QATAR UNIVERSITY

COLLEGE OF ENGINEERING

SHEAR BEHAVIOR OF GREEN CONCRETE BEAMS REINFORCED WITH BASALT FRP BARS AND STIRRUPS

BY

AYMAN AHMED EL-AHTEM

A Thesis Submitted to

the College of Engineering

in Partial Fulfillment of the Requirements for the Degree of

Masters of Science in Civil Engineering

January 2020

COMMITTEE PAGE

The members of the Committee approve the Thesis of
Ayman Ahmed El-ahatem defended on 28/11/2019.

_____

Dr.Wael I. Alnahhal
Thesis Supervisor

_____

Dr.Mohammad Irshidat
Committee Member

_____

Dr.Ghazi Abu-Farsakh
Committee Member

_____

Dr.Jamil Renno
Committee Member

Approved:

_____

Khalid Kamal Naji, Dean, College of Engineering

ABSTRACT

Ayman Ahmed Elahtem, Masters: January : 2020, Masters of Science in Civil Engineering

Title: Shear Behavior of Green Concrete Beams Reinforced with Basalt FRP Bars and Stirrups.

Supervisor of Thesis: Dr.Wael I. Alnahhal

The Reinforced concrete structures when exposed to a harsh environment it will be susceptible to the corrosion of steel reinforcement and shall lead to deterioration process. Consequently, the service lifetime of the structure will be reduced. The climatic conditions are playing an important role in accelerating corrosion; however, this corrosion needs costly repairs, and if these repairs do not start on the early stage then a catastrophic failure will happen to the structure. In order to avoid such failures and costly repairs, fiber reinforced polymer (FRP) could be used as an alternative to the steel reinforcement, which is a non-corrodible material.

Moreover, from the design prospective, the FRP cannot be used directly as an alternative to the steel bars and that's because of various differences in the physical and mechanical characteristics. One main difference in the characteristics is that the FRP bars have high tensile strength and lower modulus of elasticity compared to the steel bars. Previous studies have been examined the structure performance with different types of fiber reinforced polymers. This study will mainly focus on the shear behavior of green reinforced concrete beams with Basalt FRP (BFRP) bars and

stirrups. A total of 14No. beams with size of 200 x 300 x 2550 mm were examined in the experimental works. Sand coated Basalt FRP (BFRP) bars and stirrups are used for reinforcement of the beams as a flexural and shear reinforcements respectively. The beam will be subjected to four-point loads by the universal testing machine (UTM) till the failure takes over.

The parameters investigated in this study are span to depth ratio (i.e. a/d =2.5 and 3.5), reinforcement ratio (i.e. $\rho_1 = 2.54\rho_b \; and \; \rho_2 = 4.5\rho_b$), stirrups spacing effect (i.e. 250 mm and 350 mm) and stirrups type (Steel and Basalt). The results of the test showed that as the reinforcement ratio increase the stiffness of the beam increases. The study revealed that as the span to depth ratio increases the stiffness of the beam decreased. Results also shows that steel stirrups provide higher stiffness than the BFRP stirrups. In addition to this, it has been determined that green concrete provides high compressive strength but low flexural capacity where increasing the fly ash, affecting the flexural capacity negatively. However, it increases the workability of the concrete. It has been found that the green concrete provides high compressive strength compared to the normal concrete with the same workability properties, which increases the shear resistance by the concrete. Finally, minimizing spacing of the stirrups is not preventing occurrence of the crack, however using minimum spacing helps in decreasing the crack width.

DEDICATION

“To my grandparents, parents, my dear brother and sisters”

ACKNOWLEDGMENTS

First, I sincerely would like to thank almighty Allah for the grants he blessed me with.

Also, I would like to thank, my supervisor, Dr.Waeln Alnahhal for his continuous support throughout the two years of my master degree. As without his support, this work would have never been carried out.

The deepest gratitude after all to my dear parents for their continuous encouragement and efforts in meeting all my needs in order to finish this work.

Table of Contents

LIST OF FIGURES

LIST OF TABLES

CHAPTER ONE: INTRODUCTION

Widely, steel reinforced concrete (RC) structures in Qatar are exposed to corrosion due to the geographical location of Qatar on which the seawater is surrounding it from three directions resulting in a high concentration of chloride contents. The main critical factors initiating the corrosion is the oxygen and the moisture, when they diffuse inside the reinforcement concrete member it will reduce the compressive strength of the concrete and also affects the conventional reinforcement by degrading the diameter of the bars. This corrosion is the main cause of deterioration shown in Figure 1. So instead of using galvanized or epoxy coatings, it is recommended to use Fiber polymer bars, which eventually will solve this issue for a long-life time period.

In the last 10 years, the use of FRP reinforcement in the concrete structures has been increased because it is excellent characteristics in resisting corrosion. Also, it has good properties in the non-magnetization and high tensile strength. On the other hand, it has limitations, like low modulus of elasticity and non-yielding properties, which cause a high deflection, and cracks are getting wider in the reinforced concrete member. The most commonly available FRP in the market are aramid (AFRP), carbon (CFRP) and glass (GFRP).

Figure 1. Examples of deterioration.

1.1.Research Significance

As Qatar has been developing more buildings in order to serve the world cup 2022, more concrete will be used. In order to have a sustainable construction to provide environmentally efficient buildings, green concrete shall be highly recommended. In addition to Qatar harsh environment, the high temperature and humidity affecting the lifespan of the reinforced concrete building, an alternative such as FRP bars can be used in order to minimize the deterioration of the reinforced concrete and shall be essential to increase the lifespan and structural integrity of the building. So, from this point of view some studies has been done in order to investigate the mechanical and structural properties of the FRP in order to ensure the performance FRP bars to be used as an alternative.

1.2.Aim of the study

This study presented in this thesis aims at achieving several crucial objectives which are summarized in the following points:

This study has several aims to achieve, which can be summarized as follows:

1- Study and quantify the shear behavior of reinforced green concert beams with BFRP bars experimentally.
2- Study the effect of the span to depth (a/d) ratio effect in the shear behavior and the effect of the spacing of the stirrups. Also, the research will examine the shear behavior by using two different types of stirrups (Steel and BFRP) and other beams with No stirrups. The aim of studying beams that are not reinforced with shear reinforcement is to study the main contribution of the green concrete in the shear behavior. Comparing the experimental results with the available code equations will do this.
3- Studying the mode of failure and the failure mechanism.

1.3.Thesis Organization

The thesis is divided includes six chapters as follows:

Chapter 1 a brief introduction about the topic and the objectives of the work.

Chapter 2 includes a detailed literature review about the shear behavior of FRP-reinforced concrete using the green concrete focusing on the results developed by the previous studies.

Chapter 3 illustrates the experimental process followed in the test and also explains and evaluates the influence of the main variables.

Chapter 4 covers the results that is obtained from the experimental tests including a detailed discussion based on the results of the study by explaining each variable in the study and its effect on the behavior of the tested beam.

Chapter 5 Evaluating the accuracy of the tested beams by comparing the results with the predicted shear strength based on the equations on the design code.

Chapter 6 Includes the conclusion of the study and some recommendations for the future work.

CHAPTER TWO: LITERATURE REVIEW

2.1. Shear in Beams

Due to the applied load in beams, there will be internal forces like moment and shear in order to resist this load. Therefore, design codes are always considering these internal forces and specify a limitation for reinforcement to resist the load in order to protect the beam from the main failure, which is the flexural and the shear failure. Also, it gives a warning sign to the people who are inside the building prior collapsing. In order to ensure that before the failure occur, there will be enough time to warn the people to escape from the building.

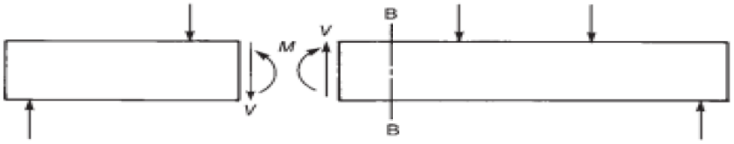

Figure 2. Internal forces on beam [4].

2.1.1. Shear Transfer Mechanisms

In the reinforced concrete members, the shear is transmitting from one plan to another in different ways. The shear behavior is mainly depending on the way of shear transmission and the failure modes. The major types of shear transfer are as follow:

(a) Shear transfer by concrete shear stress

The simplest way to transfer shear is by the shearing stresses which occurs in the un-cracked structure elements portions. The main concern in the stresses of the concrete is the low tensile stresses capacity which is not confined only as a result of the

horizontal bending stresses which caused by the bending alone [8].

(b) Interface shear transfer

Shear may transfer where the slip occurs or through a definite plan this mechanism is known as aggregate interlock mechanism. There also other mechanism where the shear can transfer known as shear friction and roughness surface transfer. Shear friction is illustrated as shown in the Figure 3 where simply can be described as saw-tooth model [8].

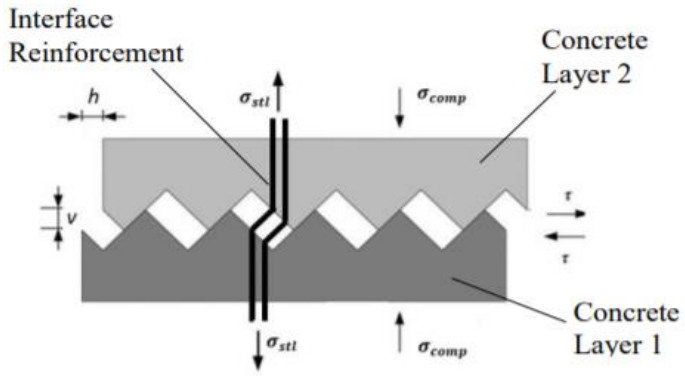

Figure 3. Shear friction model.

Shear force develops a horizontal displacement through two concrete surfaces. Due to the interlocking of the concrete surfaces, the vertical displacement developed to accompany the horizontal displacement. However, this displacement is causing tension in the reinforcement at the crossing interface. This force is the main reason of resulting friction and a clamped force between the interfaces [3,10].

(c) Dowel shear

The dowel shear force is not always dominant in the beams. The dowel shear force is mainly resisting the crack which results from the shearing displacement. The

dowel shear force is increasing the tension stress in the concrete. This tension when combined with the bars deformation resulted from wedging action. It will yield a splitting diagonally crack all over the reinforcement, which absolutely will decrease the stiffness of the concrete beam. These cracks may lead to failure; this failure commonly includes relative moment all over the crack location [4,8].

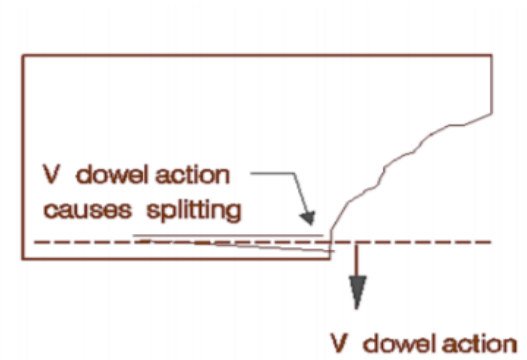

Figure 4. Dowel shear action.

(d) Arch Action

Part of the load is transmitted in the deep beams and slabs in order to support the arch action. Arch action is mainly reducing the impact of the other kinds mentioned before of the shear transfer [3].

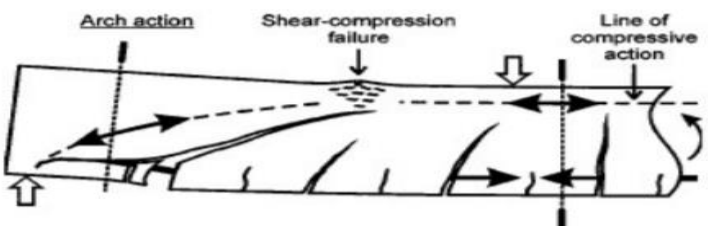

Figure 5. Arch action [5].

As the load increases the internal actions that resist the shear force be reduced which will affect the shear capacity of the beam, as consequence cracks will start to propagate and as the load increases the crack width will increase. In order to resist the internal action of the shear force, vertical reinforcement shall be provided “stirrups” which will decrease the width of the cracks that has been propagated due to the increased load. Providing stirrups will ensure that the failure that will take over will be flexural failure, if ultimate shear capacity will not be reached before the ultimate flexural capacity [5,11].

2.1.2. Predicting the shear force

Methods used to predict the shear force for RC concrete beam with FRP are mainly following the concept of considering the equilibrium of the forces through the diagonal crack [6,12,13]. The external shear forces are resisted by the internal actions that takes place inside the diagonal crack in the concrete beam which are; compression zone in the concrete denoted as (V_{cy}), aggregate interlock which denoted as (V_{ay}), the vertical stirrups (V_{sy}) and also the dowel action (V_{d}). In addition to that, the equilibrium of all the combined forces in the y-direction, which is denoted as (V). All of these forces are resisting the external shear force as shown in Figure 6.

$$\boldsymbol{V = V_{cy} + V_{ay} + V_d + V_{sy}} \qquad \boldsymbol{Eq\ (1)}$$

As the first three terms represent the contribution of the concrete shear force so the above equation can be written as following where V_C is the sum of the three terms

$$\boldsymbol{V = V_C + V_{sy}} \qquad \boldsymbol{Eq\ (2)}$$

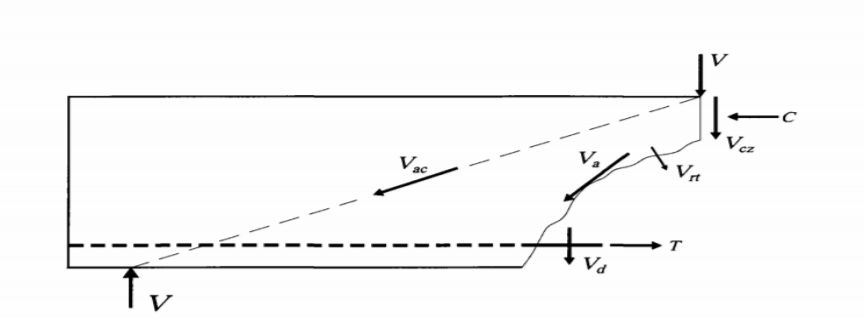

Figure 6. The internal shear force in cracked section [4].

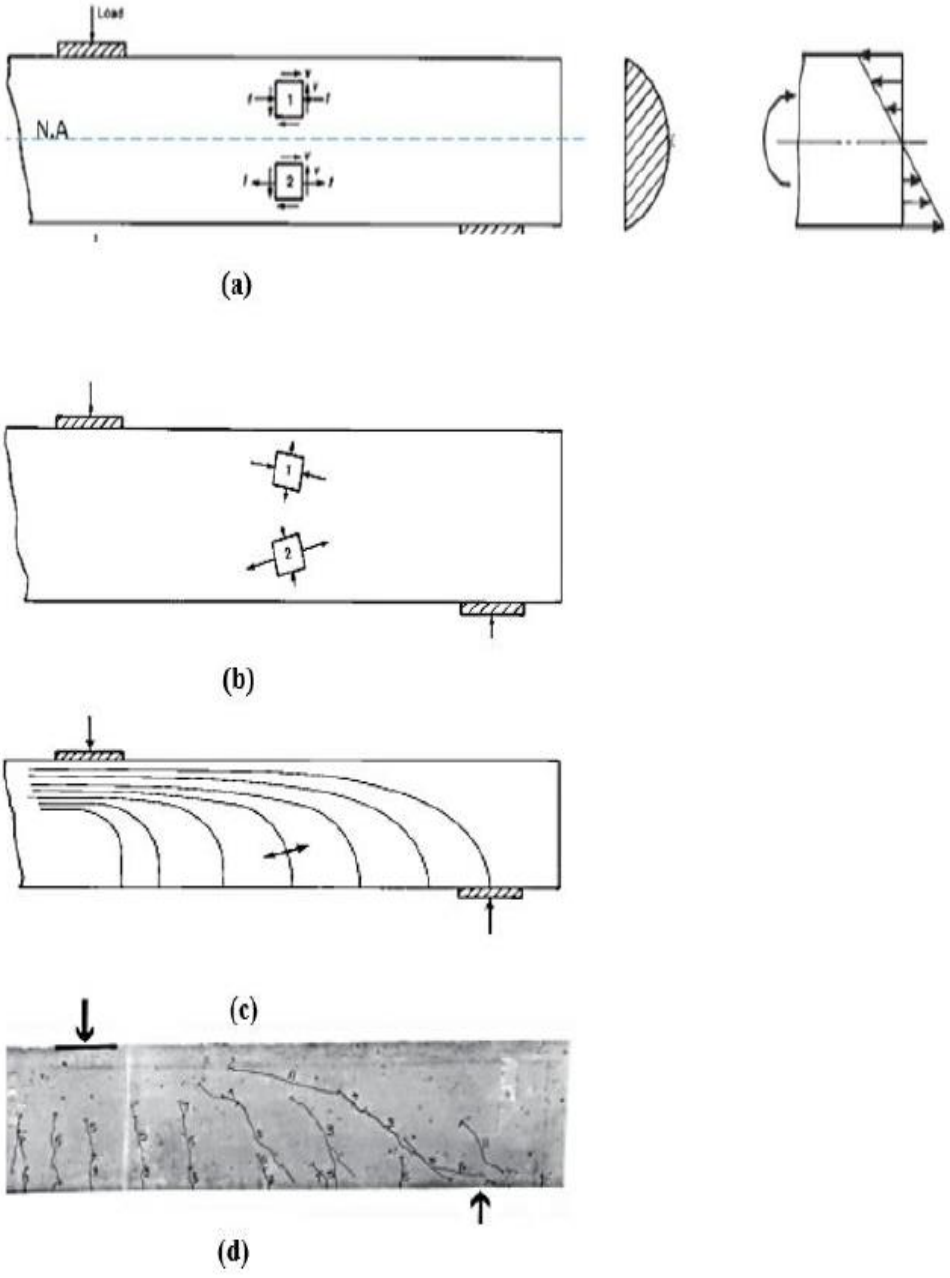

Figure 7. (a) shear flexural stresses, (b) Normal Principal stresses, (c) Compressive Stress trajectories, (d) Crack Pattern [4].

2.2. Span to depth ratio effect

ACI and ASCE committee have been classified the beams having a span to a depth ratio smaller than 2, it classifies as a deep beam; and if the span to depth ratio (a/d) exceeding 2.5 so it is classified as a shallow beam. If the ratio is in between the above ratio, the beam is classified as moderate deep beam [6]. Previous studies showed that there is a linear correlation between the span to depth ratio (a/d) and the shear strength. The same result has been predicted from the CSA S806-12 code [6]. According to F.Ashour (2015), study shows that as the (a/d) increases in CFPR-RC Carbon fiber reinforced polymer concrete beams and BFRP-RC Basalt fiber reinforced concrete beams the shear strength decrease [8,9]. There was also a correlation between the shear transfer mechanisms over the cracks and a/d ratio [41,42]. It was noted that the beams reinforced with FRP bars without shear reinforcement, the shear failure is taking place through the aggregate interlock. So, the shear strength would decrease as the crack width increase which is caused by the a/d ratio which will directly affect the shear transfer mechanism negatively [10,11].

Different type of failure occurs for different a/d ratio. Flexural failure as shown in Figure 8 (a) usually occur for beams having a/d > 2.5 which is known as very shallow beams where the first crack occurs at the maximum moment of the beam cross section due to the flexural tension. It was observed that as the load increases the tensile cracking are spreading at the regions of the less moment areas, this behavior is taking place before the failure occur. However, the failure is taking place at the maximum moment section in the beam. The second type of failure occurs is the flexure and shear cracks. This type occurs before the beam reaches the maximum flexural capacity [12].

The third type is the diagonal tension failure this take place when the load is increasing, and the cracks are keeping propagating through the beam than at a certain

stage the beam became unstable and failure occurs [12].

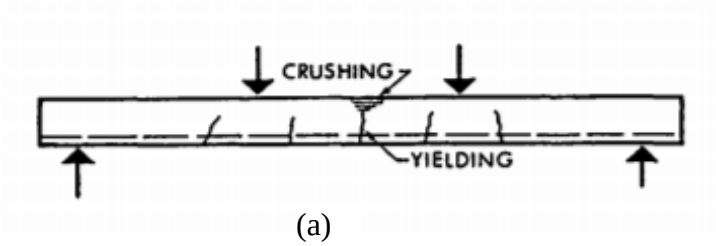

(a)

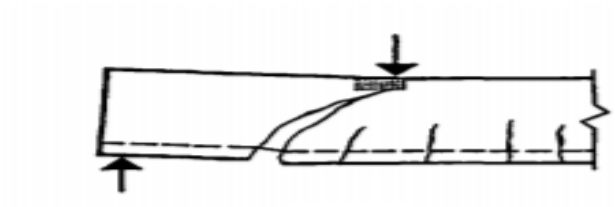

(b)

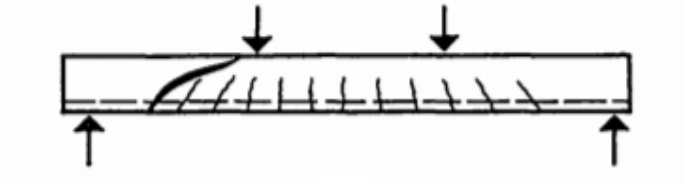

(c)

Figure 8. (a) Flexural failiure. (b) Shear-Compression failure

(c) Diagonal Tension Failure. [11].

Combination of shear and moment shall be combined in a region that the tensile crack already propagated this will result in another mode of failure. Starting from the inclined crack a secondary crack shall be propagated in the backward direction along the longitudinal reinforcement that's due to the dowel action [5,11]. This crack will cause loss of the bond, which will help the main reinforcement to slip. This shall result in the wedging action, which is playing a role in splitting the concrete with more cracks propagation. As consequence, this will lead to anchorage failure of

the longitudinal reinforcement. This crack is called shear tension failure. However, it is also noticed that the concrete which is above the upper-end of the inclined crack might be fail as a result of crushing that causing shear-compression failure.

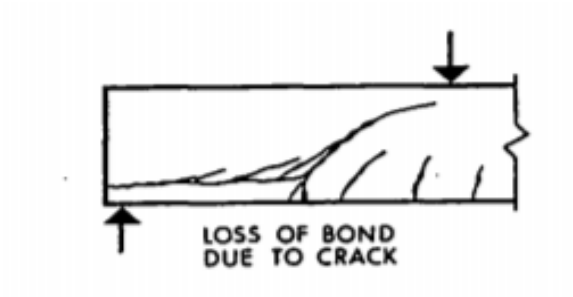

Figure 9. Shear - tension failure [11].

The effect of shear stirrups is categorized into two steps:

(a) Before the shear crack occurs -which has no effect rather than confining the concrete and to fix the top and bottom reinforcement from moving during casting.

(b) After the shear crack occur:

1- Resisting the shear across the crack.

2- Reducing the propagation of the shear crack.

3- Trying to keep the crack small by increasing the aggregate interlock.

4- Increasing the confinement in the concrete which will impact well on the bond strength between the concrete and the reinforcement.

To sum up, concrete is mainly resisting compression, but it is weak in resisting in tension stresses. For that, if the tension stresses exceeding the limit of the tension stress capacity of the concrete cracks shall be developed. Diagonal cracks will mainly result of the tension and compression stresses if the shear force is the force that governed in the beam [5]. As consequence, two types of shear cracks can be developed which is classified as follows; the first type is the diagonal tension failure: Inclined tension stress which is known as diagonal tension is resulting from the shear alone which is located in the neutral axis or the combined action of both shear and bending that exist in the beam. It may cause a disaster failure if it is considered in the design of reinforced concrete. This type occurs at the (a/d) ratio ranges between 2.5 to 6 of the beam. The crack mainly starts at the mid of the beam and starts to go upper, as the load increased the crack is getting wide till failure [7].

The second type is the shear compression failure: The failure is mainly occurring nearby the top of inclined crack usually in the beams with short span compared to the depth. This failure may cause a disaster because it crushes the concrete [8,41].

2.2.1. Modes of shear cracks

There is a lot of shapes of the cracks occur due to the shear action. Simply when the beam is loaded from the top so compression stress will be resulted due to this load and concentrated at the top and the tensile stress, will be concentrated on the bottom face of the beam. As a result of these stresses diagonal tension cracks established. The diagonal tension is pulling the beam from the supports in a form of angle, angle cracks is starting from down to the top of the beam at the cracks are mainly is starting from the quarter point of the beam from supports and then starts to go up till the top of the beam [5].

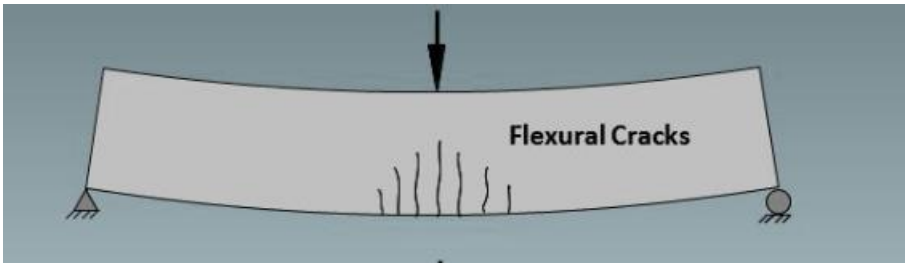

Figure 10. Flexural crack [6].

The other crack which web shear crack that is may occur either before the flexural cracks happens in the vicinity or it may develop an extension to the flexural crack. The web shear crack is developed in diagonal form in the middle of the beam height; the crack is keeping increasing and propagates in the diagonal path if the load increased. Usually, it occurs at the location where the shear is high, and the bending moment is low simply near to the simple supports where the diagonal tensile stress is high. This crack may cause failure since the shear capacity is reduced as these cracks developed. As the cracks developed the shear stresses increases and concentrate at the locations where cracks didn't take place yet [6].

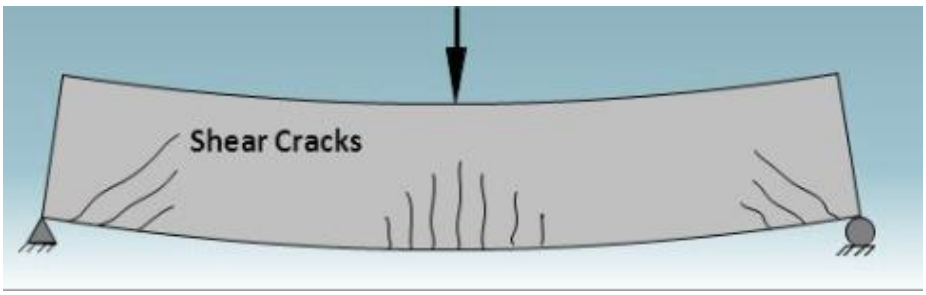

Figure 11. Web- Shear crack [6].

2.3. Shear behavior of FRP

According to Zhao (2017) who studied the stress characteristics, failure mode, deformation capacity and the stiffness of the shear behavior for different concrete which beams strengthened with different types of fibers and other forms of reinforcement will be used in the four beams which are Carbon fiber reinforced polymer, hemp fiber reinforced polymer and Glass fiber reinforced polymer (CFRP, HFRP and GFRP respectively). It is been noted that the deformation developed due to bending has been reduced under the same force applied, also it was noticed that the diagonal crack propagations were delayed from extension [14].

The FRP sheets are used in the bottom of the beam were mainly for bending reinforcement and the sheets that are installed on the sides of the beam were used for shear reinforcement. It was observed that there was a shortage in the shear capacity in the beams of the oblique section, and that's because the following factors which are the insufficient number of stirrups used, the low strength of the concrete used and finally due increasing the load if the structure system changed. It is essential to recheck the shear capacity of the oblique beam section after enhancing the bending strength by the FRP sheets to assure that the reinforcement is sufficient in order to ensure that the safety engineering requirement and the ductility requirement has been [45].

Zhao (2017) reveal that FRP reinforcement increased then the stiffness of the beam will increase and also increases the beam stiffness and it delays the extension of the diagonal cracks. It was noted that when the FRP shear strength of the concrete element reaches the ultimate failure then the concrete will be crushed specifically in the compression zone. They concluded that the effect of the reinforcement is mainly dependent in the actual strain of the fiber bars when the concrete member is cracked [47].

2.3.1. Shear behavior of geopolymer concrete beams without stirrups

New types of green concrete have been generated like geopolymer concrete in order to minimize the impact of the Ordinary Portland Cement in the environment. Whereas P. Visintin (2017), studies eight beams using geopolymer concrete beams reinforced without stirrups in order to study the contribution of the geopolymer concrete with the shear strength. The study also has been developed mechanics using the segmental approaches in order to predict the shear capacity of the reinforced geopolymer concrete without stirrups. The eight beams have been directed to the four-point load test with the lowest level of confinement and the results indicate that the geopolymer concrete has the same shear capacity of the ordinary concrete beams. That's due to the shear friction properties of the concrete which was at the same range of the ordinary concrete beams [24].

2.3.2. GFRP as shear reinforcement

N. A. Hoult (2008), noted when the axial strength of FRP stirrups is lower compared to steel it would widen the diagonal cracks also it would increase the depth of the crack; which will affect the concrete member negatively mainly in the shear transfer through the aggregate interlock. Also, it is reducing the contribution of uncracked concrete especially in the compression zone [17]. The shear contribution of the FRP through dowel action is almost negligible due the low transverse strength of the FRP [16].

After testing 12 reinforced concrete beams with BFRP with and without stirrups, the 12 beams were reinforced with different ratio of BFRP bars as a flexural reinforcement and also there was a variety in the span to depth ratio then the

following outcomes has been observed. Firstly, the mode of failure for all beams without stirrups reinforcement was shear tension failure when there was a variety on a/d ratios ranging between 5.65 and 7. The failure was more clearly in the beams that is reinforced with higher reinforcement ratios (ρf). The stiffness of the beam is decreasing when the a/d ratio increases. Also, it is noted that the stiffness of beams reinforced with and without stirrups increases while increasing the reinforcement ratio (ρ_f) while having the same span to depth ratio. All the reinforced concrete beam with stirrups has been failed in the shear compression field when the span to depth ratio is less than or equal 2.5.

Ginghis B. Maranan (2015), investigated the shear behavior of RC beams reinforced with FRP bars using geopolymer concrete. The study investigation based in two beams reinforced by steel and GFRP stirrups and one beam without stirrups in order to determine the shear contribution of the geopolymer concrete. The two beams were reinforced with a web reinforcement and then tested by using four-point loading test. The spacing of the stirrups was fixed for both beams which are 150 mm center to center. Beams have 450 mm shear span for each side and 1200 clear span. The study found that shear capacity has been doubled when the GFRP stirrups have been used compared to the beam without web reinforcement. It has been observed that crack pattern was almost the same for the beams reinforced with GFRP and steel stirrups; however, it has been observed that wider cracks have been developed for the beams that have a lower modulus of elasticity of GFRP bars comparable with the beam with steel bars [30]. The failure of the beam reinforced with steel stirrups caused by the yielding of the steel, however for the beam reinforced with GFRP stirrups the failure caused due to the failure of lap splice of stirrups also it is noticed that the final failure of the beam reinforced with GFRP stirrups was more explosive than the beam

reinforced with steel stirrups. It was observed that stirrups have prevented the longitudinal splitting of the beam due to the confining effect. Finally, from the results provided the GFRP stirrups can be used as an alternate of the steel stirrups [31,56].

2.3.3. Shear behavior of GFRP composite spirals

G.B. Maranan (2018), studied the shear behavior of geopolymer-concrete beams reinforced with continuous (GFRP) composite spirals in order to examine its effect in the shear behavior. Eight beams were tested investigate the effect of the configuration of the web reinforcement, spiral pitch, ratio of the longitudinal reinforcement and the span to depth ratio. It was observed that beams stiffness has been increased by 120% when the spiral reinforcement in the beams were used compared to the normal stirrups. The enhancement was due to either the close spacing of the spiral which has a main factor to increase the shear performance which increases also the confinement in the concreate which playing a role in increasing the shear capacity of the beam compared to the wide spacing stirrups [29]. The other reason which used to analyze this improvement was the inclination of the spirals was almost normal to the direction of the shear cracks. The beam which reinforced with GFRP spiral reinforcement are viable alternative to use and can be substituted with the ordinary closed GFRP stirrups.

2.4. Deflection behavior

The load-deflection test has been done in 24 concrete beams reinforced with glass and carbon FRP. The concrete members were reinforced with extensive ratios of reinforcement in order to measure the flexural response. Because the FRP has low modulus of elasticity and special bond characteristics it was expected to have large deformation in the FRP reinforced concrete beams. As a result of these characteristics of the FRP the service limit is governing in the design procedures [19]. In order to

calculate the service limits accurately it requires doing integration to the curvatures and also allow shear and bond deformation to occur. However, this calculation is not appropriate design because it requires time to calculate it. For this reason, it is important to establish a simplified method in order to evaluate the deflection of the concrete elements with acceptable accuracy [20, 21].

The simple analysis models require calculation of the effective moment of inertia in order to describe the actual stiffness of the cracked member. The effective moment of inertia has proved its effectiveness in determining the deflection of the concrete members reinforced with the steel, so it is also adopted with the FRP reinforced concrete members.

2.5. Crack development in concrete beams

The low modulus of elasticity of the FRP results in crack width deflection which should be controlled in the design of the concrete beams reinforced with FRP bars. The paper is testing 5 beams reinforced with different FRP reinforcement ratios in order to evaluate the initiation of the crack and the crack pattern and studying the impact of the reinforcement ratio in crack width. P. Visintin (2011), tested the bending behavior of concrete beams reinforced with Carbon and Glass FRP (CFRP and GFRP) to examine the flexural behavior in term of deflection behavior and crack shape [34]. It was observed that the GFRP reinforced concrete beams made the cracks denser and scatters the cracks symmetrically compared to the CFRP reinforced concrete beams. P. Visintin (2011), concludes with significant finding that the result of the experiment shows that when the reinforcement ratio increases then the crack width and the crack spacing decrease. Also, it was observed that the crack width of concrete members reinforced with FRP is larger than the concrete members reinforced with normal steel reinforcement [29].

2.6. Green concrete

Concrete is a very important element in different types of structures such as bridges, high-rise buildings, conventional structures and many others. Due to its cost and desired technical properties of resisting loads and giving strength to the structure, it is found to play a big role in construction. However, concrete might also give negative impact on the environment in terms of the manufacture of its materials and sustainability. The main component of making concrete is the Portland cement. According to the studies that producing one ton of Portland cement is missioning 1 ton of CO2 to the atmosphere which is affecting the environment negatively [36]. In the past decades, scientists have been searching for alternatives materials to be used in normal concrete in-order to achieve what's called as green concrete. The word green is not limited to the color it's related to the environment and sustainability. The alternatives of the Portland cement were like the fly ash, silica fume and blast furnace slag. The study revealed that the silicon (Si) and aluminum could react with the alkaline liquid to produce binder. Green Concrete is mainly made form concrete wastes which considered to be eco-friendly. Measures and introduction to alternative materials are taken into consideration in the mix-design; insuring a long-life cycle with low maintenance surface leading to a sustainable structure. The main goals that are achieved by green concrete is energy savings, reduction of Co_2 emissions and the use of waste products in replacement with fossil fuels used in the production of the normal concrete materials. Using these products in the concrete will positively have an environmental impact and would play an important role in the reduction of natural disasters [38]. Some of the criteria for a green material as follow:

- Reusable or Recyclable

- Locally Available
- Indoor Air Quality
- Reducing the Co_2 emissions
- Water Conservation
- Salvaged or re manufactured
- Resource and Energy efficiency

According to Parbat, Dhale (2015), Portland cement needs about 1.5 tons of raw materials for its production and in-turn about one ton of carbon dioxide is released to the environment during the process of production and this would increase the impact of global warming in the environment. It was studied also that fly-ash acts as partial replacement to Portland cement that could reach 60% percent replacement of high-level volume leading to reduced carbon dioxide emissions.

Whereas Doye (2017) showed that studies found that the optimum replacement level is around 30%. It was mentioned that the fly-ash would improve the performance of the concrete in the softened and hardened state. It is also possible to replace Portland cement with a fly-ash by 100% having a concrete of 100% fly-ash as cement replacement and mainly percentages above the 80% would need a chemical activator [37].

According to Meyer (2015) Ground Granulated blast furnace slag has an optimum cement replacement level between 70% to 80%. It can improve the durability and the mechanical properties of the concrete [38].

Ingredients of the green concrete that could replace the cement content

Fly-Ash

Fly-ash is produced during the combustion of coal. It has a lot of good features, which improves the workability and strength of the concrete. Many tests showed that it generates less heat of hydration, so this is an advantage for mass concrete applications [38,41]. It also improves the durability of hardened concrete and the workability of plastic concrete.

Figure 12. Fly ash.

Ground Granulated Blast-Furnace Slag

Blast- Furnace slag is outstanding Cementitious material, which is Produced when molten iron slag form in the blast furnace. Then it goes through a water stream to produce the granular product that is dried and grounded. Another advantage is that Blast slag is producing less heat of hydration which will reduce the cracks which generated due to the non-uniform expansion of concrete body. It also improving the durability of the concrete [39].

Silica Fumes

Silica Fume (SF) is mainly obtained as a by-product of silicon and ferrosilicon alloy production. SF has a shape of spherical particles of about 150nm diameter. The main advantage of using the SF is it improves the durability and the bonding strength of the concrete in addition of increasing the concrete compressive strength [56].

Recycled Concrete Aggregate:

M. Etxeberria (2006), compared 24 samples of concrete beam specimens (made with RCA) with analytical models for regular concrete. The samples varied in the percentage of RCA used to replace the natural aggregate. By replacing the natural aggregate by the recycled one this will help in conserving natural resources and give a positive impact on landfill by reducing their capacity [50].

It was found from the results of the experiment that beams made with RCA did not significantly affect the flexural capacity of the RC beams especially when shear reinforcement is used. It is important to note that in the case where there was no shear reinforcement a 25% replacement of aggregates with RCA showed no change in the shear failure values however a percentage of 50 or more showed a 11 to 15% decrease in shear strength [51]. However, this may not be a problem as in construction stirrups are always provided.

And although the deflections of RC beams made with RAC where more than that of RC beams made with regular concrete [50, 52] the flexural failure was observed to occur after the yielding of the steel reinforcement. This means that the typical methods for moment calculations can still be applied. However, if the deflection problem is controlled and stirrups are used then RCA beams should act in a way that is similar to that of regular concrete beams.

Doye (2017) mentioned that Recycled concrete and masonry aggregates would act as a good sustainable material. As fine aggregates query dust may be used as it's durability under sulphate attack is much higher compared to conventional concrete, also the effects of quarry dust on the elastic modulus property are good with conventional concrete containing natural sand [37].

Steel Slag:

Again, these tests were performed in order to compare how will RC beams made with steel slag aggregate (SSA) perform versus RC beams made with regular concrete.

Zaki and Metwally [53] reported that the failure mode of SSA RC beams was similar to that of regular RC beams with no horizontal cracks; this means that the bond between the concrete and the steel reinforcement was not affected by the steel slag aggregates. Furthermore, the deflection problem found in RCA beams was not found in SSA beams, as SSA beams acted very similarly to regular concrete beams.

The compressive strength of SSA concrete cube samples was found to increase with an increase in the percentage of steel slag aggregates that replaced regular aggregates and the same was reported about the tensile strength of SSA concrete [56,57]. This was reflected on SSA RC beams where the flexural and shear strength of the beams was also higher than that of regular concrete beams. However, one issue that appeared during testing was that the SSA concrete if prepared with the same water to cement ratio as regular concrete the workability was reduced. This is not seen as a problem as it was proposed to use plasticizers [55] or water to cement ratio of 0.6 to improve workability.

Advantages of green concrete:

- Less impact on the environment.
- 30% reduction in CO2 emissions from concrete plants.
- Use of residual products in concrete industry increases by 20%.
- Green concrete production is cheaper than conventional concrete.
- Good durability and workability.

Limitation of green concrete:

- Green concrete has less tensile strength than the conventional concrete [68].
- Green concrete has higher creep and shrinkage [68].

CHAPTER THREE: EXPERIMENTAL PROGRAM

3.1. Materials

3.1.1. Basalt Fiber Reinforced Polymers Bars

Fiber reinforced polymer is mainly obtained by introducing high strength fibers to a polymer matrix which is mainly classified into two groups which is thermosetting resins like polyesters and thermoplastic resins like nylon. The matrix is the basic material of composite also it is providing protection to the fibers from exposing to the environment which protects the structures elements. Fibers are relatively composed of ductile matrix polymer like vinyl ester and epoxy which dominating about 30 to 60% of the volume of the composite [1]. In the past composite materials were used mainly in aerospace and in the sporting goods where the high strength compared to the weight is the most priority in their characteristics. The type that was used in this study is the basalt FRP (BFRP). Different nominal diameters were used (12 and 16 mm). BFRP are characterized by some features that attracts engineers to like it due to high thermal and corrosion resistance [60]. As per Sim et al. study it was noticed that the BFRP maintain its mechanical properties and its shape till 2 hours of exposing to 1200 C heats. However, Sim et al observed that glass and basalt fiber are experiencing a higher reduction of tensile strength after leaving them in 1 molar of sodium hydroxide solution for 28 days. On the other hand, slight reduction observed on the tensile strength of the carbon fiber. The main source of the BFRP bars is the igneous rock which contains of numerous forms of silica oxides about 51.6 to 57.5%. Generally, above 46% of silica oxide is adequate composition for production of the basalt fiber. Vinyl ester is the polymeric resin used in the production of the BFRP bars. The characteristics of the BFRP bar provided by the manufacturer are listed below in the Table 1. A (BFRP) stirrups used in this study has a nominal diameter of

9.5 mm. As shown in the Figure 13 geometry of the stirrup which is satisfying the requirement of the ACI minimum radius bend which is minimum rb to bar diameter (db) ratio (rb/ db) of 3.

(a)

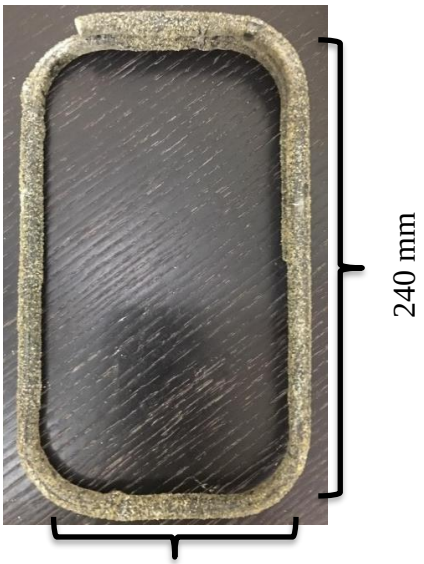

(b)

Figure 13. (a) BFRP Bar; (b)Stirrup Used in the Study.

Table 1 Material Properties for the Used BFRP Bars in this Study

Material Properties	BFRP sand coated bars	
Diameter of the bar (mm)	16	12
Tensile Strength (MPa)	1056	1230
Elastic Modulus (GPa)	60	72

3.1.2. Concrete Mix

Concrete mix used in the study was aiming for compressive strength of 40 MPa. In this study, a green concrete mix has been made which means a partial replacement of the cement content has been made. Materials which replaces the content of the cement was the fly ash and silica fume with a 60 and 80 Kg respectively with a total proportion of 50% of the cement content. At the beginning, a trial mix has been made to validate the mix design and to ensure that aimed strength will be reached.

3.1.3. Mix Design

In order to ensure that the mix design is correct for the green concrete, 8 specimens have been casted then tested after 7 and 28 days. The proportions used in the trail mix are as shown in Table 2.

Table 2 Mix of the Concrete Design

Materials	Mix proportion
Cement	260 Kg/m^3
Silica Fume	80 Kg/m^3
Fly Ash	60 Kg/m^3
20 mm lime stone	481 Kg/m^3
10/14 mm lime stone	633 Kg/m^3
Sand	750 Kg/m^3
Superplasticizers	4.5 Kg/m^3
Water	149 Kg/m^3

3.2.*Beam Tests*

This section is showing the procedures of testing the shear behavior of 14 green concrete beams reinforced with BFRP bars and stirrups. The tested span of beams was 2250 mm with simply supported supports and two points load and with a cross-section dimension of 300mm depth and 200mm width. The beams were designed to achieve the shear failure prior the flexural failure, generally the flexural capacity was high compared to the shear capacity.

3.2.1. Test Setup and Instrumentation

Four-point loads test was conducted for the study using Universal Testing Machine with a maximum load of 1500 KN capacity at Qatar University lab. All the mid-span deflection of the beams was measured using the LVDT (Linear Variable Differential Transducer). All crack patterns have been recorded at every increment of the load. Crack transducers have been fixed diagonally between the support and the point load specifically at the mid-height of the shear span of the beam. FRP and concrete strains were recorded by using the strain gauges manufactured in Japan by (Tokyo Sokki Kenkyujo Co. Ltd. (TML). All beams were tested till the failure occurs. After assembling BFRP reinforcement cages the BFLA-5-8-5L (for composite reinforcement) strain gauges of 5-mm was placed at the mid-span of the bars from the bottom. However, the concrete strain was measured using a specialized strain gauge of 60 mm length (PL-60-11-3L) placed at the top surface mid-span of the concrete beam.

A data acquisition system (TML Data Logger Multi-Channel Digital Strain meter DRA-30A) was linked to a master plan that connected to the strains and transducers and the LVDT. The electrical signals of the connected strains and transducers were

transformed to a digital signal by the data acquisition system, finally displayed then recorded at the system this procedure is for every incremental of the load.

(a) (b)

Figure 14. (a) FRP strain gauge; (b) Concrete strain guage.

3.2.2. Testing Variables

In this study, the factors affecting the shear behavior of the beam would be studied. The main factor that will be studied is to distinguish the influence of the green concrete on the shear behavior on the beams reinforced with FRP bars. Beams will be divided into two major groups and one minor group first group will be casted with BFRP stirrups with two different reinforcement ratios which are $2.54\ \rho_b\ and\ 4.5\ \rho_b$ and different span to depth ratios (a/d) 2.5 and 3.5 with different stirrups spacing of 250 mm and 350 mm. The second group casted with steel stirrups will be with two different reinforcement ratios which are $2.54\ \rho_b\ and\ 4.5\ \rho_b$ and 3.5 span to depth ratio with different stirrups spacing of 250 mm and 350 mm. The minor group that contains of three beams will be casted with no stirrups. Reinforced with two different reinforcement ratios which are $2.54\ \rho_b\ and\ 4.5\ \rho_b$ and with 3.5 and 2.5 span to depth ratio.

3.2.3. Beams Designations

The beams designation will be segregate in a different four parts of variables, starting with the stirrups type used B,S, NS which BFRP stirrups ,Steel stirrups, No stirrups respectively. Then,the second part indicating the renforcment ratio ρ_1 which corrspondes for the 6ϕ12 and ρ_2 corrospondes with 5ϕ16.Third part is the span to depth ratio which is 2.5 and 3.5. Finally, the last part indectates the stirrups spacing used which is 250 mm and 350 mm. For example, B-1-B-ρ_1-2.5-250 refer to (B-1) which is reinforced with BFRP stirrups, and reinforced with a ρ_1 which corrspondes with 6ϕ12 BFRP bars, with a span to depth ratio of 2.5 and 250 mm spacing between stirrups.

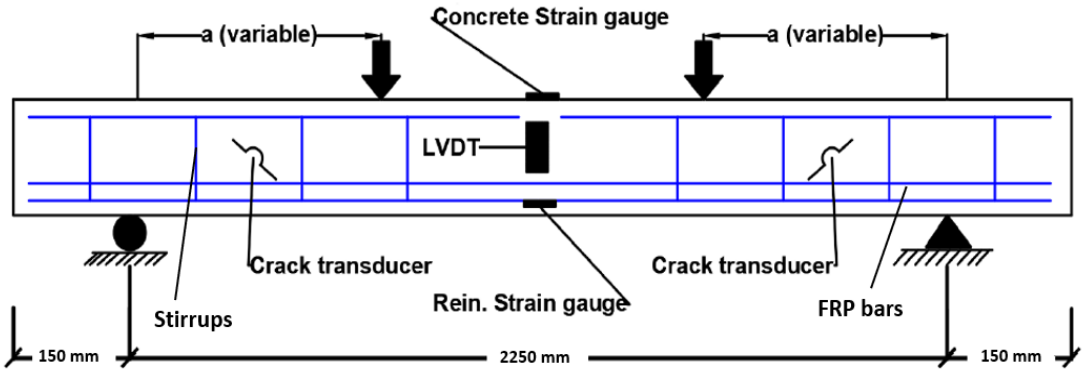

Figure 15. Detailed sketch of the beam.

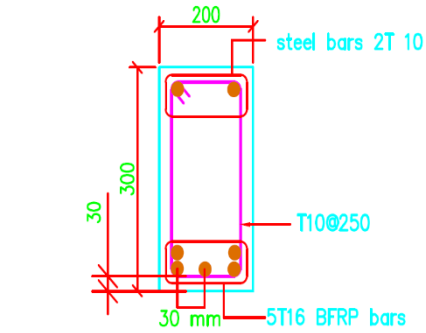

5T16 BFRP bars with STEEL stirrups spacing 250 mm a/d =2.5

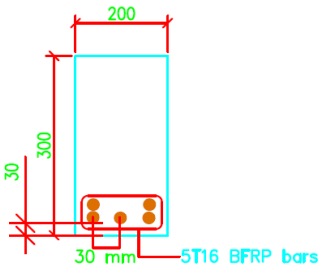

5T16 BFRP bars without stirrups a/d =3.5

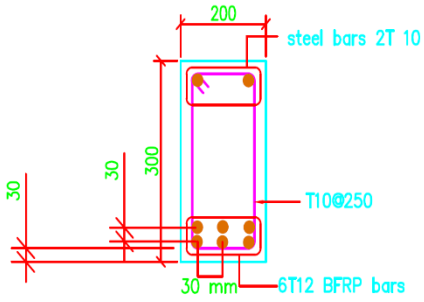

6T12 BFRP bars with BFRP stirrups spacing 250 mm a/d =2.5

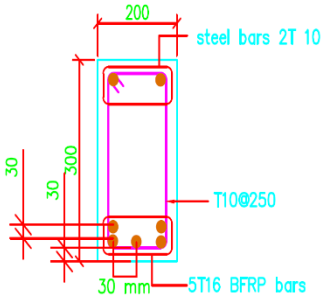

5T16 BFRP bars with BFRP stirrups spacing 250 mm a/d =3.5

Figure 16. Beam sections detailing with deginations .

Table 3 Detailed Testing Matrix

Beam No.	Beam designation	Target Comp. Strength (MPa)	Reinforcement ratio	Spacing (mm)	a/d ratio	Type of the stirrups
B-1	**B-ρ_1-2.5-250**	40	2.54 ρ_{fb}	250	2.5	**BFRP**
B-2	**B-ρ_1-2.5-350**	40	2.54 ρ_{fb}	350	2.5	**BFRP**
B-3	**B-ρ_1-3.5-350**	40	2.54 ρ_{fb}	350	3.5	**BFRP**
B-4	**B-ρ_1-3.5-250**	40	2.54 ρ_{fb}	250	3.5	**BFRP**
B-5	**B-ρ_2-3.5-250**	40	4.5 ρ_{fb}	250	3.5	**BFRP**
B-6	**B-ρ_2-2.5-250**	40	4.5 ρ_{fb}	250	2.5	**BFRP**
B-7	**B-ρ_2-2.5-350**	40	4.5 ρ_{fb}	350	2.5	**BFRP**
B-8	**B-ρ_2-3.5-350**	40	4.5 ρ_{fb}	350	3.5	**BFRP**
B-9	**S-ρ_1-2.5-250**	40	2.54 ρ_{fb}	250	2.5	**Steel**
B-10	**S-ρ_1-2.5-350**	40	2.54 ρ_{fb}	350	2.5	**Steel**
B-11	**S-ρ_2-2.5-250**	40	4.5 ρ_{fb}	250	2.5	**Steel**
B-12	**NS-ρ_2-3.5**	40	4.5 ρ_{fb}	-	3.5	**No-stirrups**
B-13	**NS-ρ_2-2.5**	40	4.5 ρ_{fb}	-	2.5	**No-stirrups**
B-14	**NS-ρ_1-2.5**	40	2.54 ρ_{fb}	-	2.5	**No-stirrups**

3.2.4. Beams *Preparation*

Figure 17. Shuttering used to cast beams

Figure 18. Assembly of the reinforcment cages

Figure 19. Installation of the strain gauges for the BFRP bars.

Figure 20. Installing Reinforcment cages in the shuttering.

Figure 21. Casted beams.

Figure 22. Beams ready for test.

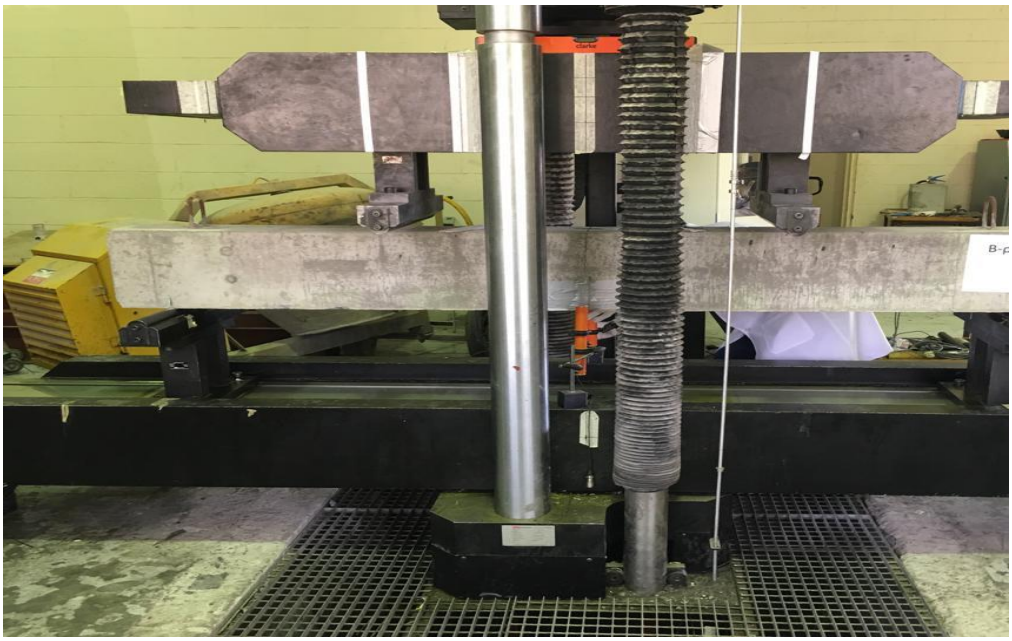

Figure 23. Universal Testing Machine used in the Study.

CHAPTER FOUR: TEST RESULTS AND DISCUSSION

4.1.Introduction

This chapter will illustrate the test results of the tested specimens. The behavior of the beams will be presented in terms of deflection response, flexural strain and failure mode. Also, the results of the mechanical properties of the casted concrete will be shown in this chapter. In addition, the shear behavior will be illustrated and discussed specifically the shear cracking load and cracking pattern. The analysis will mainly focus in four parameters, which are stirrups spacing, type of the stirrups, a/d ratio and reinforcement ratio. Eight beams were reinforced with BFRP stirrups, three with steel stirrups and three with no stirrups as discussed earlier in chapter 3.

4.2.The Mechanical Properties of Fresh Concrete

4.2.1. Slump *Test*

Slump test has been carried out to check the workability and the consistency of the concrete test procedures according to the ASTM (C143). The slump result of the casted concrete was 200 mm which was within the range of the mix allowable slump which is 150 mm $\pm$ 50 mm. The workability of the concrete mix was high compared to the normal concrete with the same compressive strength .

Figure 24. Slump Test.

4.3.The Mechanical Properties of Hardened Concrete

4.3.1. Compressive Test Results

In order to measure the compressive strength of the casted concrete in 5 cylinders with size of 150 mm x 300 mm have been casted. The test has been conducted in the standard compression testing machine with a capacity of 2000 KN. Compressive strength test has been taken place after 28 days of curing, the average result of the compressive strength of the concrete was 44.5 MPa as the designed mix. Table 4 showing the compressive test results.

Figure 25. Compressive stength test for the cylinders.

Table 4 Compression Test Results

Cylinder NO.	Actual Compressive Strength (MPa)	Average Compressive Strength (MPa)
1	45.23	
2	41.63	
3	44.72	44.5
4	45.68	
5	45.42	

4.3.2. Flexural Test Results

In order to determine the flexural tensile strength of the casted concrete, a simply supported prism of concrete subjected to two points load test has been conducted. The test has been carried out for three prisms and the average flexural strength was 4.42 MPa. The variety in the results was due to many reasons one of them is the handling and the transportation of the prisms from the site to the lab. Table 5 show the test results of the prisms.

Table 5 Flexural Test Results

Prism NO.	**Actual Flexural Strength (MPa)**	**Average Flexural Strength (MPa)**
1	4.2	4.42
2	4.53	
3	4.53	

(a) (b)

Figure 26. (a) Carrying out the flexural test ; (b) Failure of the prism under the flexural test.

4.3.3. Tensile *test for the FRP bars*

In order to design the BFRP reinforced concrete beam it is necessary to test the characteristics of BFRP bars and to know the actual yielding strength. In this experiment, 5 bars have been chosen randomly from each diameter used in the study that is 12 mm and 16 mm, in total 10 samples have been tested.

BFRP bars were installed in the center of the steel pipe and the gap has been filled by expansive grout to be used as an end restrainer and to provide the confinement pressure on the bar [26,61]. Procedures have been taken as per ACI-440.15 provisions [26], the steel pipe which have anchors of 305 mm long, the bar length was determined as follows, bar length shall be $40d_b$ and add to this 2La. La tends to the length penetration of the BFRP bar inside the steel pipe (anchorage length) and d_b tends to the diameter of the bar which will be used in the test . The penetration part of the bar shall be aligned perfectly in order to prevents any undesired failure also plastic caps has been used at both ends of the steel pipe one of the ends was installed with a drilled plastic cab which the bar inserted to ensure that the bar is centered as shown in the Figure 27 (b). The grout was in liquid condition initially then after 24 hours it starts to harden then the specimen can be turned then the second anchor can be prepared.

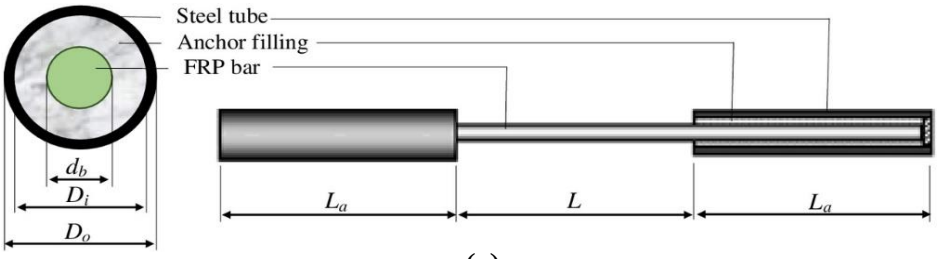

(a)

(b)

Figure 27. (a) Tensile test prepertration; (b) Specimens of BFRP bars before test.

Universal Testing Machine was used to conduct the tensile test. The tested sample fixed from the top and bottom by two steel plates as shown in the Figure 28 (a). At the middle of the bar length, an extensometer has been fixed to measure changes in the length of the bar and to measure the tensile capacity of the bar as shown in the Figure 28 (a). Load test starts in a constant rate of load speed till the failure occur as shown in the Figure 28(b).

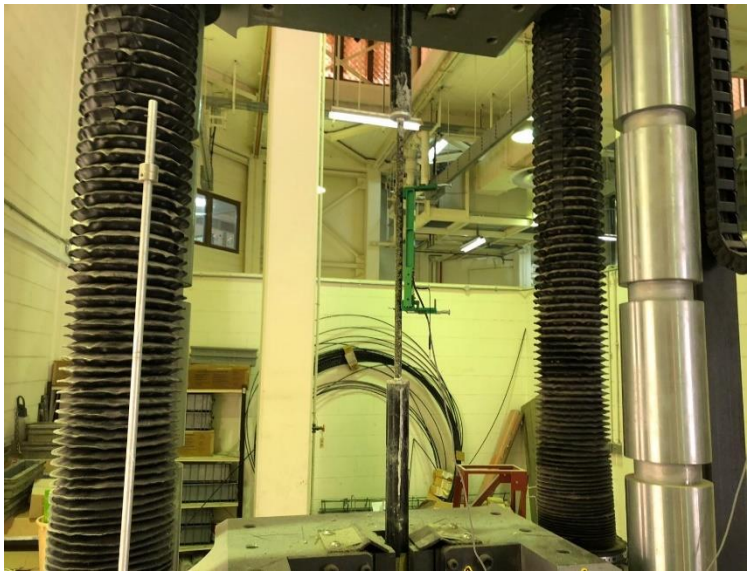

(a)

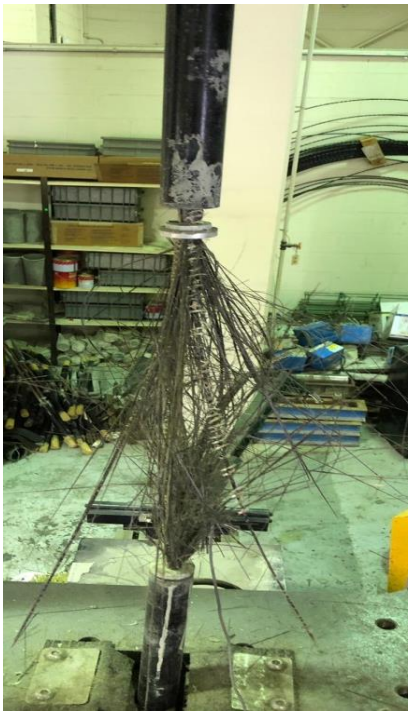

(b)

Figure 28. (a) Tensile test ; (b) Failiure of the sample.

4.4.Large- Scale Beams Results

This section will mainly be focused in presenting the behavior of the tested beams in stages starting from the condition of the beam before initiating the test till the failure occur.

4.4.1. Beam B-1 (B-ρ_1-2.5-250)

Beam B1 consists of 6Ø12 BFRP bars as flexural reinforcement and with BFRP stirrups as shear reinforcement spaced with 250 mm, span to depth ratio of the beam was 2.5. At the beginning no cracks were visible till the load reaches 41 KN, the first flexural crack was initiated specifically at the extreme tension fiber of the concrete within the zone of the constant moment. While the load was increasing more flexural cracks were propagated near the neutral axis and first crack start to widen more, it was noticed that the mid-span deflection was close to constant manner till load reaches 48 KN then it starts to increase faster as the moment of inertia start to be reduced due to cracks propagation. When the load reaches the 82 KN cracks started to be shift in the shear span, however the flexural crack started to be developed from the extreme tension fiber of the concrete beam spreading toward upward beam. As the load increasing flexural shear cracks were obvious in the span approximately equal to a beam depth from the support and the diagonal crack in the shear span begin to extend toward point load. When the load reaches around 230 KN the diagonal crack start to widen more and lower part of the crack expanded diagonally passing through the level of the main reinforcement, diagonal tension failure occurs with an angle of approximately 45° the failure occurs suddenly when the rupture of the BFRP stirrups happen where diagonal crack has been expanded as shown in the Figure 29 and 30.

As mentioned earlier that no slippage for main reinforcement occur and no

spallation of concrete at the failure stage. The maximum mid-span deflection recorded was about 35.1 mm and the maximum compressive strain for concrete was 0.002 however the maximum tensile strain for the BFRP was 0.009.

Figure 29. Beam B-1 (Diagonal tension failure).

Figure 30. Rupture of the BFRP stirrups.

4.4.2. Beam B-2 (B-ρ_1-2.5-350)

Beam B2 consist of 6Ø12 BFRP bars as flexural reinforcement and with BFRP stirrups as shear reinforcement spaced with 350 mm, shear span to depth ratio of the beam was 2.5. At the beginning, no cracks were visible till the load reaches 47 KN the first flexural crack was initiated specifically at the extreme tension fiber within the zone of the constant moment. While the load was increasing more flexural cracks were propagated slowly toward neutral axis and the first crack start to widen more, it was noticed that the mid-span deflection was close to constant manner till load reaches 56 KN then it starts to increase faster as the moment of inertia start to be reduced since more cracks propagated. When the load reaches the 94 KN cracks started to be shift in the shear span, however the flexural crack starts to be developed and it expand from the bottom portion of the beam toward compression zone at the mid-span of thee beam. As the load increasing flexural shear cracks was obvious in the span approximately equal to a beam depth from the support and the diagonal crack in the shear span begin to extend toward point load. When the load reaches around 130 KN the diagonal crack start to widen more and lower part of the crack expanded diagonally passing through the level of the main reinforcement, diagonal tension failure occurs with an angle of approximately 48° the failure occurs suddenly when the BFRP stirrups has been ruptured where diagonal crack has been expanded as shown in the Figure 31 and 32.

As mentioned earlier that no slip for main reinforcement occur and no spallation of concrete at the failure stage. The maximum mid-span deflection recorded was about 18.1 mm and the maximum compressive strain for concrete was 0.001 however the maximum tensile strain for the BFRP was 0.005.

Figure 31. B-2 Diagonal tension failure.


Figure 32. Rupture of the stirrups B-2.

4.4.3. Beam B-3 (B-ρ_1-3.5-350)

Beam B3 consist of 6Ø12 BFRP bars as flexural reinforcement and with BFRP stirrups as shear reinforcement spaced with 350 mm, shear span to depth ratio of the beam was 3.5. At the beginning no cracks were visible till the load reaches 39 KN the first flexural crack was initiated specifically at the extreme concrete tension fiber within the zone of the constant moment. While the load was increasing more flexural cracks were propagated slowly toward neutral axis. However, the first flexural crack starts to widen more. It was noticed that the mid-span deflection was close to constant

manner till load reaches 49 KN then it starts to increase faster as the moment of inertia start to be reduced since more cracks propagated. When the load reaches the 88 KN cracks started to be shift in the shear span. However, the flexural crack starts to be developed and it expand from the bottom portion of the beam toward compression zone at the mid-span of thee beam. As the load increasing flexural shear cracks was obvious in the span approximately equal to a beam depth from the support and the diagonal crack in the shear span begin to extend toward point load. When the load reaches around 105 KN the diagonal crack starts to widen more and lower part of the crack expanded diagonally passing through the level of the main reinforcement, diagonal tension failure occurs with an angle of approximately 45° the failure occurs where diagonal crack has been expanded as shown in the Figure 33.

As mentioned earlier that no slip for main reinforcement occur and no spallation of concrete at the failure stage. The maximum mid-span deflection recorded was about 20.26 mm and the maximum compressive strain for concrete was 0.0017 however the maximum tensile strain for the BFRP was 0.0075.

Figure 33. Beam B-3 Diagonal tension failure.

4.4.4. Beam B-4 (B-ρ_1-3.5-250)

Beam B4 consist of 6Ø12 BFRP bars as flexural reinforcement and with BFRP stirrups as shear reinforcement spaced with 250 mm, shear span to depth ratio of the beam was 3.5. At the beginning no cracks were visible till the load reaches 34 KN them first flexural crack was initiated specifically at the extreme tension fiber within the zone of the constant moment. While the load was increasing more flexural cracks were propagated slowly toward neutral axis however the first flexural crack starts to widen more, it was noticed that the mid-span deflection was close to constant manner till load reaches 45 KN then it starts to increase faster as the moment of inertia start to be reduced since more cracks propagated. When the load reaches the 80 KN cracks started to be shift in the shear span, however the flexural crack starts to be developed and it expand from the tension fiber of the concrete beam toward compression zone at the mid-span of thee beam. As the load was increasing flexural shear cracks was obvious in the span approximately equal to a beam depth from the support and the diagonal crack in the shear span begin to extend toward point load. When the load reaches around 179.7 KN more flexural shear crack start to propagate faster. Then the diagonal crack start to widen more and lower part of the crack expanded diagonally passing through the level of the main reinforcement. While in unloading process were in progress the beam experienced crushing of concrete from the top near to the point load and also in the diagonal crack zone. Shear compression failure occurs with an angle of approximately 40° the failure occurs suddenly when the BFRP stirrups has been ruptured where diagonal crack has been expanded as shown in the Figure 34 & 35.

As mentioned earlier that no spallation of concrete at the failure stage. The maximum mid-span deflection recorded was about 34 mm and the maximum

compressive strain for concrete was 0.003 however the maximum tensile strain for the BFRP was 0.012.

Figure 34. Beam B-4 Shear compression failure.

Figure 35. Rupture of the stirrups B-4.

4.4.5. Beam B-5 (B-ρ_2-3.5-250)

Beam B5 consists of 5Ø16 BFRP bars as flexural reinforcement and with BFRP stirrups as shear reinforcement spaced with 250 mm. The shear span to depth ratio of the beam was 3. At the beginning of the test there were no cracks visible till the load reaches 38 KN. After a while the first flexural crack was initiated specifically at the extreme tension fiber within the zone of the constant moment. While the load was increasing more flexural cracks near to the first crack were propagated slowly toward neutral axis however the first flexural crack starts to widen more, it was noticed that the mid-span deflection was close to constant manner till load reaches 48 KN then it starts to increase faster as the moment of inertia start to be reduced since more cracks propagated. When the load reaches the 110 KN cracks started to be shifted in the shear span, however the flexural crack starts to expand from the tension fiber of the concrete beam toward compression zone at the mid-span of thee beam. As the load was increasing a diagonal crack starts to become visible in the span equal to a beam depth from the support. This crack starts to expand towards the point load and downward towards the bottom of the flexural reinforcement. When the load reaches around 185.3 KN beam starts to displace downward dramatically. Then the load starts to decrease gradually while the crushing in the concrete happen near the point load and the diagonal crack has been expanded below the point load and the failure occur. Diagonal tension failure occurs with an angle of approximately 38°. as shown in the Figure 36 & 37.

Although it was noticed that there was no spallation of concrete occur at the failure stage. The maximum mid-span deflection recorded was about 28.2 mm and the maximum compressive strain for concrete was 0.0027 however the maximum tensile strain for the BFRP was 0.008.

Figure 36. Beam B-5 Shear Compression failure.

Figure 37. Shear Compression failure.

4.4.6. Beam B-6 (B-ρ_2-2.5-250)

Beam B6 consist of 5Ø16 BFRP bars as flexural reinforcement and with BFRP stirrups as shear reinforcement spaced with 250 mm, shear span to depth ratio of the beam was 2.5. At the beginning of the test there were no cracks visible till the load reaches 54 KN. After a while the first flexural crack was initiated specifically at the extreme tension fiber within the zone of the constant moment. While the load was increasing more flexural cracks near to the first crack were propagated toward neutral axis. However, the first flexural crack starts to widen more. It was noticed that the mid-span deflection was close to constant manner till load reaches 59 KN it starts to

increase faster as the moment of inertia start to be reduced due to more cracks propagation. When the load reaches the 86 KN cracks started to be shifted in the shear span, however the flexural crack starts to expand from the tension fiber of the concrete beam toward compression zone at the mid-span of thee beam. As the load was increasing flexural shear cracks was visible in the span approximately equal to a beam depth from the support and the diagonal crack in the shear span begin to extend toward point load. When the load reaches around 230.4 KN more flexural shear cracks start to propagate faster however the diagonal crack start to widen more and lower portion of the crack expanded diagonally passing through the level of the main reinforcement, diagonal tension failure occurs with an angle of approximately 35°. The load reaches 247 KN then the load starts to decrease gradually when the diagonal crack has been expanded and widened then failure happen as shown in the Figure 38.

As mentioned earlier that no slip for main reinforcement happen during the test and no spallation of concrete occur at the failure stage. The maximum mid-span deflection recorded was about 28 mm and the maximum compressive strain for concrete was 0.0026 however the maximum tensile strain for the BFRP was 0.007.

Figure 38. Beam B-6 Diagonal tension failure.

4.4.7. Beam B-7 (B-ρ_2-2.5-350)

Beam B7 consists of 5Ø16 BFRP bars as flexural reinforcement and with BFRP stirrups as shear reinforcement spaced with 350 mm, shear span to depth ratio of the beam was 2.5. At the beginning of the test there were no cracks visible till the load reaches 45 KN. After a while the first flexural crack was initiated specifically at the extreme tension fiber within the zone of the constant moment. While the load was increasing more flexural cracks near to the first crack were propagated slowly toward neutral axis however the first flexural crack starts to widen more, it was noticed that the mid-span deflection was close to constant manner till load reaches 55 KN then it starts to increase faster as the moment of inertia start to be reduced since more cracks propagated. When the load reaches the 63 KN cracks started to be shifted in the shear span. However, the flexural crack starts to expand from the tension fiber of the concrete beam toward compression zone at the mid-span of the beam. As the load was increasing flexural shear cracks was visible in the span approximately equal to a beam depth from the support. The diagonal crack in the shear span begin to extend toward point load. When the load reaches around 97 KN more flexural shear cracks start to propagate faster. However, the diagonal crack start to widen more and lower portion of the crack expanded diagonally passing through the level of the main reinforcement, diagonal tension failure occurs with an angle of approximately 43°. The load reaches 175 KN then the load starts to decrease gradually, and the diagonal crack has been expanded and widened then crack occur as shown in the Figure 39.

As mentioned earlier that no slippage for main reinforcement happen during the test and no spallation of concrete occur at the failure stage. The maximum recorded mid-span deflection was about 19 mm and the maximum compressive strain for concrete was 0.0016 however the maximum tensile strain for the BFRP was 0.006.

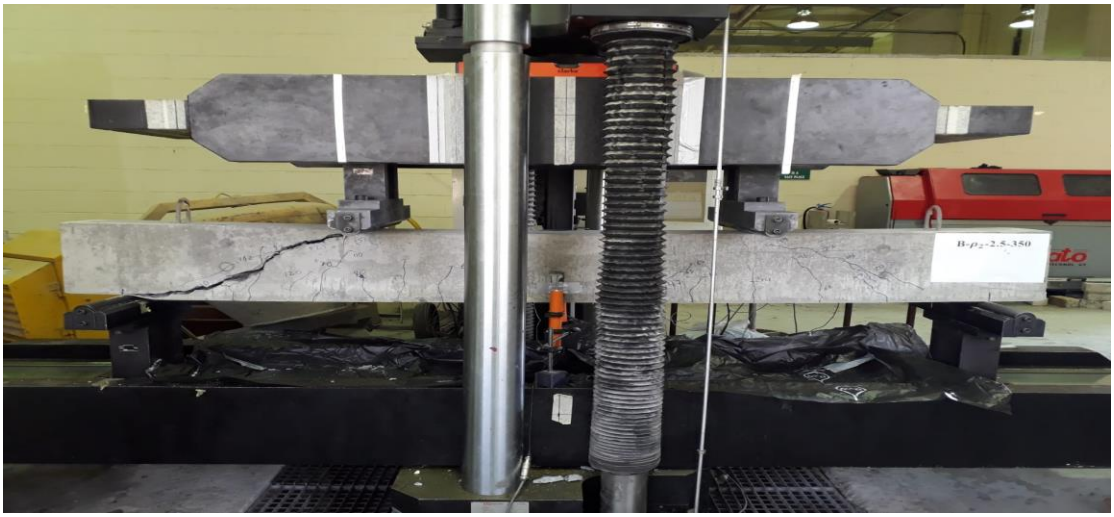

Figure 39. Beam B-7 Diagonal tension failure.

4.4.8. Beam B-8 (B-ρ_2-3.5-350)

Beam B8 consist of 5Ø16 BFRP bars as flexural reinforcement and with BFRP stirrups as shear reinforcement spaced with 350 mm, shear span to depth ratio of the beam was 3.5. At the beginning no cracks were visible till the load reaches 27 KN them first flexural crack was initiated specifically at the extreme tension fiber within the zone of the constant moment. While the load was increasing more flexural cracks were propagated slowly toward neutral axis however the first flexural crack starts to widen more, it was noticed that the mid-span deflection was close to constant manner till load reaches 47 KN it starts to increase faster as the moment of inertia start to be reduced since more cracks propagated. When the load reaches the 72 KN cracks started to be shift in the shear span, however the flexural crack starts to be developed and it expand from the tension fiber of the concrete beam toward compression zone at the mid-span of thee beam. As the load was increasing flexural shear cracks was obvious in the span approximately equal to a beam depth from the support and the

diagonal crack in the shear span begin to extend toward point load. When the load reaches around 130.5 KN more flexural shear crack start to propagate faster than the diagonal crack. Lower part of the crack expanded diagonally passing through the level of the main reinforcement. Diagonal tension failure occurs with an angle of approximately 45° the failure occurs suddenly when the BFRP stirrups has been ruptured where diagonal crack has been expanded as shown in the Figure 40 & 41. As mentioned earlier that no slip for main reinforcement occur and no spallation of concrete at the failure stage. The maximum mid-span deflection recorded was about 20 mm and the maximum compressive strain for concrete was 0.0017 however the maximum tensile strain for the BFRP was 0.005.

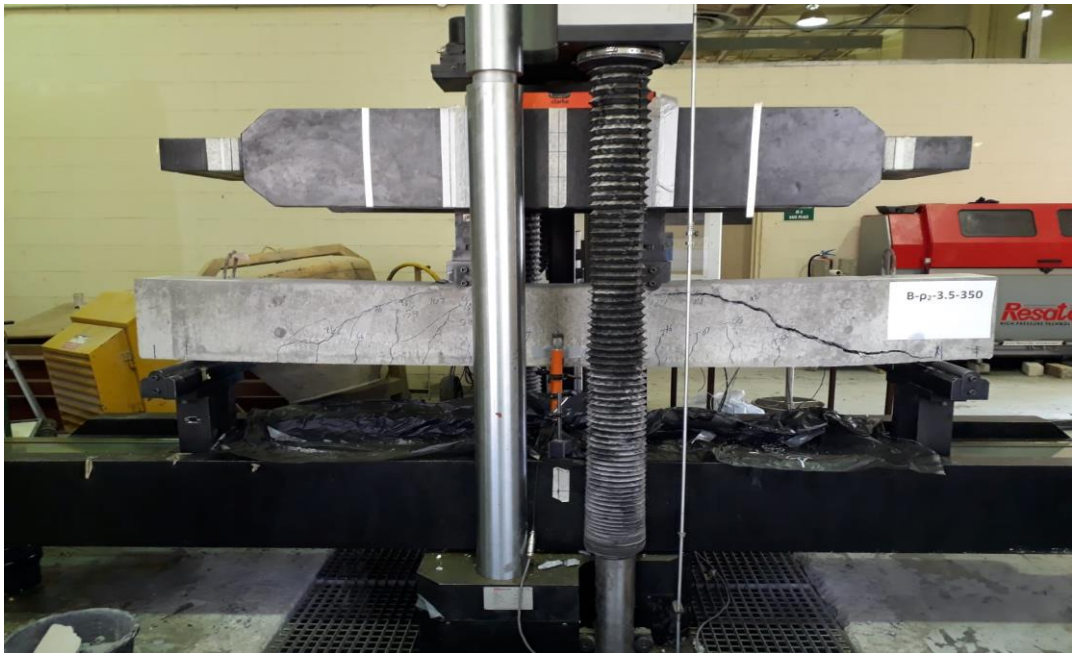

Figure 40. Beam B-8 Diagonal tension failure.

Figure 41. Rupture of the stirrups B-8.

4.4.9. Beam B-9 (S-ρ_1-2.5-250)

Beam B9 consist of 6Ø12 BFRP bars as flexural reinforcement and with Steel stirrups as shear reinforcement spaced with 250 mm, shear span to depth ratio of the beam was 2.5. At the beginning of the test there were no cracks visible till the load reaches 28 KN. After a while the first flexural crack was initiated specifically at the extreme tension fiber within the zone of the constant moment. While the load was increasing more flexural cracks near to the first crack were propagated slowly toward neutral axis however the first flexural crack starts to widen more, it was noticed that the mid-span deflection was close to constant manner till load reaches between the range of 28 and 34 KN it starts to increase faster as the moment of inertia start to be reduced since more cracks propagated. When the load reaches the 93 KN cracks started to be shifted in the shear span, however the flexural crack starts to expand

from the tension fiber of the concrete beam toward compression zone at the mid-span of thee beam. As the load was increasing a diagonal crack starts to be visible in the span of the compression zone this crack starts to expand with some adjacent cracks starts to expand towards the point load and downward towards the bottom of the flexural reinforcement level. When the load reaches around 284 KN beam starts to displace downward dramatically then the load starts to decrease gradually while the crushing in the concrete happen at the compression zone and one flexural widened crack was visible before failure as shown in the Figure 42.

Although it was noticed that there was no slip for main reinforcement happen during the test and no spallation of concrete occur at the failure stage. The maximum mid-span deflection recorded was about 39 mm and the maximum compressive strain for concrete was 0.0027 however the maximum tensile strain for the BFRP was 0.012.

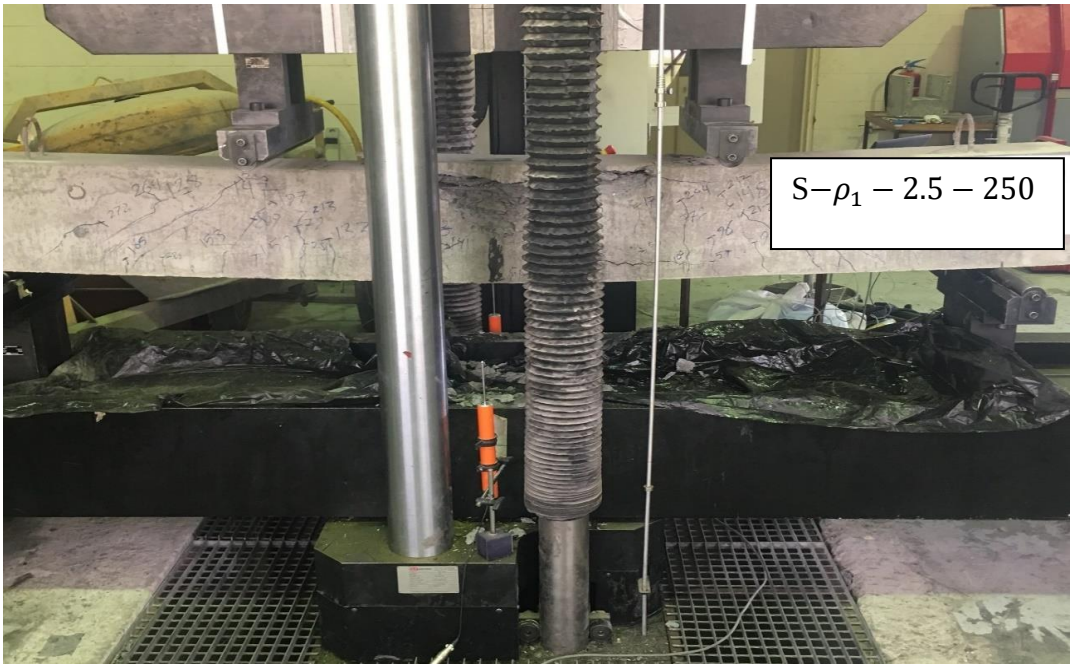

Figure 42. compression flexural failiure B-9.

4.4.10. Beam B-10 (S-ρ_1-2.5-350)

Beam B10 consist of 6Ø12 BFRP bars as flexural reinforcement and with Steel stirrups as shear reinforcement spaced with 350 mm, shear span to depth ratio of the beam was 2.5. At the beginning of the test there were no cracks visible till the load reaches 52 KN. After a while the first flexural crack was initiated specifically at the extreme tension fiber within the zone of the constant moment. While the load was increasing more flexural cracks near to the first crack were propagated slowly toward neutral axis however the first flexural crack starts to widen more, it was noticed that the mid-span deflection was close to constant manner till load reaches 58 KN then it starts to increase faster as the moment of inertia start to be reduced since more cracks propagated. When the load reaches the 77 KN cracks started to be shifted in the shear span, however the flexural crack starts to expand from the tension fiber of the concrete beam toward compression zone at the mid-span of thee beam. As the load was increasing flexural shear cracks was visible in the span approximately equal to a beam depth from the support and the diagonal crack in the shear span begin to extend toward point load. When the load reaches around 180.6 KN more flexural shear cracks start to propagate faster however the diagonal crack start to widen more and lower portion of the crack expanded diagonally passing through the level of the main reinforcement, diagonal tension failure occurs with an angle of approximately 45°. The load reaches 180 KN then the load starts to decrease gradually, and the diagonal crack has been expanded and widened then crack occur as shown in the Figure 43 & 44.

As mentioned earlier that no slip for main reinforcement happen during the test and no spallation of concrete occur at the failure stage and no rupture for the steel stirrups during the failure. The maximum mid-span deflection recorded was about 20

mm and the maximum compressive strain for concrete was 0.0015 however the maximum tensile strain for the BFRP was 0.006.

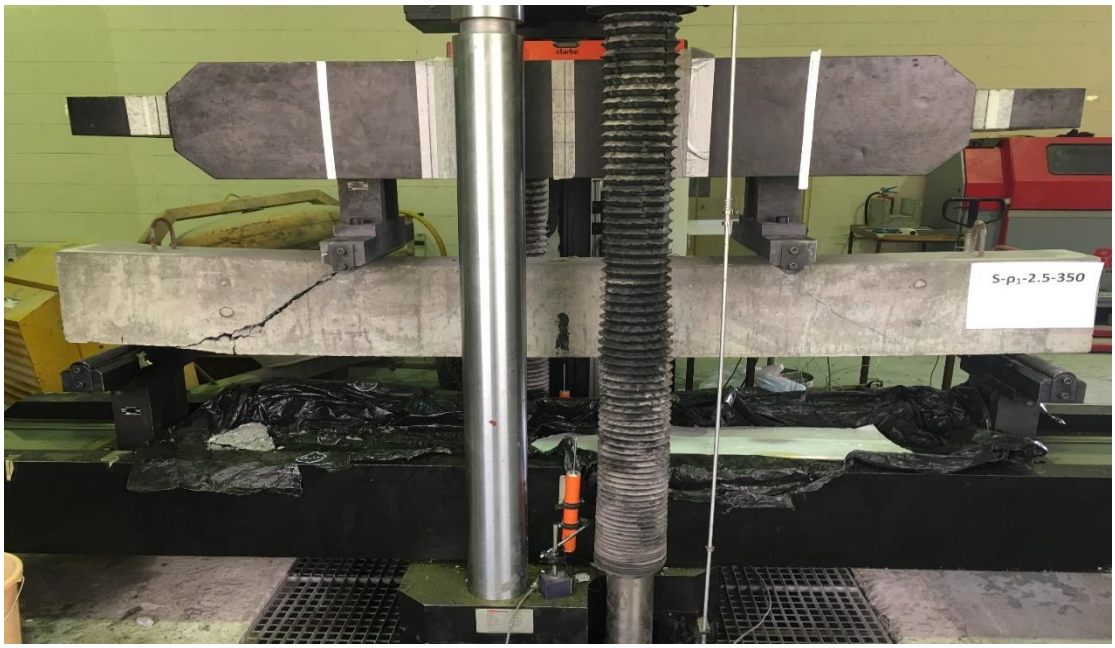

Figure 43. Beam B-10 Diagonal tension failure.

Figure 44. Steel stirrups after failiure.

4.4.11. Beam B-11 (S-ρ_2-2.5-250)

Beam B11 consist of 5Ø16 BFRP bars as flexural reinforcement and with Steel stirrups as shear reinforcement spaced with 250 mm, shear span to depth ratio of the beam was 2.5. At the beginning of the test there were no cracks visible till the load reaches 44 KN. After a while the first flexural crack was initiated specifically at the extreme tension fiber within the zone of the constant moment. While the load was increasing more flexural cracks near to the first crack were propagated slowly toward neutral axis however the first flexural crack starts to widen more, it was noticed that the mid-span deflection was close to constant manner till load reaches 54 KN then it starts to increase faster as the moment of inertia start to be reduced since more cracks propagated. When the load reaches the 98 KN cracks started to be shifted in the shear span, however the flexural crack starts to expand from the tension fiber of the concrete beam toward compression zone at the mid-span of thee beam. As the load was increasing a diagonal crack starts to be visible in the span approximately equal to a beam depth from the support this crack starts to expand with some adjacent cracks starts to expand towards the point load and downward towards the bottom of the flexural reinforcement level. When the load reaches to around 284 KN, the beam starts to displace downward dramatically. Due to this, the load starts to decrease gradually while the crushing in the concrete happen near the point load. The diagonal crack has been expanded below the point. While unloading process, the concrete near to the crack starts to crush and fall. Shear compression failure occurs with an angle of approximately 38°. as shown in the Figure 45 & 46.

Although it was noticed that there was no slip for main reinforcement happen during the test and no spallation of concrete occur at the failure stage. The maximum mid-span deflection recorded was about 32 mm and the maximum compressive strain

for concrete was 0.0027 however the maximum tensile strain for the BFRP was 0.0083.

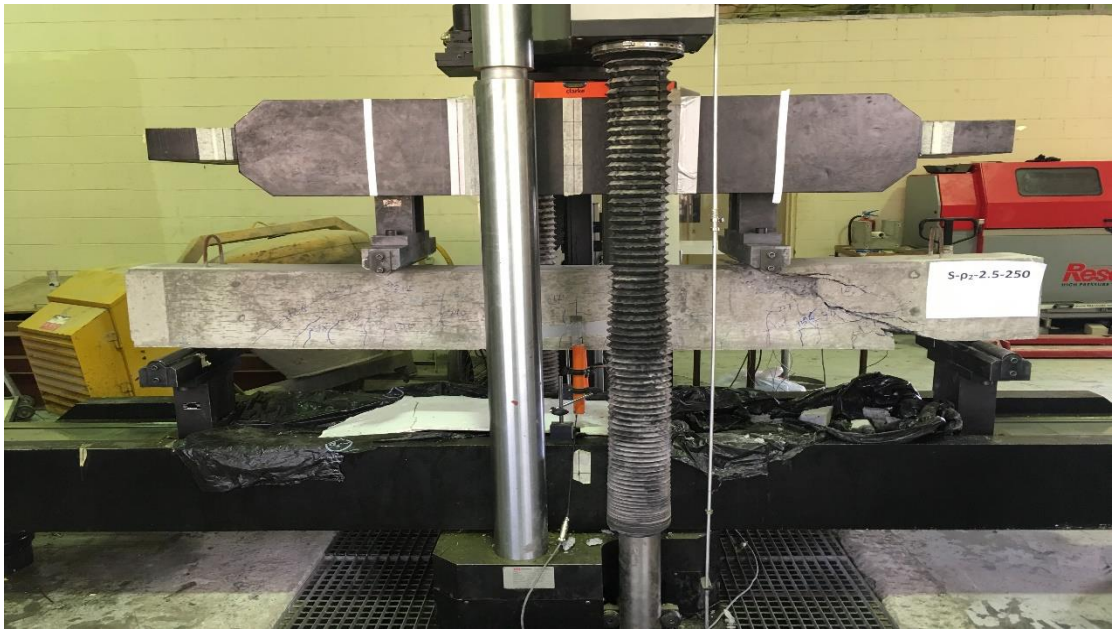

Figure 45. Beam B-11 Shear compression failure.

Figure 46. Crushing of the concrete located at the diagonal crack.

4.4.12. Beam B-12 (NS-ρ_2-3.5)

Beam B12 consist of 5Ø16 BFRP bars as flexural reinforcement and without stirrups. Which means that the beam has no shear reinforcement in order to test the contribution of the green concrete with shear resistance. The shear span to depth ratio of the beam was 3.5. At the beginning of the test there were no cracks visible till the load reaches 40 KN. After a while the first flexural crack was initiated specifically at the extreme tension fiber within the zone of the constant moment. While the load was increasing more flexural cracks near to the first crack were propagated slowly toward neutral axis however the first flexural crack starts to widen more, it was noticed that the mid-span deflection was close to constant manner till load reaches 48 KN then it starts to increase faster as the moment of inertia start to be reduced since more cracks propagated. When the load reaches the 93 KN cracks started to be shifted in the shear span, however the flexural crack starts to expand from the tension fiber of the concrete beam toward compression zone at the mid-span of thee beam. As the load was increasing a diagonal crack starts to be visible in the span approximately equal to a beam depth from the support this crack starts to expand and widened with some adjacent cracks starts to expand towards the point load and downward towards the flexural reinforcement level. When the load reaches around 109.4 KN beam starts to displace downward dramatically then the load starts to decrease gradually as the failure occurs. Shear tension failure occurs with an angle of approximately 40°. as shown in Figure 47 & 48.

Although it was noticed that there was no spallation of concrete occur at the failure stage. The maximum mid-span deflection recorded was about 13 mm and the maximum compressive strain for concrete was 0.0013 however the maximum tensile strain for the BFRP was 0.004.

Figure 47. Beam B-12 Shear tension failure.

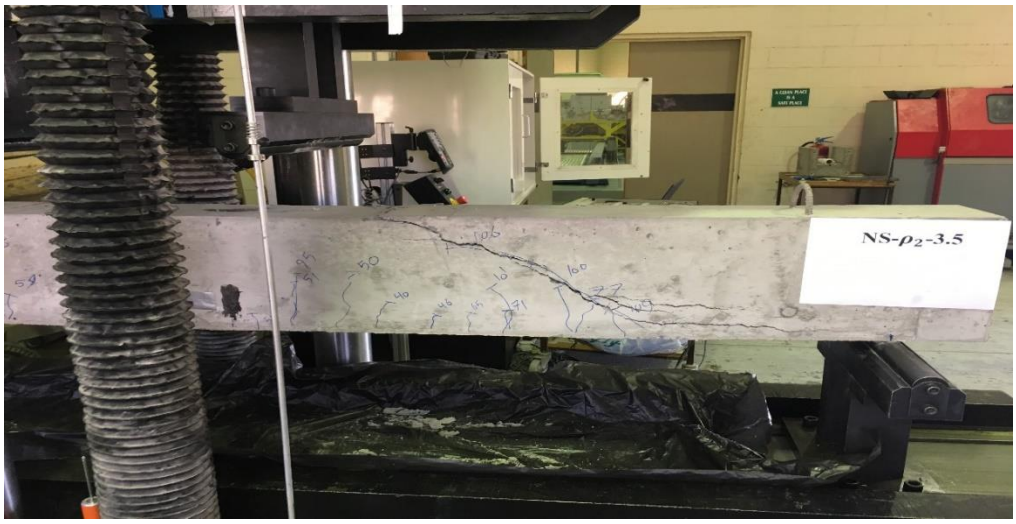

Figure 48. Shear tension failure.

4.4.13. Beam B-13 (NS-ρ_2-2.5)

Beam B13 consist of 5Ø16 BFRP bars as flexural reinforcement and without stirrups which means that the beam has no shear reinforcement in order to test the contribution of the green concrete with shear resistance, shear span to depth ratio of the beam was 2.5. At the beginning of the test there were no cracks visible till the load reaches 44 KN. After a while the first flexural crack was initiated specifically at the

extreme tension fiber within the zone of the constant moment. While the load was increasing more flexural cracks near to the first crack were propagated slowly toward neutral axis however the first flexural crack starts to widen more. It was noticed that the mid-span deflection was close to constant manner till load reaches 52 KN then it starts to increase faster as the moment of inertia start to be reduced since more cracks propagated. When the load reaches the 78 KN cracks started to be shifted in the shear span, however the flexural crack starts to expand from the tension fiber of the concrete beam toward compression zone at the mid-span of thee beam. As the load was increasing a diagonal crack starts to be visible in the span approximately equal to a beam depth from the support this crack starts to expand and widened with some adjacent cracks starts to expand towards the point load and downward towards the bottom of the flexural reinforcement level. When the load reaches around 176.7 KN beam starts to displace downward dramatically then the load starts to decrease gradually as the failure occurs. Diagonal tension failure occurs with an angle of approximately 48°. as shown in the Figure 49.

Although it was noticed that there was no slippage for main reinforcement and no spallation of concrete occur at the failure stage. The maximum mid-span deflection recorded was about 17 mm and the maximum compressive strain in concrete was 0.0017 however the maximum tensile strain in the BFRP was 0.0045.

Figure 49. Beam B-13 Diagonal tension failure.

4.4.14. Beam B-14 (NS-ρ_1-2.5)

Beam B14 consist of 6Ø12 BFRP bars as flexural reinforcement and without stirrups which means that the beam was not shear reinforced in order to test the contribution of the green concrete with shear resistance. The shear span to depth ratio of the beam was 2.5. At the beginning of the test there were no cracks visible till the load reaches 40 KN. After a while the first flexural crack was initiated specifically at the extreme tension fiber within the zone of the constant moment. While the load was increasing more flexural cracks near to the first crack were propagated slowly toward neutral axis however the first flexural crack starts to widen more, it was noticed that the mid-span deflection was close to constant manner till load reaches 59 KN then it starts to increase faster as the moment of inertia start to be reduced since more cracks propagated. When the load reaches the 97 KN cracks started to be shifted in the shear span, however the flexural crack starts to expand from the tension fiber of the concrete beam toward compression zone at the mid-span of thee beam. As the load was increasing a diagonal crack starts to be visible in the span approximately equal to a beam depth from the support this crack starts to expand and widened with some adjacent cracks starts to expand towards the point load and downward towards the

bottom of the flexural reinforcement level. When the load reaches around 122 KN beam starts to displace downward dramatically then the load starts to decrease gradually as the failure occurs. Diagonal tension failure occurs with an angle of approximately 45°. as shown in the Figure 50.

Although it was noticed that there was no slip for main reinforcement happen during the test and no spallation of concrete occur at the failure stage. The maximum mid-span deflection recorded was about 11 mm and the maximum compressive strain for concrete was 0.0041 however the maximum tensile strain for the BFRP was 0.004.

Figure 50. Beam B-14 Diagonal tension failure.

4.5.Discussion of test results

This section will discuss in detail the test results mentioned above, Table.6 summarizes the test results showing the beam designation, maximum corresponding load at failure, max deflection at the mid-span, max strain for the flexural BFRP bars and concrete for each beam at the failure stage. In addition, it shows the cracking moment and the failure type for the tested beams.

As shown in the results earlier that most of the mode failures for the beams reinforced with BFRP stirrups were shear diagonal tension failure except Beam No.5 and Beam No.4 which has experienced a shear compression failure. That is due to the confinement of the BFRP stirrups which was spaced by a 250 mm. Which helped in preventing the beam from the longitudinal splitting, thus the struts were subjected to high compressive stress and a lateral expansion at the compression field located between the support and the point load. This resulted in a failure of lap splice specifically at the zone of the stirrups bent which lead to beam failure. In addition, both beams also experienced concrete crushing at the flexural compression area near to the point loads. However, there were different cases for the control beams reinforced with steel stirrups. Beam No.9 which reinforced with steel stirrups at 250 mm has experienced a flexural compression failure and by comparing Beam-9 failure with Beam-10 which experienced a shear diagonal tension failure having the same reinforcement ratio, with same span to depth ratio and also reinforced with steel stirrups. It was noticed that such failure is normal due to the different spacing of the steel stirrups for Beam No.9 compared with Beam No.10 of 250 mm spacing stirrups helped in preventing the beam from the longitudinal splitting, thus the struts were subjected to high compressive stress and there was a high resistance form the stirrups which lead to the flexural compression failure due to the low of the top longitudinal

reinforcement for the beam. For the beams which was not reinforced with any of stirrups by comparing beam No.12 and 13 which have the same reinforcement ratio and different span to depth ratio. It was noticed that beams which have 2.5 span to depth ratio was experienced a shear diagonal tension failure and beams which have a span to depth ratio of 3.5 exhibited to shear tension failure which caused loss of the bond between the reinforcement and concrete which will help the main reinforcement to slip that will result anchorage failure. Detailed comparison between various variables studied is shown in Table.6. To sum up, five beams have been failed due to the FRP stirrups rupture. One beam which was reinforced with a steel stirrup failed due to the shear compression failure. The rest of beams failure will be discussed in detail below. Generally, most of the beams failed under the shear force was in diagonal shear failure mode. It was noticed that during the test that no slip condition of the flexural reinforcement has been found.

Table 6 Summery of test results

Beam No.	Beam designation	Max load P (KN)	Max ε FRP	Max ε concrete	Mcr (KN.m)	Failure type
B-1	B-ρ1-2.5-250	230	0.0086	0.002	41	Diagonal tension
B-2	B-ρ1-2.5-350	130	0.0053	0.001	47	Diagonal tension
B-3	B-ρ1-3.5-350	105	0.0075	0.0017	45	Diagonal tension
B-4	B-ρ1-3.5-250	179.2	0.012	0.0034	34	Shear comp
B-5	B-ρ2-3.5-250	185.3	0.008	0.0027	38	Shear comp
B-6	B-ρ2-2.5-250	230.4	0.0074	0.0026	54	Diagonal tension
B-7	B-ρ2-2.5-350	175	0.006	0.0016	45	Diagonal tension
B-8	B-ρ2-3.5-350	130	0.005	0.0017	27	Diagonal tension
B-9	S-ρ1-2.5-250	284	0.012	0.00275	51	Flexural-compression
B-10	S-ρ1-2.5-350	180.6	0.0062	0.00145	59	Diagonal tension
B-11	S-ρ2-2.5-250	284	0.0083	0.0027	58	Shear comp
B-12	NS-ρ2-3.5	109.4	0.004	0.0013	40	shear tension
B-13	NS-ρ2-2.5	176.7	0.0045	0.0017	43	Diagonal tension
B-14	NS-ρ1-2.5	122	0.0041	0.00135	49	Diagonal tension

4.6.Effect of stirrup type

In nature stirrups is main element to resist the shear force in the concrete beams. It gives adequate advance warning before failure occurs. Also, it prevents the brittle failure of the concrete beams. Thus, using stirrups is very important in order to ensure that the concrete beam will develop the full flexural capacity. As mentioned earlier that the stirrups are enhancing the stiffness of the beam by the following factors:

1. Enhancement of the contribution of dowel action.
2. Provide confinement for the cross-section when the spacing of the stirrups is close. Which will improve the compressive strength of the concrete. Also, it helps in preventing of the arch action at the zones, which is affected by it.
3. Controlling the crack width of the shear diagonal cracks also it preserves contribution, which is provided by aggregate interlock.
4. Prevention of the splitting cracks which developed by the dowel force at the anchorage zones.

Comparison between BFRP and Steel stirrups

In this study there were 8 beams reinforced with BFRP stirrups, 3 with steel stirrups and 3 without stirrups. The results show that beams reinforced with steel stirrups owning a highest shear force before failure and deflection capacity. However, there was a little difference between the beams reinforced with steel stirrups and BFRP stirrups. Where the difference on the stiffness is between 15 to 20%. It has been noticed that a wider crack has experienced by the beams reinforced with BFRP stirrups compared with reinforced steel stirrups. That is due to the low elastic modulus

of the BFRP stirrups compared to steel stirrups. This result was done as per the comparison between B-1 and B-9, B-2 and B-10, and B-6 and B-11 respectively. There was a difference in the failure modes of beams. B-1 and B-2 experienced a diagonal tension failure due to the rupture of the BFRP stirrups at the bent zone due to the high compressive stress at the struts. However, B-9 exhibit compression failure and as mentioned earlier, that is due to 250 mm spacing stirrups which helped in preventing the beam from the longitudinal splitting. Thus, the struts were subjected to high compressive stress and there was a high resistance formed in the stirrups that lead to the flexural compression failure due to the low of the top longitudinal reinforcement for the beam. B-11 has another mode of failure which was shear compression failure and that is due to the crush of the concrete beam near to the point load above the diagonal crack. There was no difference in failure between B-6 and B-10.

Comparison between BFRP stirrups and without stirrups

Results show that beams without shear stirrups with a span to depth ratio of 3.5 exhibited shear tension failure, as B-12 failure and that can be explained simply when the diagonal crack approaches the flexural reinforcement level, the BFRB bars starts to slip from the concrete. Although, comparing B-12 with B-5 and B-4 that has same criteria of reinforcements and span to depth ratio, it was noticed that B-5 and B-4 experienced a shear compression failure. This can be illustrated due to the confinement of the BFRP stirrups with spacing of 250 mm that helped in preventing the beam from the longitudinal splitting. Thus, the struts were subjected to high compressive stress. However lateral expansion at the compression field located between the support and the point load resulted in a failure of lap splice at the zone of

the stirrups bent that led to beam failure. However, there were no differences in failure modes for the rest of the no-stirrups beams compared with BFRP ones by comparing B-1 with B-14 and B-2 with B-14. It was observed that beams reinforced with BFRP stirrups have a higher shear force and higher deflection capacity by approximately 54 to 70 %, no-stirrups beams mean that the green concrete can resist almost 30 % of the shear capacity of the beams. Also, it was noticed that beams reinforced with BFRP stirrups have higher strain of the flexural reinforcement as shown in the Figure 51.

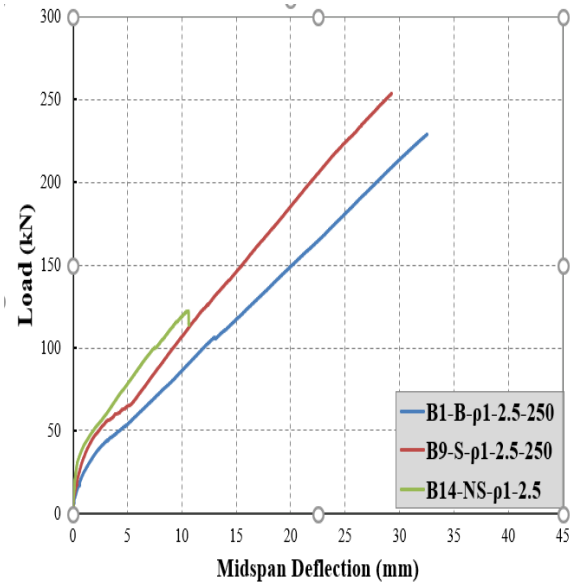

(a) B-1 vs B-9 vs B-14

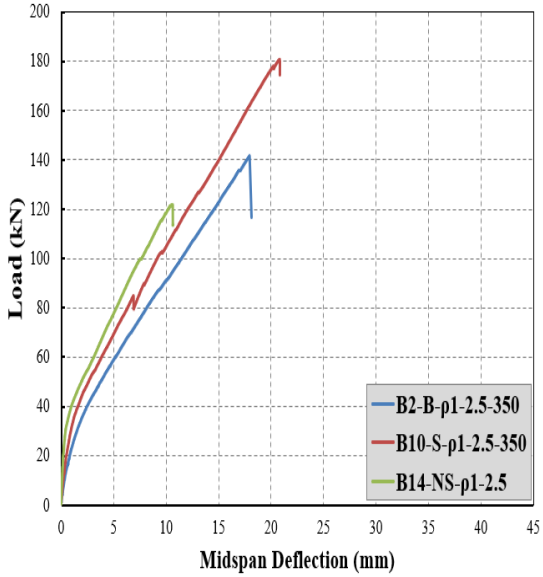

(b) B-2 vs B-10 vs B-14

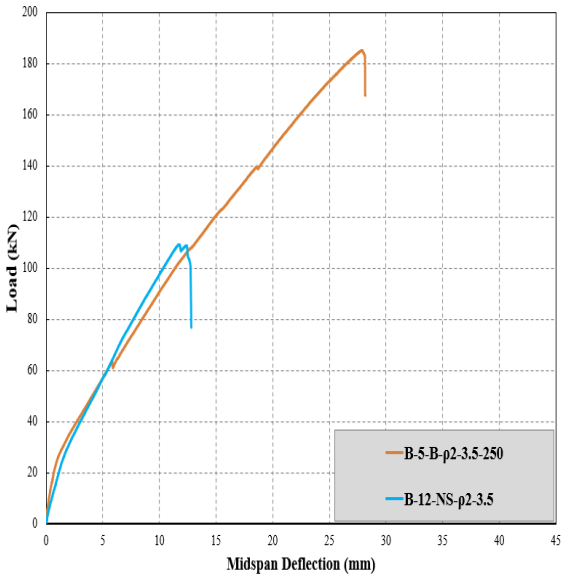

(c) B-5 vs B-12

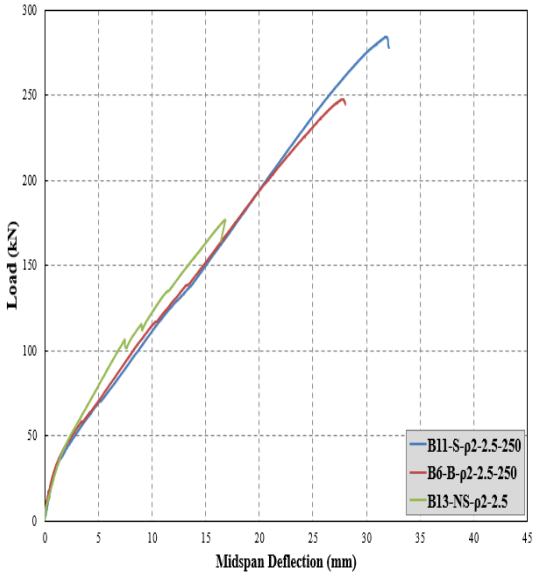

(d) B-11 vs B-6 vs. B-13

Figure 51. Load vs load displacment diagrams for identical beams with different type of stirrups, some without stirrups.

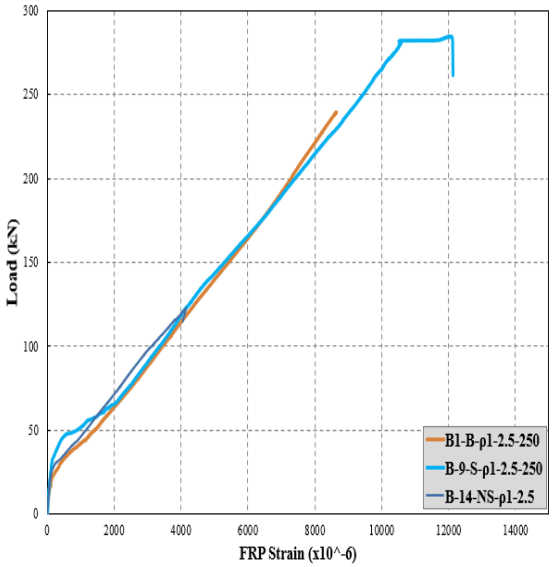

(a) B-1 vs B-9 vs B-14

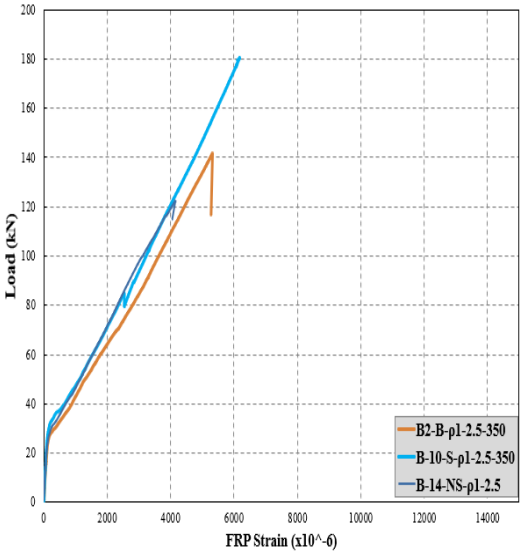

(b) B-2 vs B-10 vs B-14

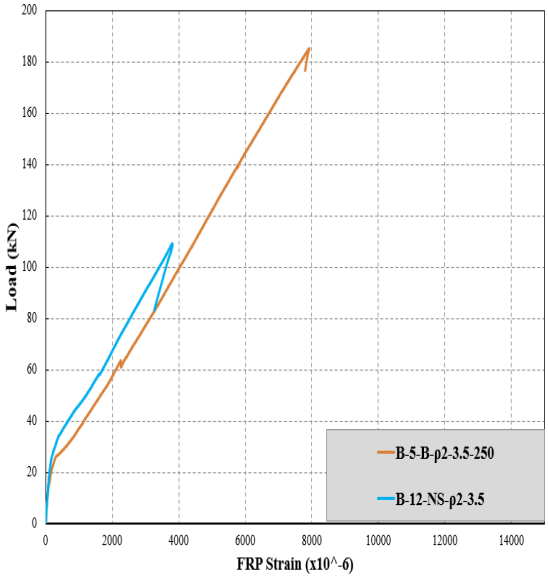

(c) B-5 vs B-12

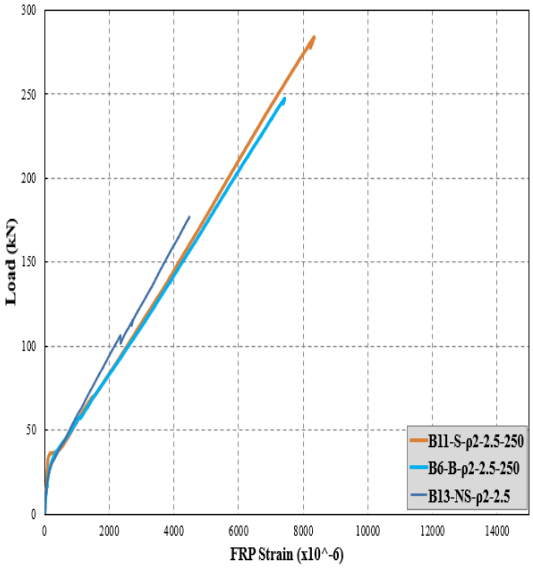

(d) B-11 vs B-6 vs B-13

Figure 52. Load vs longitudinal FRP strain diagrams for identical beams with different type of stirrups, some without stirrups.

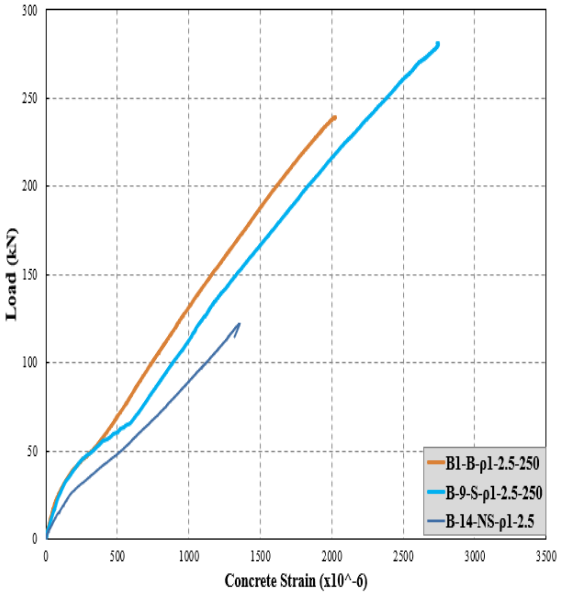

(a) B-1 vs B-9 vs B-14

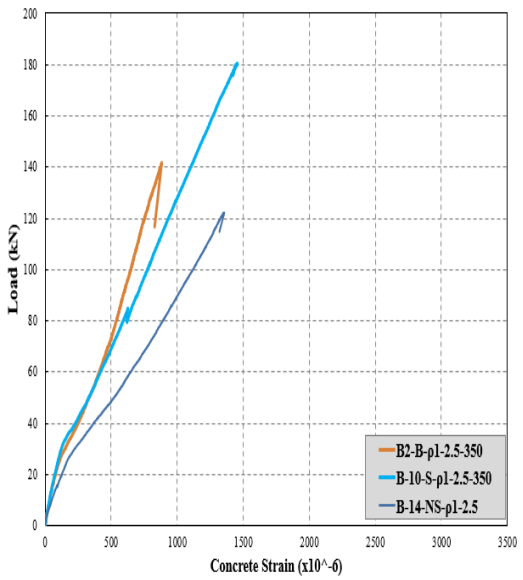

(b) B-2 vs B-10 vs B-14

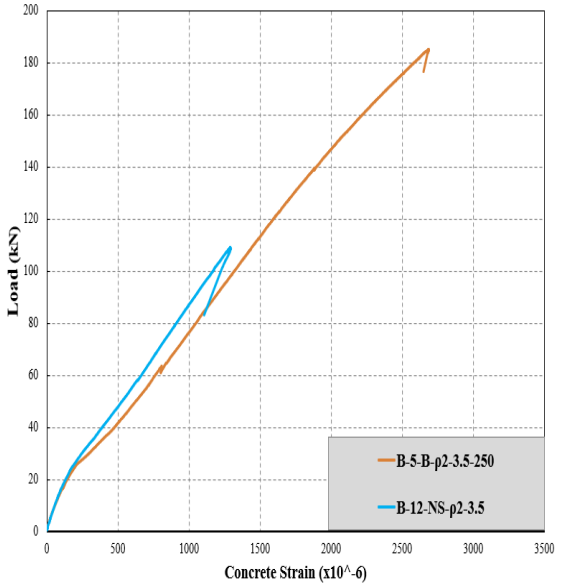

(c) B-5 vs B-12

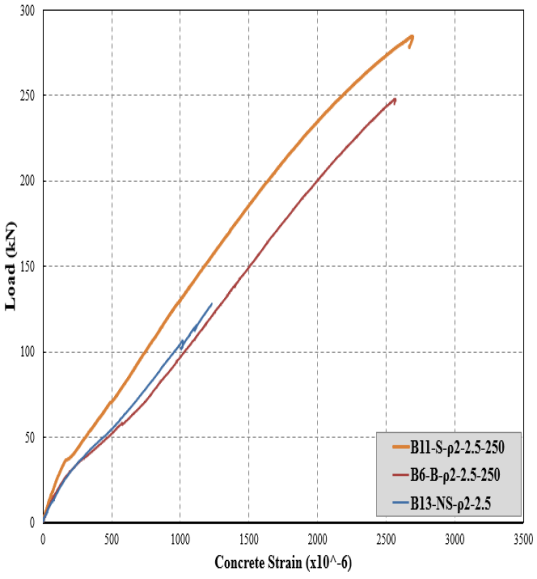

(d) B-11 vs B-6 vs. B-13

Figure 53. Load vs Concrete strain diagrams for identical beams with different type of stirrups , some without stirrups.

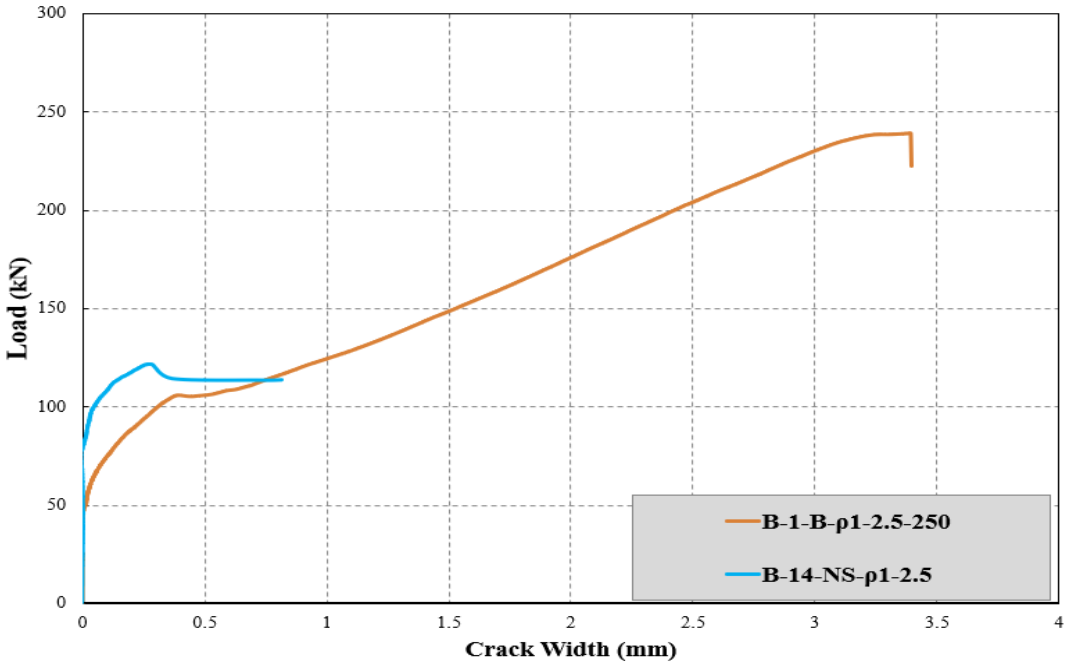

(a) B-1 vs B-14

Figure 54. Load vs crack width diagrams for identical beams with different type of stirrups , some without stirrups.

4.7.Effect of the Spacing

Test results show that there was an enhancement in the shear strength while minimizing the spacing between stirrups. By comparing B-1 which has a spacing of 250 mm and B-2 with spacing of 350 mm, B-1 shows a high resistance of ultimate load and owning high mid-span deflection capacity by about 40% and 48% respectively, as shown in Figure 55. However, it has been noticed that the difference of percentage in load vs. longitudinal FRP strain found between B-3 compared with B-4, B-5 with B-8, B-6 with B-7 and B-9 with B-10 are almost the same.

As mentioned earlier, B-5 experienced a shear compression failure due to the wider crack width resulted in breakdown of aggregate interlock. Consequently, resulting in shear compression failure that causes crushing of the concrete at the compression zone above neutral axis. In addition, B-4 experienced a similar type of failure but the BFRP stirrups was also ruptured. It has been noticed the Beams with spacing of 350 mm stirrups experienced a diagonal tension failure. A different scenario happened with beams reinforced with steel stirrups. B-9 has failed on a different type of compression flexural failure. At the beginning, there was a shear diagonal cracks devolved at the shear span but due to the high shear reinforcement ratio and low compression reinforcement, the concrete crushed due to the high compressions stress in the upper mid-span that exceeds the allowable compression capacity of the concrete. Generally, low stirrups spacing preventing the beam from the longitudinal splitting. Thus, the struts were subjected to high compressive stress and there was a high resistance formed in the stirrups.

Results revealed that while minimizing stirrups spacing is increasing the shear force capacity of the beam due to the usage of more stirrups that will counterattack the widening of diagonal shear crack width and that can be explained due to the

distribution of the shear force among a high number of stirrups that acts as a dowel. To sum up, minimizing spacing of the stirrups is not preventing occurrence of the crack. However, using minimum spacing helps in decreasing the crack width as shown in Figure 58. Also, it helps in improving the aggregate interlock.

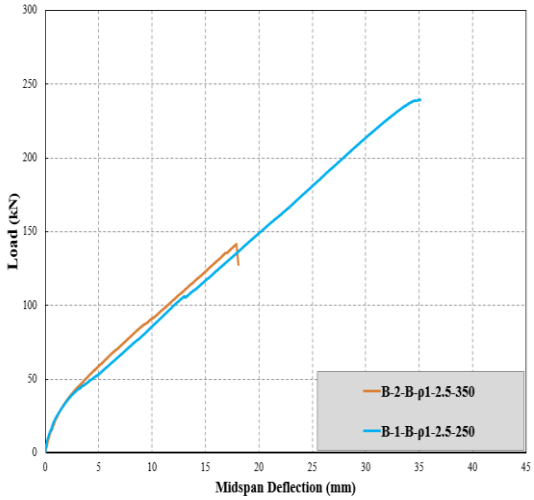

(a) B-2 vs B-1

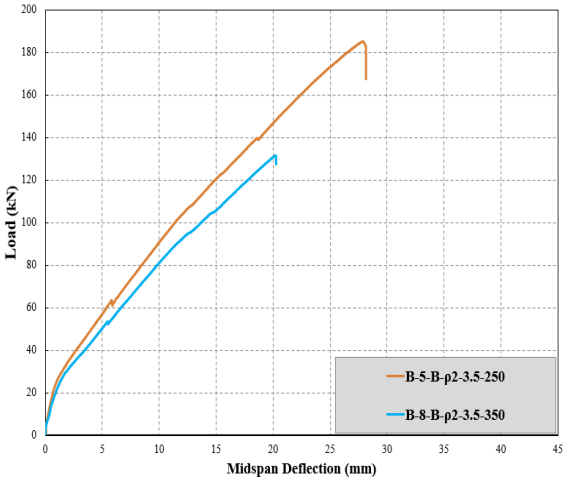

(b) B-5 vs B-8

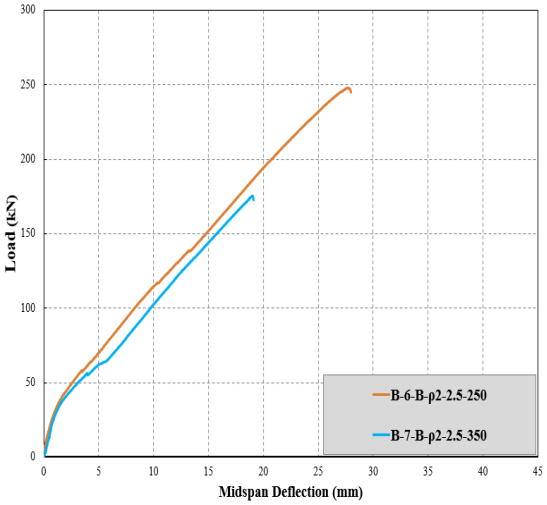

(c) B-6 vs B-7

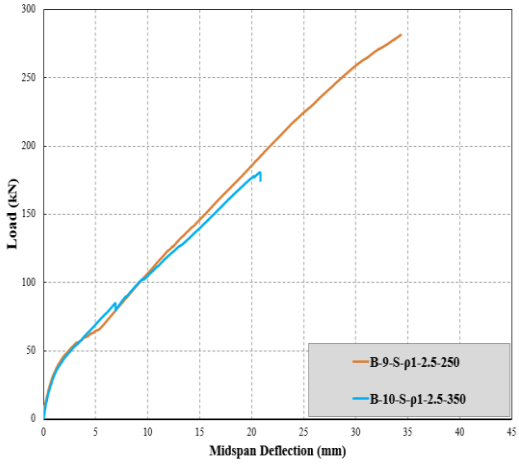

(d) B-9 vs B-10

Figure 55. Load vs load displacement diagrams for identical beams with different stirrups spacing.

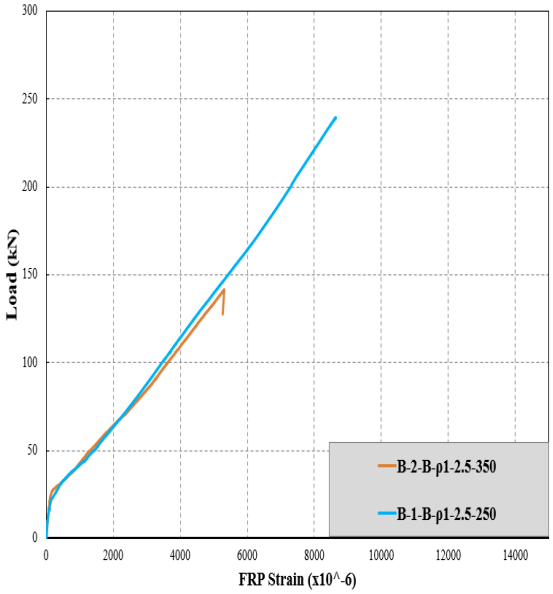

(a) B-2 vs B-1

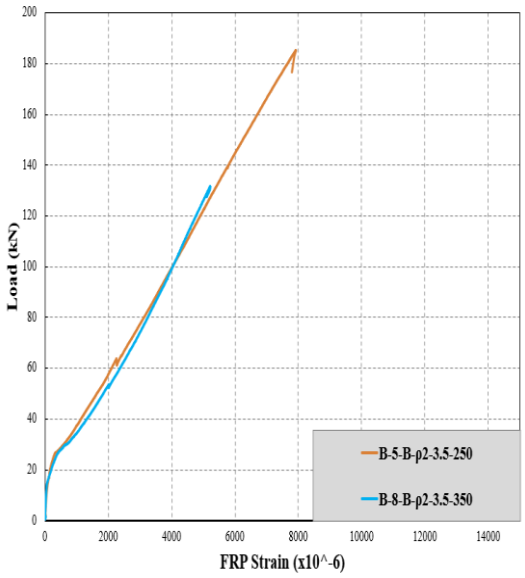

(b) B-5 vs B-8

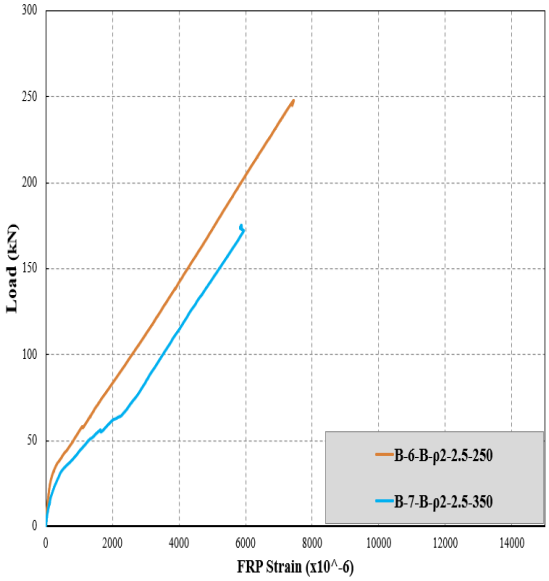

(c) B-6 vs B-7

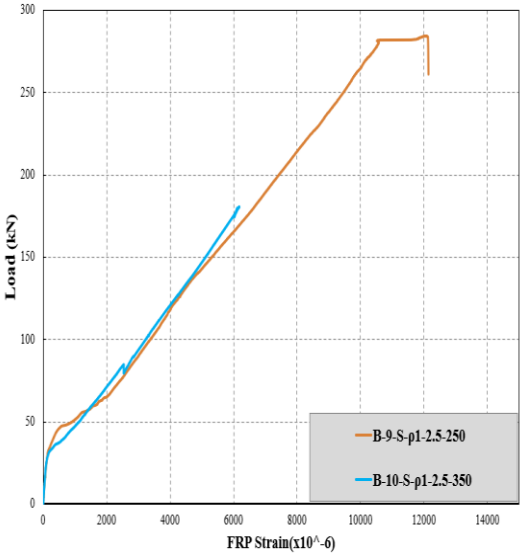

(d) B-9 vs B-10

Figure 56. Load vs longitudinal FRP strain diagrams for identical beams with different stirrups spacing.

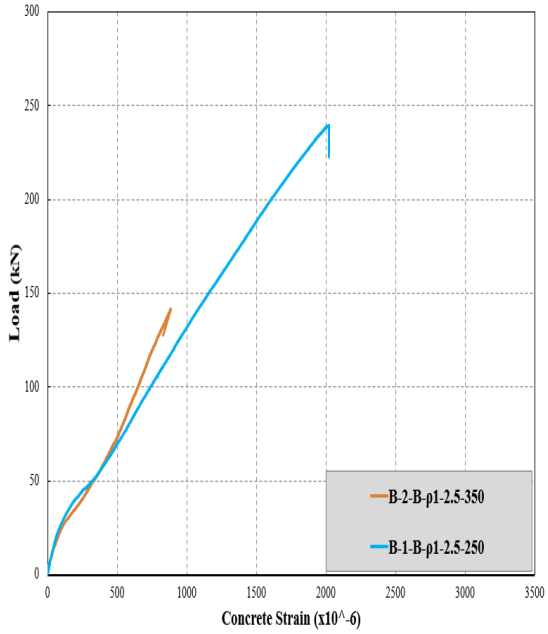

(a) B-2 vs B-1

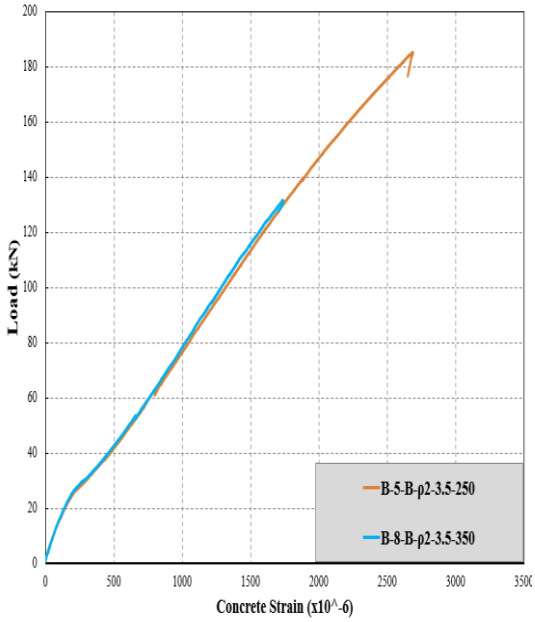

(b) B-5 vs B-8

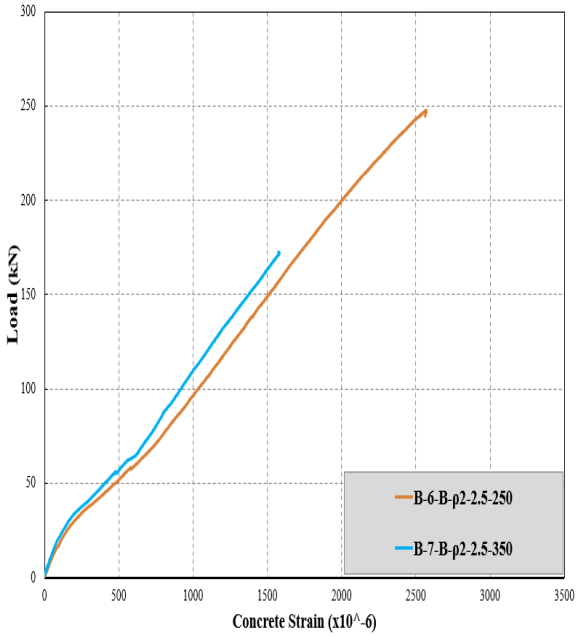

(c) B-6 vs B-7

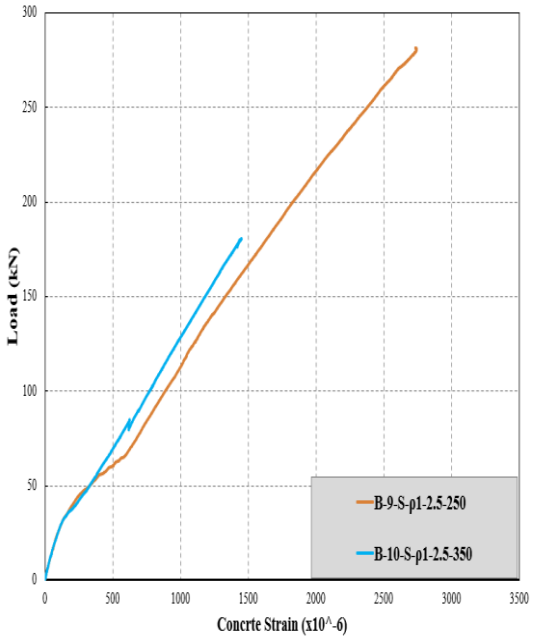

(d) B-9 vs B-10

Figure 57. Load vs concrete strain diagrams for identical beams with different stirrups spacing.

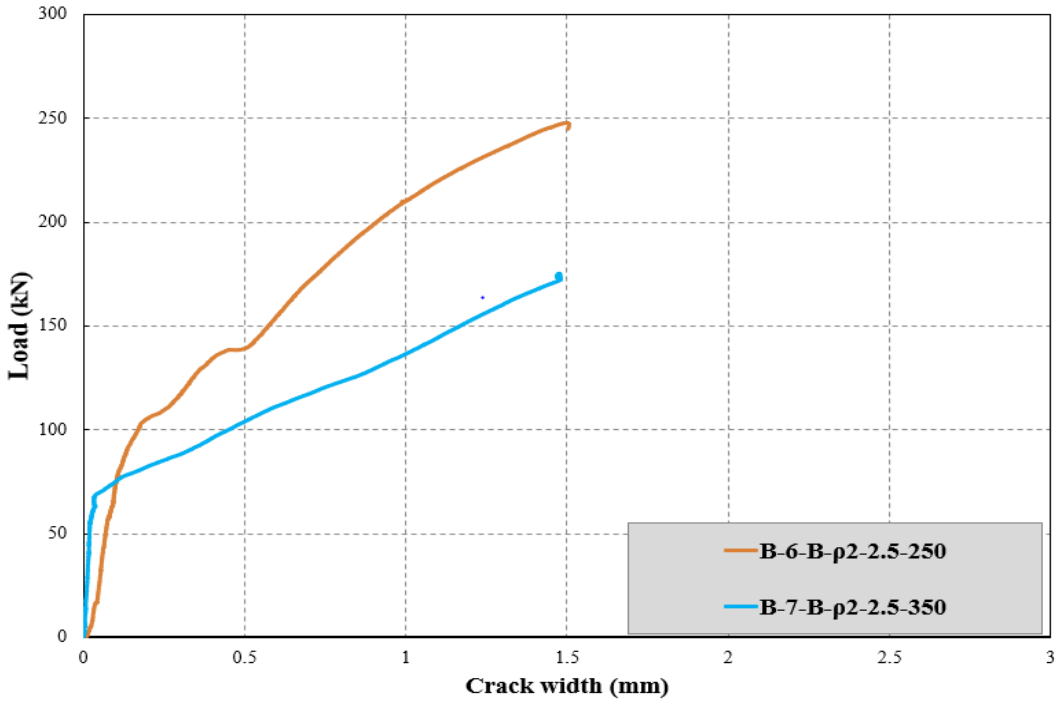

(a) B-6 vs B-7

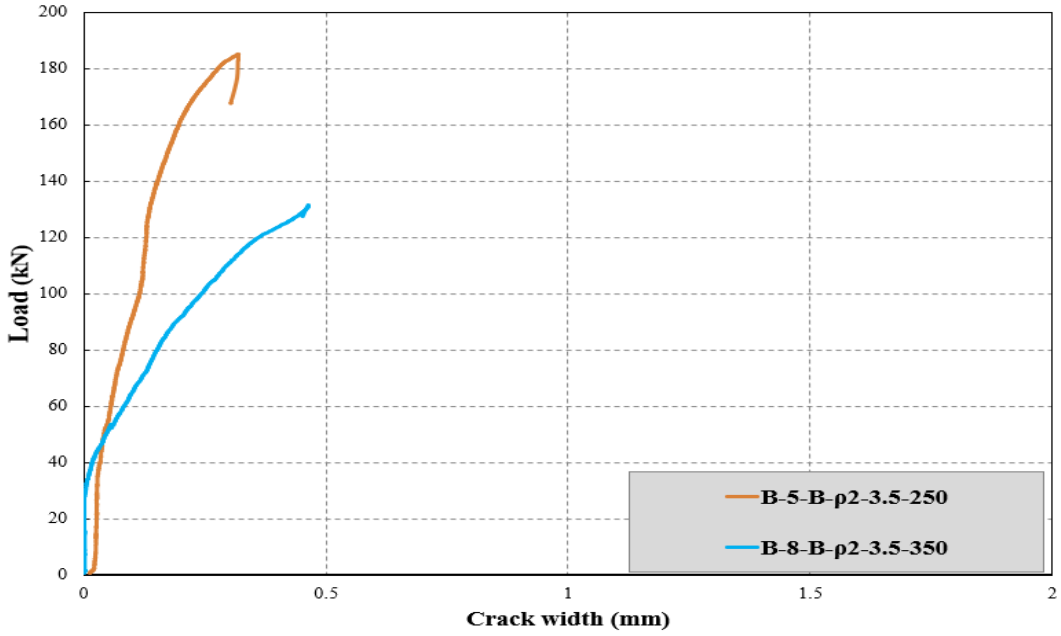

(b) B-5 vs B-8

Figure 58. Load vs crack width diagrams for identical beams with different stirrups spacing.

4.8.Effect of Span to depth ratio

Span to depth ratio used in this study was 2.5 and 3.5. The results show that there was an enhancement in the load capacity of the beam. Also, in the deflection capacity with about 25% of the beams has a span to depth ratio of 2.5. It has been noticed that span to depth affects directly the stiffness of the beam negatively. When the a/d ratio is increasing, the stiffness of the beams is decreased and vice versa. This can be observed when comparison made between beams with a/d ratios of 2.5 and 3.5. This resulted when the beam has high a/d, the beam will have a long moment arm. This means, shear span will also be longer that will make the initiation of the flexural cracks at the early stages at a high moment value compared to the beams with low a/d. That is due to the high-tension stresses and high number of cracks at the beam that will reduce directly the beam stiffness. As a result, comparing the beams with high a/d and with low ratio at the equal loading level, it was found that beams with high a/d experienced a high tensile strain for the flexural reinforcement and its concrete specifically at the mid-span as shown in the Figure 59. The load capacity of the beams B-1, B-2 has a/d of 2.5 were higher by 20 to 25 % respectively than that of the beams B-3 and B-4 which has a/d of 3.5.

It was interesting to observe that all beams with a span to depth ratio of 2.5 experienced a diagonal tension failure except the steel beams which exhibited to another mode of failure as illustrated before for B-9 and B-11. However, the diagonal crack was initiated and widened but it is due to the high shear reinforcement that inhibits the diagonal shear failure to occur. The failure of B-9 could be analyzed also due to the increase of the flexural cracks at the zone where there was no change in moment close to the compression fiber of the beam and that consequently will reduce the stiffness of the beam causing the compression failure. For B-11, which has

experienced shear compression mode failure, the reason could be due to the minimum spacing of the stirrups that contributes in preventing the beam from the longitudinal splitting. Thus, the struts were subjected to high compressive stress and a lateral expansion at the compression field located between the support and the point load. Hence, resulting in a failure of lap splice located at the zone of the stirrups bent that leads to beam failure.

However, by comparing beams without stirrups having different a/d, it was found that beams with a/d 2.5 (B-13) exhibited to a diagonal tension failure and beam with a/d 3.5 (B-12) have different mode of shear failure; which was shear tension failure. The B-12 has experienced shear tension failure could be due to the high deformation and high stresses concentration of the BFRP bars that leads to forming cracks and losing the bond between the bars and the concrete. Results show that B-13 has high load and shear strength compared to B-12 by 31 % as shown in the load displacement diagrams Figure 59. It has also been noticed that beams having a/d of 3.5 experienced different types of failure. That is shear tension failure and shear compression failure. And only one of the beams with a/d of 3.5 experienced the diagonal shear failure and this can be due to the larger spacing between the stirrups.

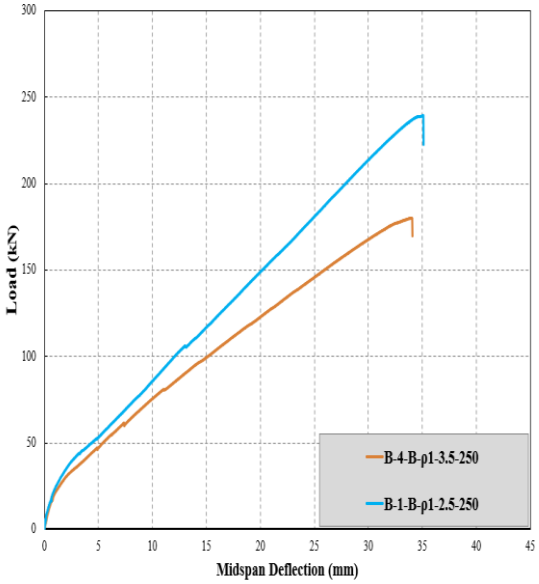

(a) B-4 vs B-1

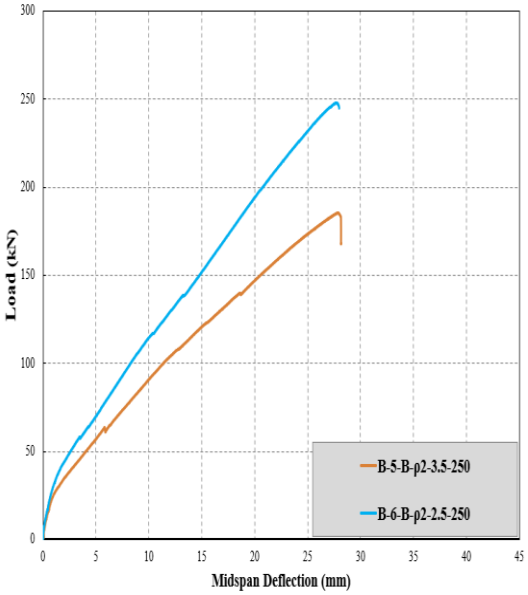

(b) B-5 vs B-6

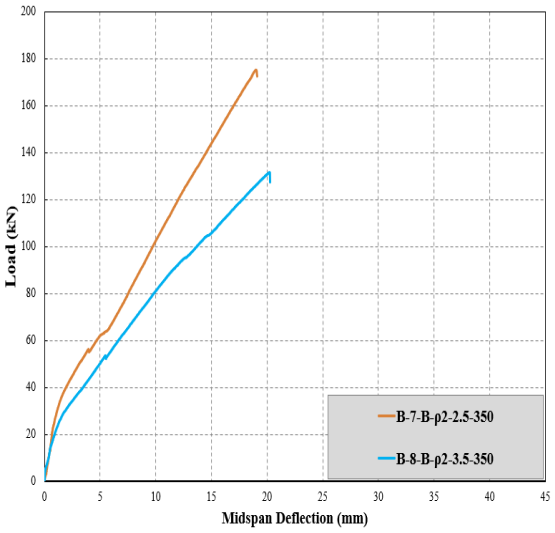

(c) B-7 vs B-8

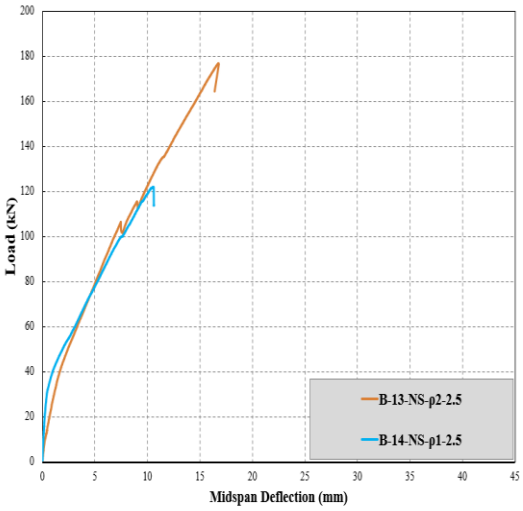

(d) B-12 vs B-13

Figure 59. Load vs load displacment diagrams for identical beams with different span to depth ratio.

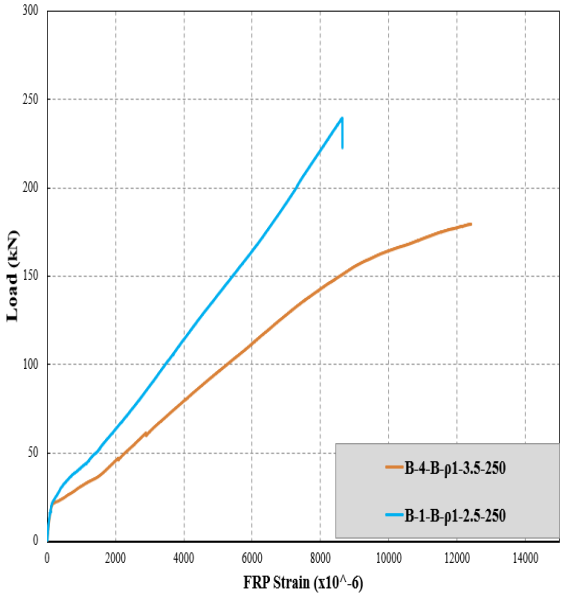

(a) B-4 vs B-1

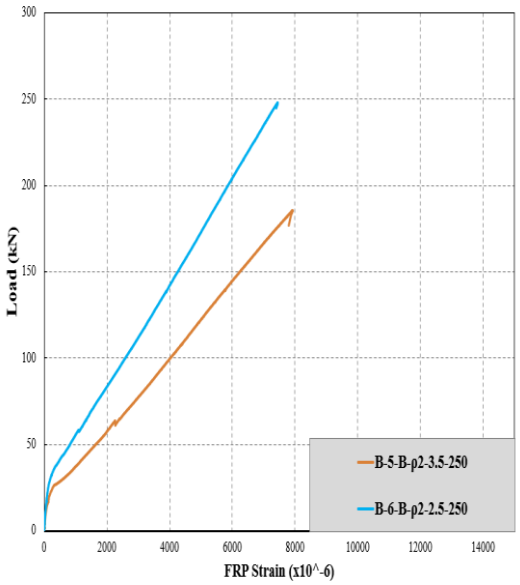

(b) B-5 vs B-6

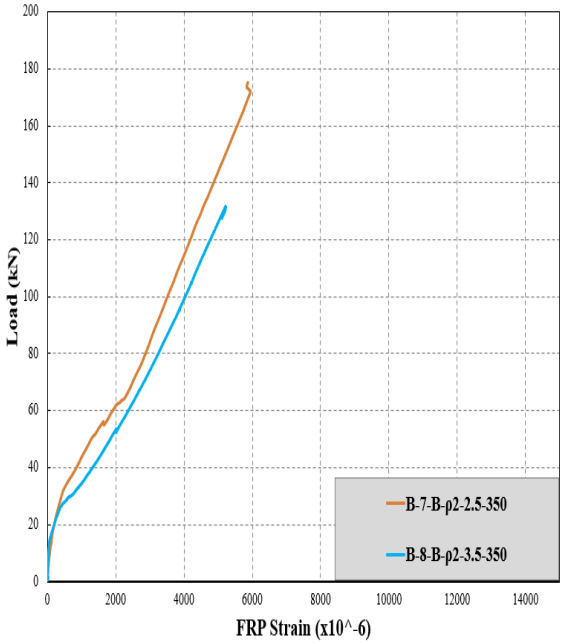

(c) B-7 vs B-8

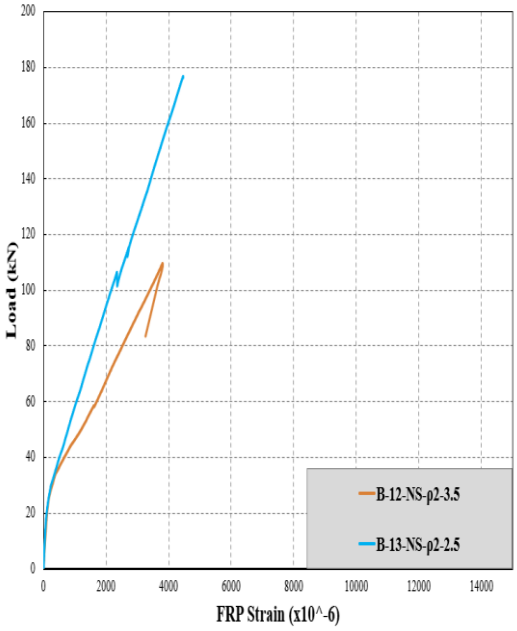

(d) B-12 vs B-13

Figure 60. Load vs longitudinal FRP strain diagrams for identical beams with different span to depth ratio.

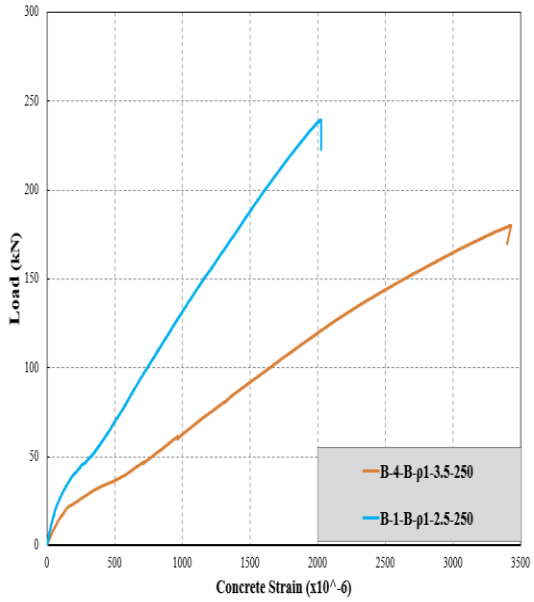

(a) B-4 vs B-1

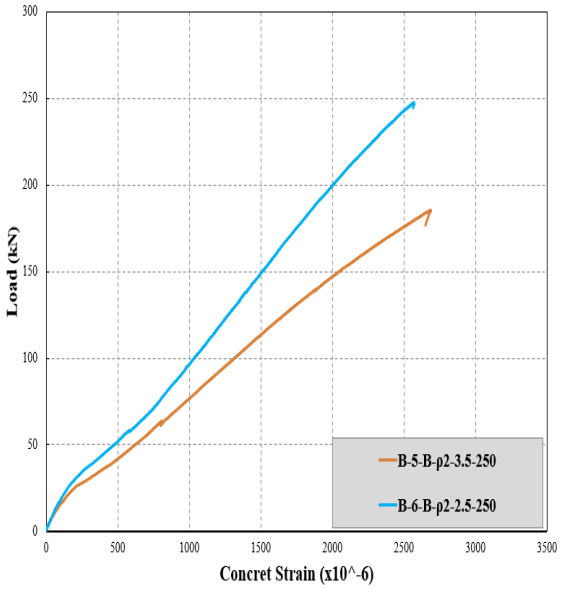

(b) B-5 vs B-6

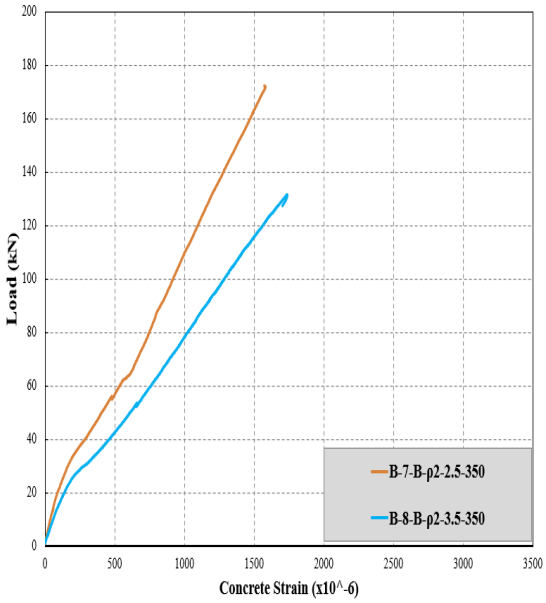

(c) B-7 vs B-8

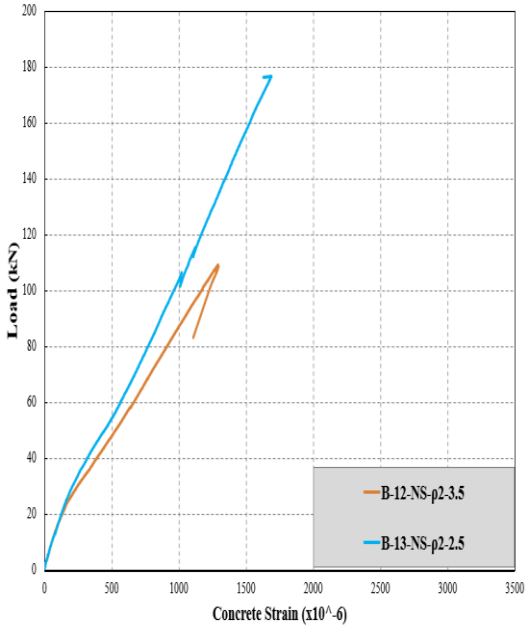

(d) B-12 vs B-13

Figure 61. Load vs concrete strain diagrams for identical beams with different span to depth ratio.

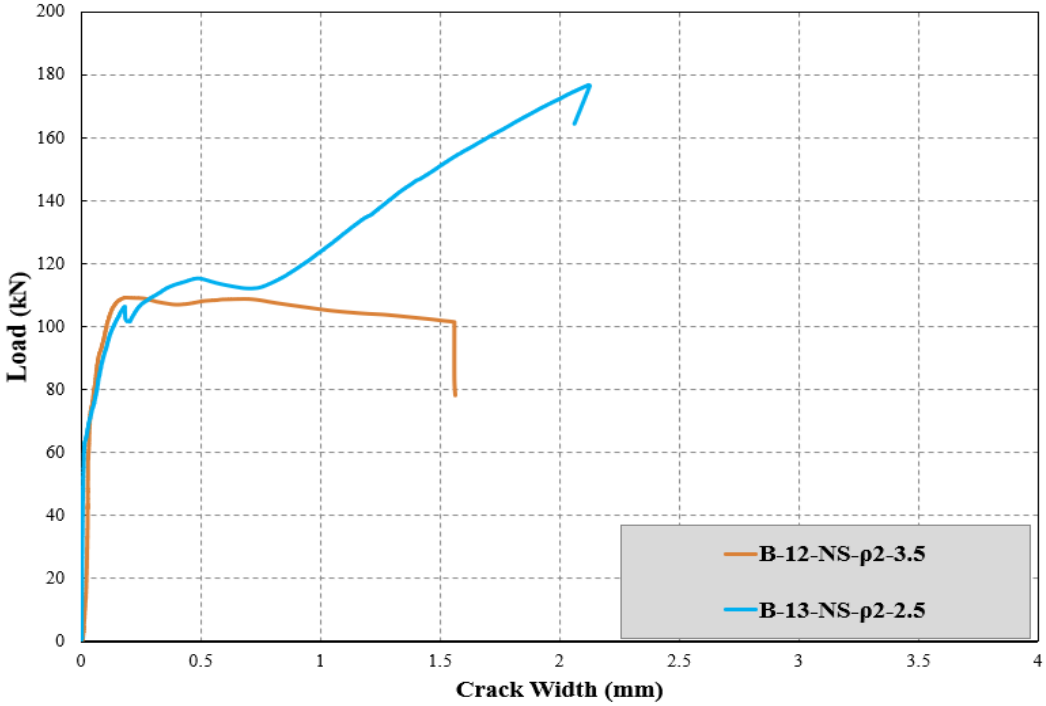

(a) B-12 vs B-13

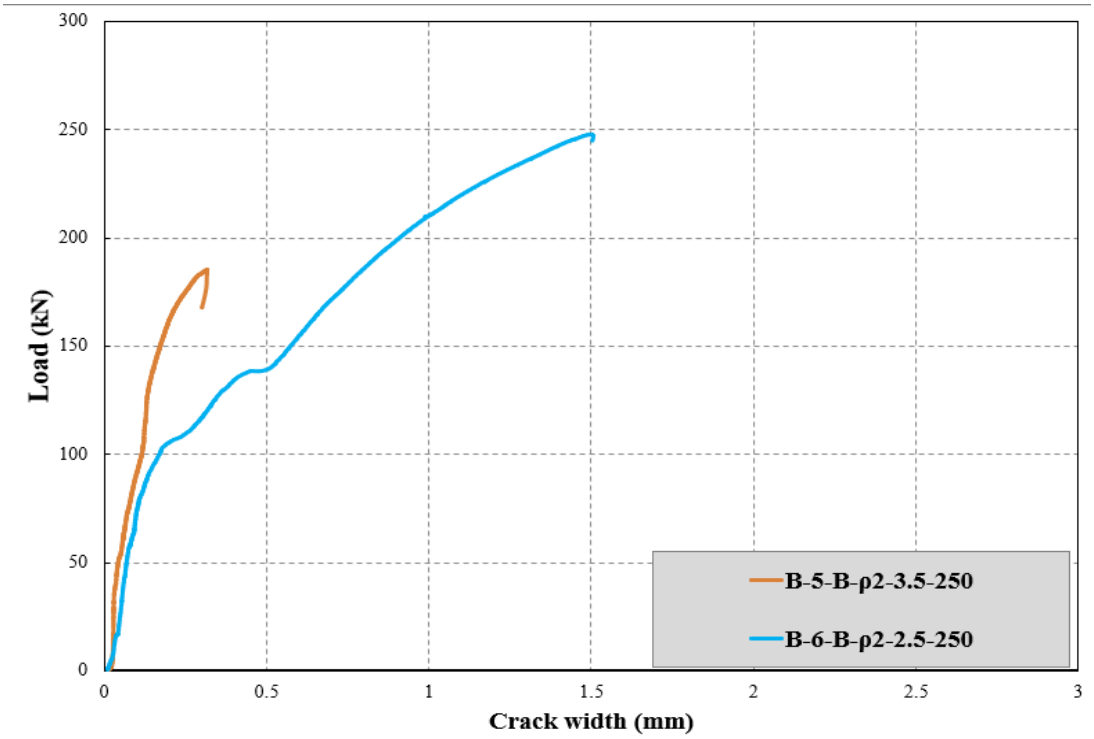

(a) B-5 vs B-6

Figure 62. Load vs crack width diagrams for identical beams with different span to depth ratio.

4.9.Effect of the Reinforcement ratio

Results revealed that increasing the reinforcement ratio has improved the beam and deflection capacity and shear strength by approximately 30 % as shown in the load-displacement graphs Figure 63 comparing the experimented beams B-1, B-2, B-3, B-4, B-9 with B-6, B-7, B-8, B-5 and B-11 respectively. However, while comparing the deflection and load capacity of beams with non-reinforced stirrups (B-13 Vs. B-14), it was found that the deflection capacity was increased by approximately 55% when the reinforcement ratio increased. This could be a result of the shear transfer mechanism at the uncracked sections between the reinforcement bars and the concrete, which will preserve the mechanism of the aggregate interlock. Also, it could be result of increasing the dowel action capacity.

As mentioned earlier, when all of the beams exhibited to a constant linear behavior in the mid-span deflection till the first flexural crack was initiated, the behavior starts to change significantly as the crack propagation starts to increase. This is due to the moment of inertia that started to reduce as an effect of this cracks. It can be observed that this reduction of the stiffness was influenced by reinforcement ratio. However, using high reinforcement ratio enhances the stiffness of the beam starting from the first flexural crack stage which can be visible at this point till the failure occur as shown in the Figure 63. It has been noticed that the strain values of the concrete and the continual reinforcement bars have been affected by the reinforcement ratio. This can be obtained from Figure 64 & 65 which indicates the strain values are lower when the used reinforcement ratio is high at the same load level.

In addition, it was observed that after the initiation of the first flexural crack the strain of the flexural reinforcement starts to increase dramatically. This could be a

result of the transmission large portion of the tensile stress from the concrete to the flexural reinforcement BFRP bars that characterized with low modulus of elasticity. There has no difference in the mode of failure that was observed for beams reinforced with different reinforcement ratio.

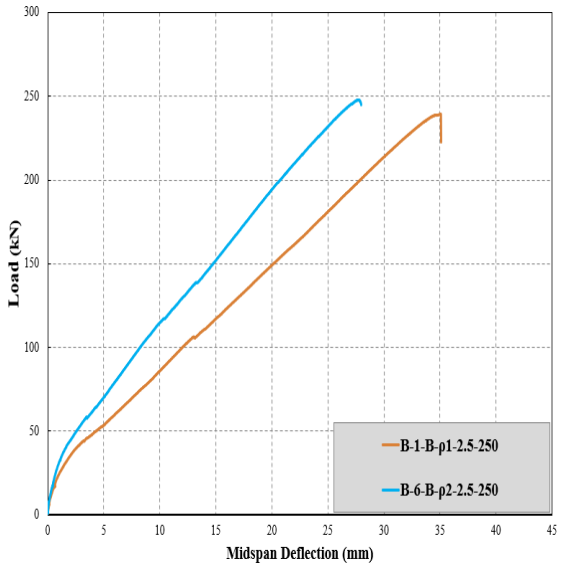

(a) B-1 vs B-6

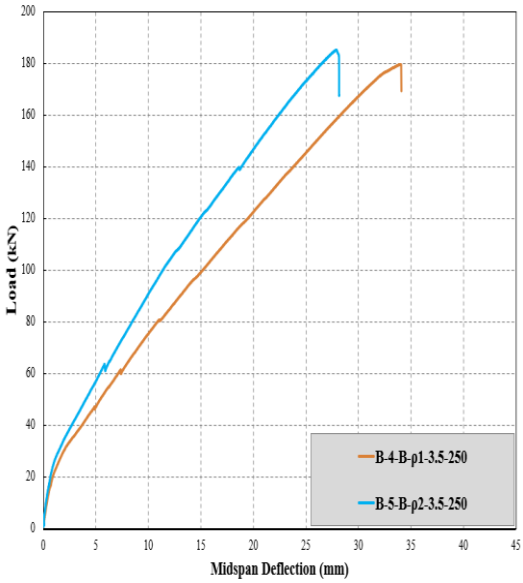

(b) B-4 vs B-5

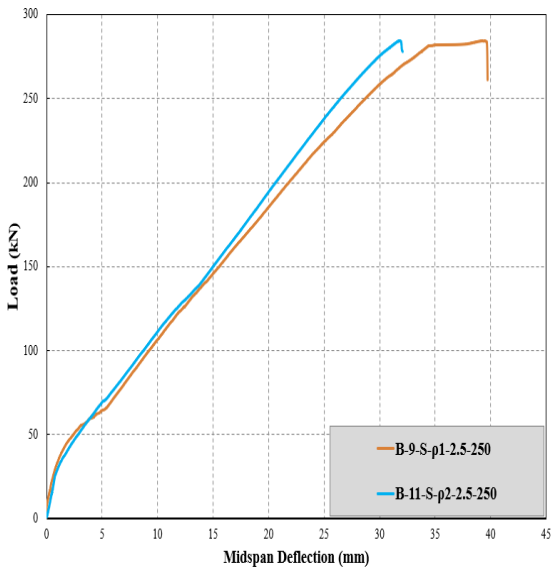

(c) B-9 vs B-11

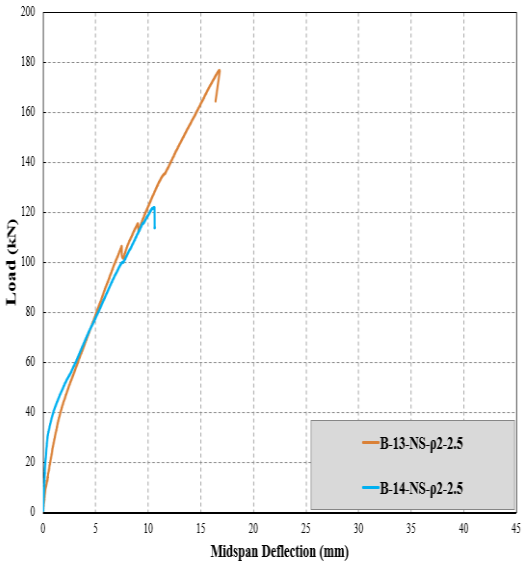

(d) B-13 vs B-14

Figure 63. Load vs load displacement diagrams for identical beams with different reinforcement ratio.

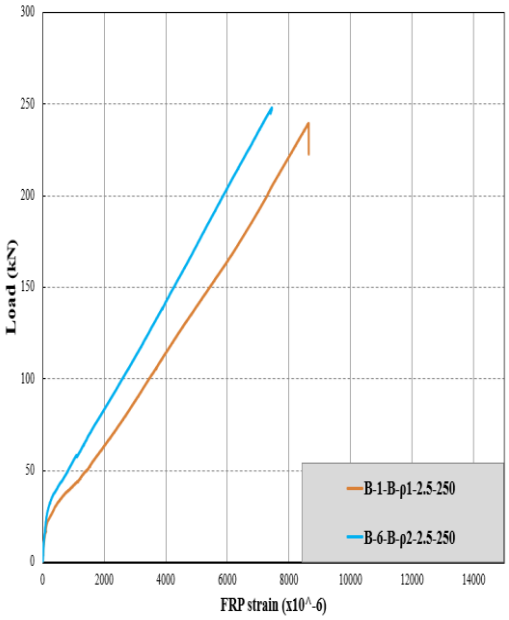

(a) B-1 vs B-6

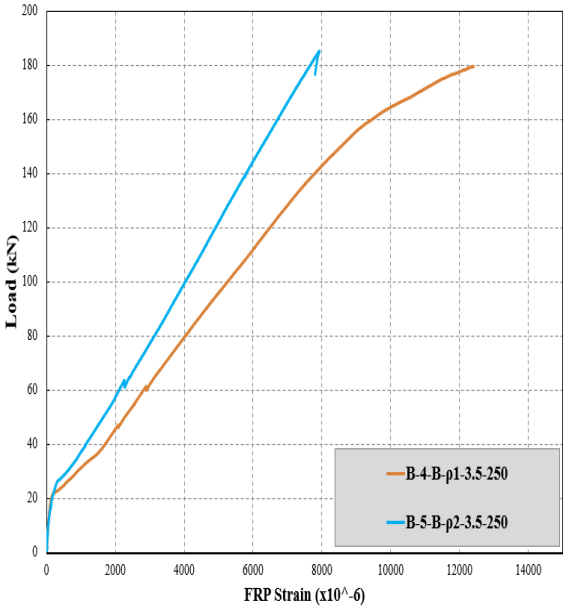

(b) B-4 vs B-5

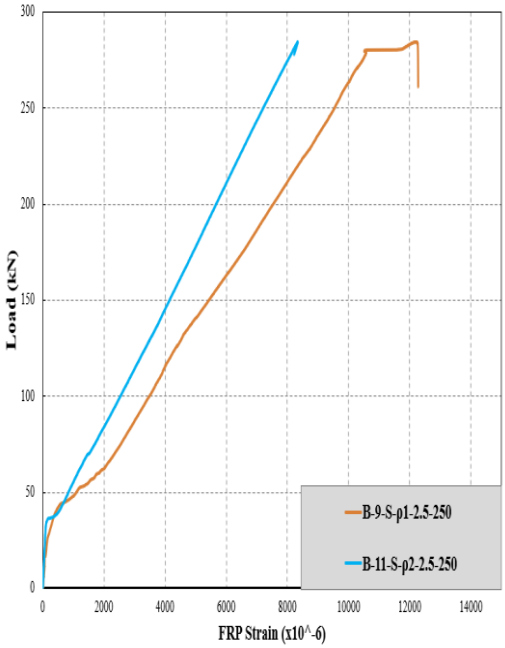

(c) B-9 vs B-11

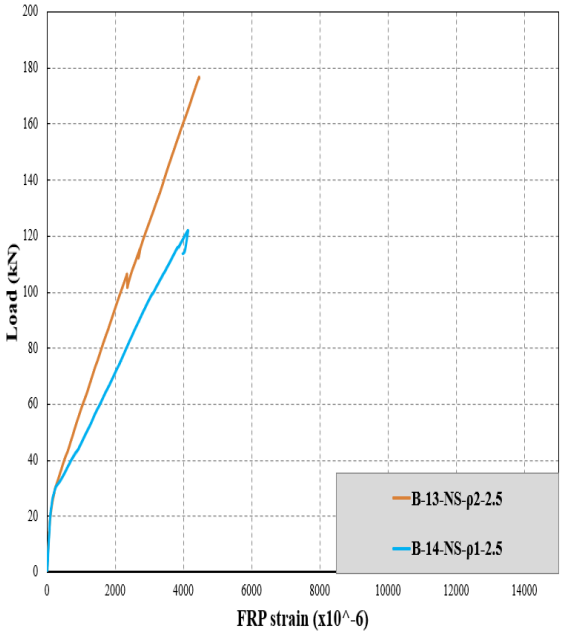

(d) B-13 vs B-14

Figure 64. Load vs longitudinal FRP strain diagrams for identical beams with different reinforcement ratio.

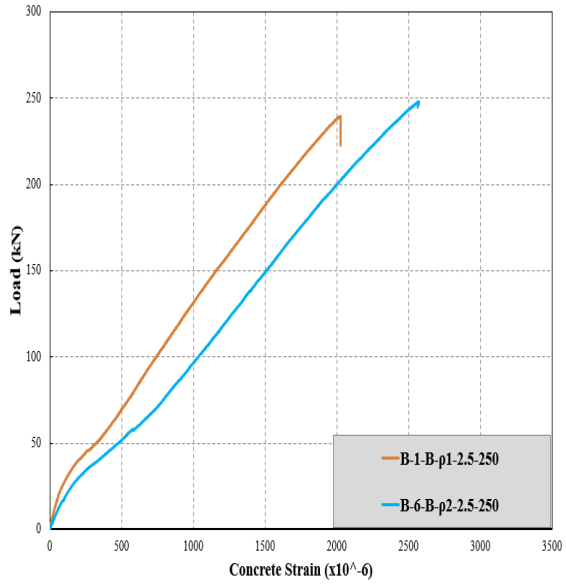

(a) B-1 vs B-6

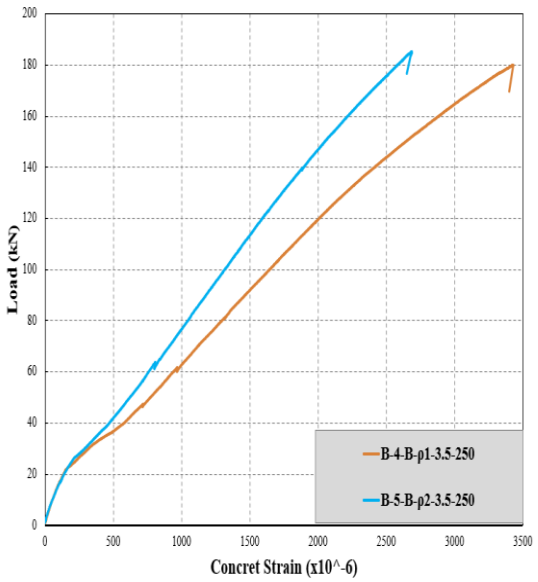

(b) B-4 vs B-5

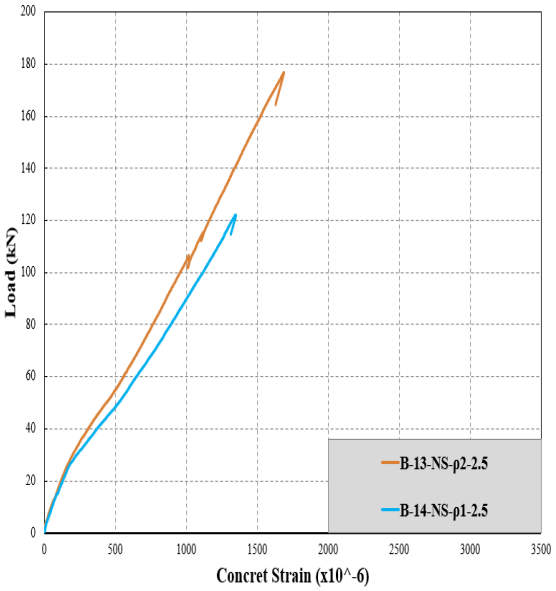

(c) B-13 vs B-14

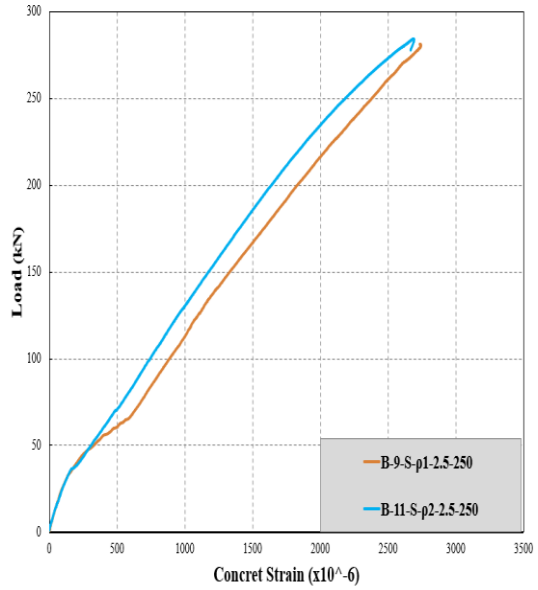

(d) B-9 vs B-11

Figure 65. Load vs concrete strain diagrams for identical beams with different reinforcement ratio.

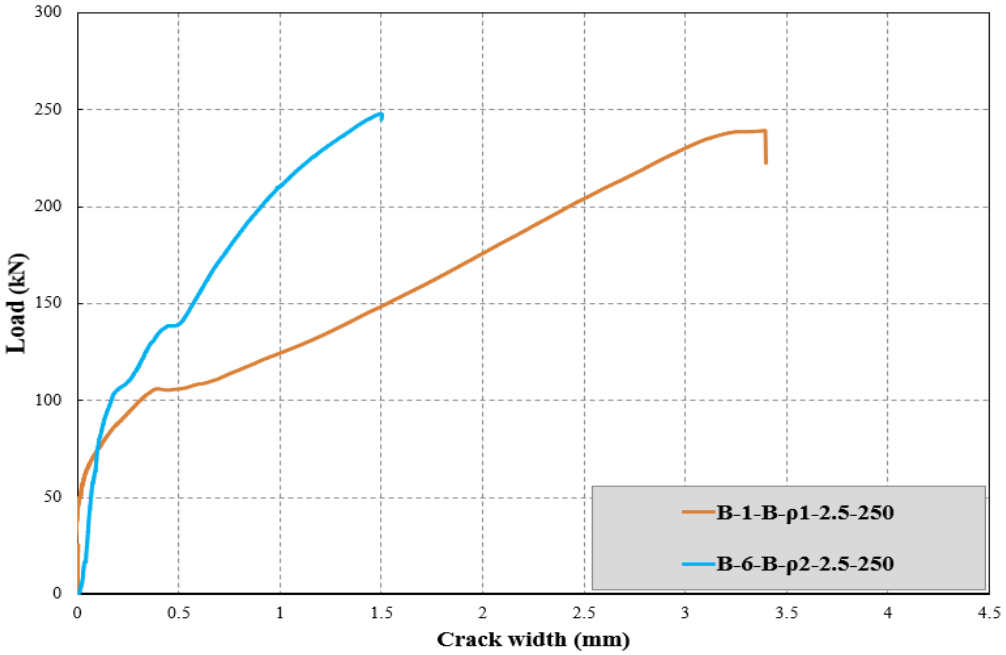

(a) B-1 vs B-6

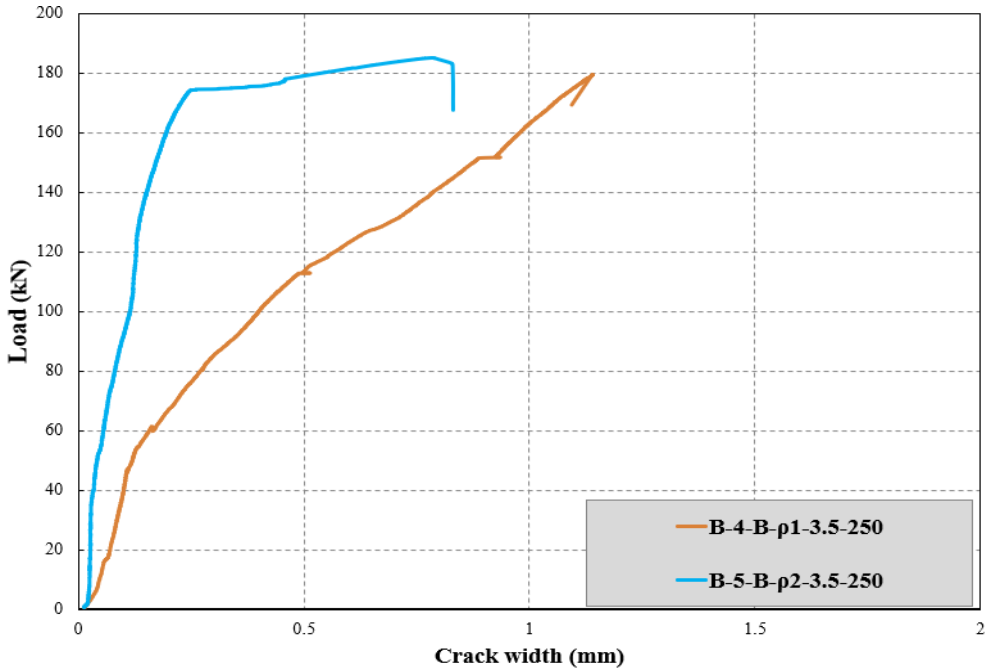

(b) B-4 vs B-5

Figure 66. Load vs crack width diagrams for identical beams with different reinforcement ratio.

CHAPTER FIVE: ANALYTICAL MODELLING OF SHEAR BEHAVIOR

This chapter will present the analytical model for the shear behavior of the green concrete beams reinforced with BFRP stirrups using available codes equations to assess the shear capacity of the experimented beams. Also, to validate the findings of the study using available codes equations and to evaluate the green concrete contribution in the shear capacity of the beams. As well as, the contribution of the spacing of the stirrups, the stirrups type effect, reinforcement ratio and finally the span to depth ratio for the beams reinforced with BFRP bars.

Several guidelines addressed designing and constructing the structure concrete elements which reinforced with glass, carbon and aramid with FRP bars. However, these guidelines are not providing any provisions for the structural elements reinforced with BFRP bars. The main guidelines are the ACI, ISIS and CSA. All of these guidelines have assumed the shear contribution of the transverse reinforcement (stirrups) and the contribution of the concrete are resisting the shear independently as the ultimate shear capacity of the concrete beam reinforced with FRP bars are the resultant of both contributions as follows $Vn = Vfrp + Vc$ where V_{frp} tends to the FRP stirrups contribution resisting the shear and V_c tends to the capacity of the shear that can be resisted by the concrete.

5.1.Design Equations for Shear Strength

5.1.1. ACI 440.1R-15 [26]

$$V_c = \frac{2}{5}\sqrt{f_c'}\, b_w kd \qquad (10)$$

Where, V_c tends to the shear resistance by the concrete

$b_w = width\ of\ web\ \ in\ (mm)$

$f'c =\ compressive\ strength\ of\ the\ concrete\ in\ \ (MPa)$

$d = effective\ depth\ of\ the\ section\ in\ (mm)$

$c = kd,\ \ cracked\ transformed\ section\ neutral\ axis\ depth\ in\ (mm).$

$k = \sqrt{2\rho n + (\rho n)^2} - \rho n$

$\rho = \frac{A}{b_w d}$

A = Area of the main reinforcement in (mm^2)

$V_f = \frac{A_{fv} f_{fv} d}{s}$ (11)

Where, $V_f\ \ tends\ to\ the\ \ shear\ resistance\ \ capacity\ provided\ by\ FRP\ stirrups.$

$A_{fV} = Area\ of\ \ shear\ reinforcement\ provided\ \ in\ \ (mm^2)$

f_{fv} *= tensile strength of FRP taken as the smallest of design tensile strength* f_{fu}, *strength of bent portion of FRP stirrups* f_{fb}, *or stress corresponding to* $0.004E_f$,*(MPa).*

$s = Spacings\ of\ FRP\ stirrups.$

5.1.2. CSA-S806-12 [7]

$V_c = 0.05\lambda k_m k_r (f'c)^{\frac{1}{3}} b_w d_v,\ \ for\ d \leq 300\ mm$ (12)

$provided\ that\quad 0.11\sqrt{f'c}\ \ b_w d_v \leq V_c \leq 0.22\sqrt{f'c}\ \ b_w d_v$

$k_m = \sqrt{\frac{V_f d}{M_f}}\ \leq 1.0, \qquad where\ \left(\frac{V_f d}{M_f}\right) is\ equivalent\ to\ \left(\frac{d}{a}\right)$

$k_r = 1 + (E_f \rho)^{\frac{1}{3}}$

$E_f = elastic\ modulus\ of\ the\ longitudinal\ FRP\ reinforcement$

d_v *is taken as the greater of* 0.9 d *or* 0.72 h, *where* $\boldsymbol{h}$ *is the overall thickness of a member*

$V_f =$ *ultimate shear,* $M_f =$ *ultimate moment*

$$V_f = \frac{0.4\Phi_f A_{fv} f_{fu} d_v}{s} cot\theta \quad (13)$$

$f_{fu} \leq 0.005 E_f$

$\theta = 30^o + 7000\varepsilon_l$

$provided\ that\ \ 30^o \leq \theta \leq 60^o$

$$\varepsilon_l = \frac{\frac{M_f}{d_v} + V_f + 0.5N_f}{E_f A_{fV}},$$

$N_f =$ *axial load normal to the member cross section. In this study it will qual to* 0

5.1.3. ISIS 2007 [26].

$$V_c = 0.2\lambda\sqrt{f'c} b_w d \sqrt{\frac{E_f}{E_s}} \quad (14)$$

$$V_f = \frac{A_{fV} f_{fv} d_v cot\theta}{s} \quad (15)$$

$d_v = 0.9d$

$$f_{fv} = \frac{\left(0.05\left(\frac{rb}{db}\right)+0.3\right) f_{fuv}}{1.5}, \quad or\ f_{fv} = E_{fv}\varepsilon_{fwd1} \quad (16)$$

5.2.Design Equations for Concrete Beams Reinforced with Longitudinal FRP Bars.

It was noticed that the codes have been used with the same concept of the reinforced steel concrete section equations when developing the FRP reinforced sections equations. Due to the different characteristics between the FRP and the steel, some

modifications have been made in the equations especially in the shear equations; the main modification was in the axial stiffness effects ($E_f\rho_f$) for the FRP bars when it is used in reinforcing the concrete section. As the FRP bars have low Modulus of elasticity compared to steel bars that resulted to wide crack width, it affects the stiffness of the concrete section. Also, it affects the uncracked compression region due to the reduction in the depth of the uncracked section that will affect directly the shear strength of the concrete member.

A study has been made to ensure the validation accuracy of the equation codes to the experimental program. The study experimented about 86 concrete beams reinforced with FRP bars. The study compared the predicted shear which was obtained from the ACI -440, ISIS, JSCE and CSA S806-12 and the experimented shear. Different beams were reinforced with BFRP bars as a flexural reinforcement, the results have been added to the database [60,3,64]. All reduction safety factor in the design equations was used as 1.

The Figure 67 shows the experimental and predicted shear results; Y-axis and X-axis represent the shear results from the experimental program and predicted shear results respectively. The diagonal line in the graph shows the scattered experimental shear results from the predicted shear, shown in the Figure 68. It can be noticed clearly that the reinforced BFRP concrete sections bars have the same trend of the other FRP bars like GFRP and AFRP due to close modulus of elasticity. As a result, it was concluded that section reinforced with BFRP bars have a close shear behavior to the other FRP bars.

From the comparison made between the experimental work and codes equations, it was noticed that the predicted shear is close to the experimented ones specifically the CSA S806-12 with a ratio of Vexp/Vpredict of 1.12 code and that's

because the code has been taken in consideration many factors like span to depth ratio, compressive strength of the concrete, stirrups spacing and reinforcement ratio. However, the ACI 440.1R-15 considers same factors except the span to depth ratio. Hence, it was observable that the predicted shear was conservative and far from the experimented shear as can be noticed from the Table 7; that the ratio was 1.89. However, ISIS equations prediction was close to the experimented beams with a ratio of Vexp/Vpredict of 1.26 with some overestimation from the ISIS equations in a small number of beams and that's can be due to the neglection of the ISIS equations to the reinforcement ratio effect in the shear strength. A large scattering can be noticed while comparing the experimented shear results with the ACI, and ISIS from the Figure 67. And it could be resulted of not considering the span to depth ratio effect in the equations, which have an effect as illustrated before and cannot be neglected.

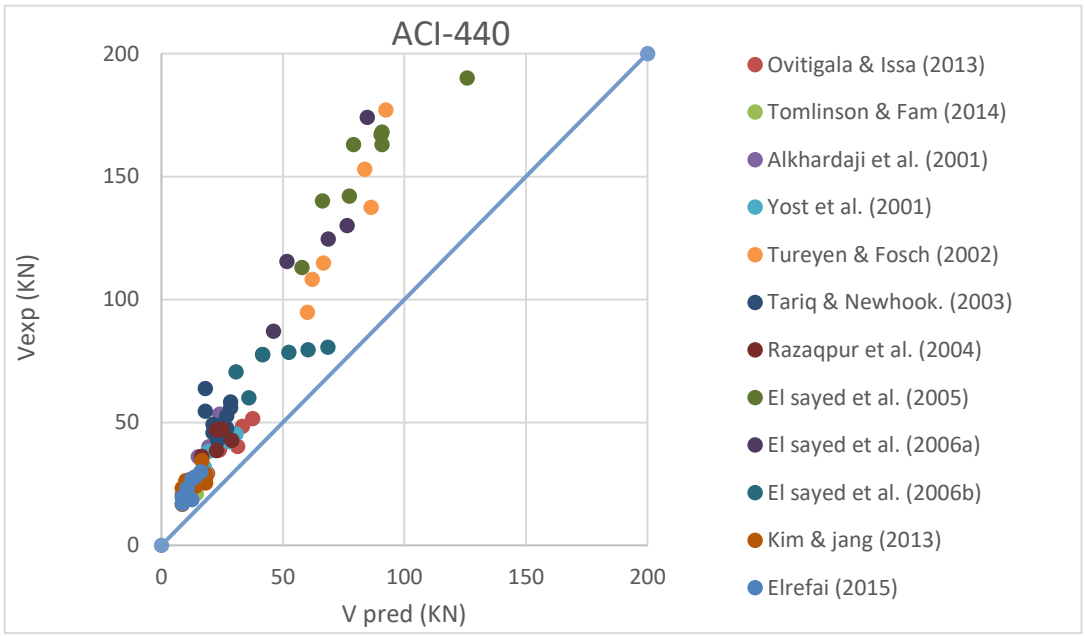

(a)

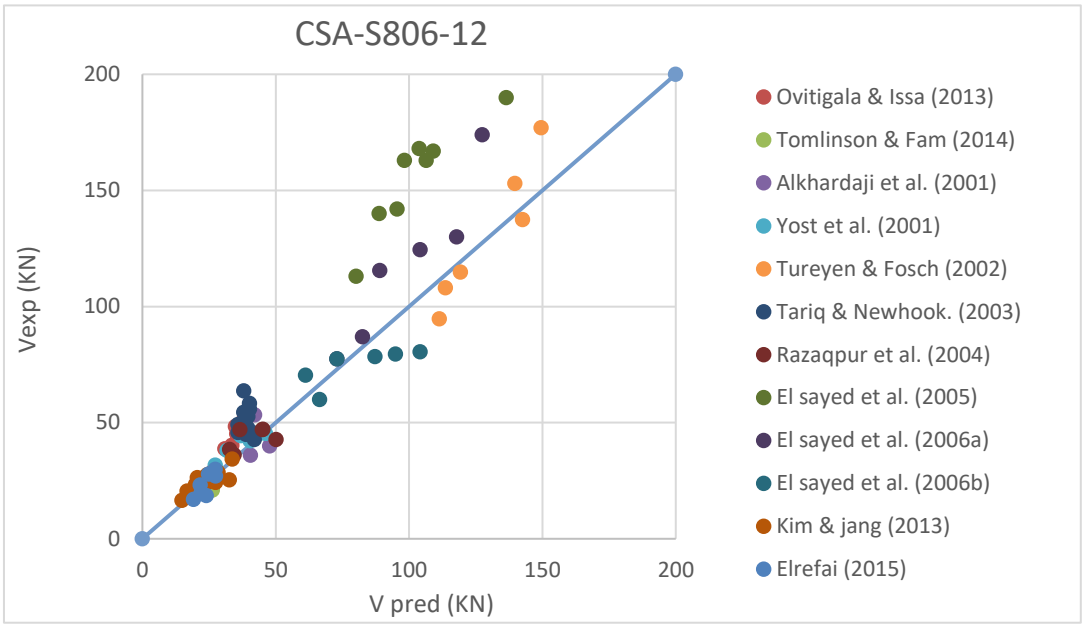

(b)

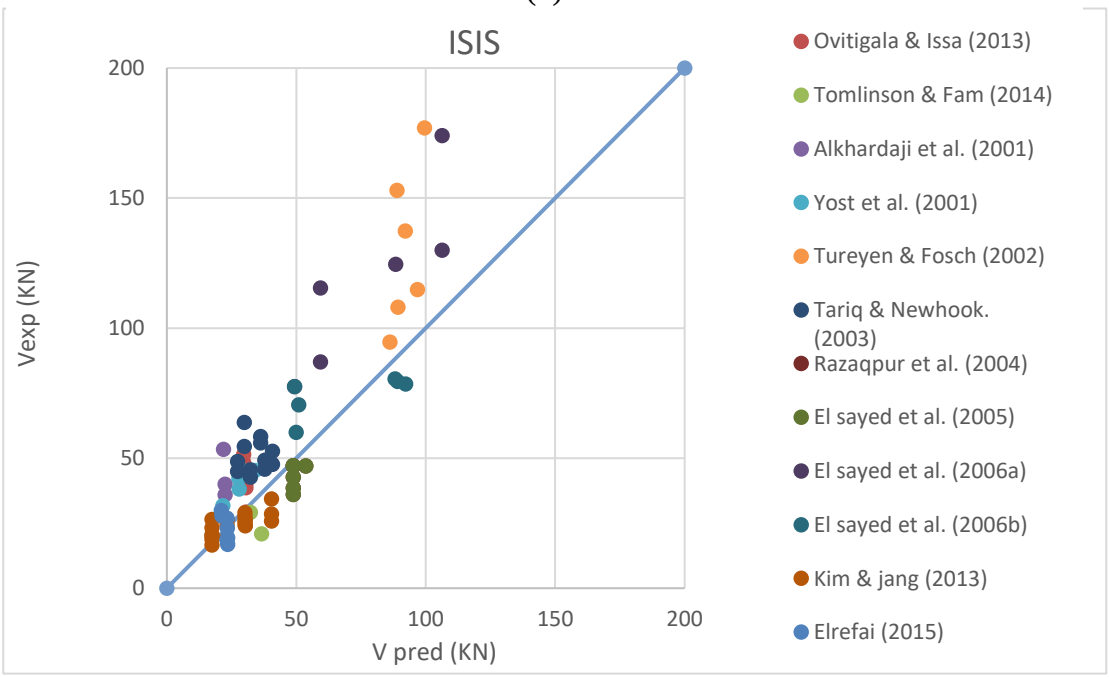

(c)

Figure 67. Comparison of experimental and predicted shear strength for beams reinforced with longitudinal FRP bars only. Comparison made with following codes (a) ACI-440 (b) CSA-S806-12; (c) ISIS.

Table 7 Summary for the experimental concrete shear capacity compared to the predicted ones

	V_{exp}/V_{pre}		
	ACI 440-15	CSA-S806-12	ISIS
Mean	1.89	1.12	1.26
St. Dev.	0.37	0.21	0.37
Coeff. Of. Var. (%)	20	18.9	29.6

5.3.Design Equations for Beams with FRP Stirrups

In order to ensure the accuracy of the stirrups design equation, a database has been made to include about 92 concrete beams reinforced with FRB bars and stirrups [7,6,3]. Comparison was made between the experimental shear results with the predicted shear results. The reduction safety factor has been taken as 1.

In order to ensure that the structural member can control the crack width and a failure at the bent region can be avoided, design codes has been specified an upper limit to the stress and strain for the developed stirrups due to the low modules of elasticity of the FRP.

The allowable strain ranges from 0.0025 to 0.004 in the different design guidelines like ACI & ISIS, noticeable that the FRP shear reinforcement can reach a large strain at the failure stage. ACI-440 code stated that the upper limit of the stirrups strain is 0.004 to prevent the degradation of the aggregates that interlocked with the bounded concrete. Figure 69 show the comparison between the predicted shear results and the experimental shear results. It has been noticed from the ISIS was the overestimating shear results with a high a ratio between the Vexp. /Vpred about 2.84. However, the ACI-440 and CSA-S806-12 the shear results were close to the experimented beams with Vexp. /Vpred. of 1.47 and 1.38 respectively. The difference

between the ACI-440 and CSA-S806-12 in the stress level of the stirrups f_{fv} is that ACI is considering the strain 0.004 and the CSA consider it as 0.005, which is a small difference. The maximum stress of the FRP stirrups can be calculated based on the following equation provided by the ACI code

$$f_{fv} = 0.004 * E_{fv} \leq f_{fb} \quad (17)$$

Where $f_{fb} = \left(0.05\left(\frac{rb}{db}\right) + 0.3\right) f_{fuv} \leq f_{fuv}$

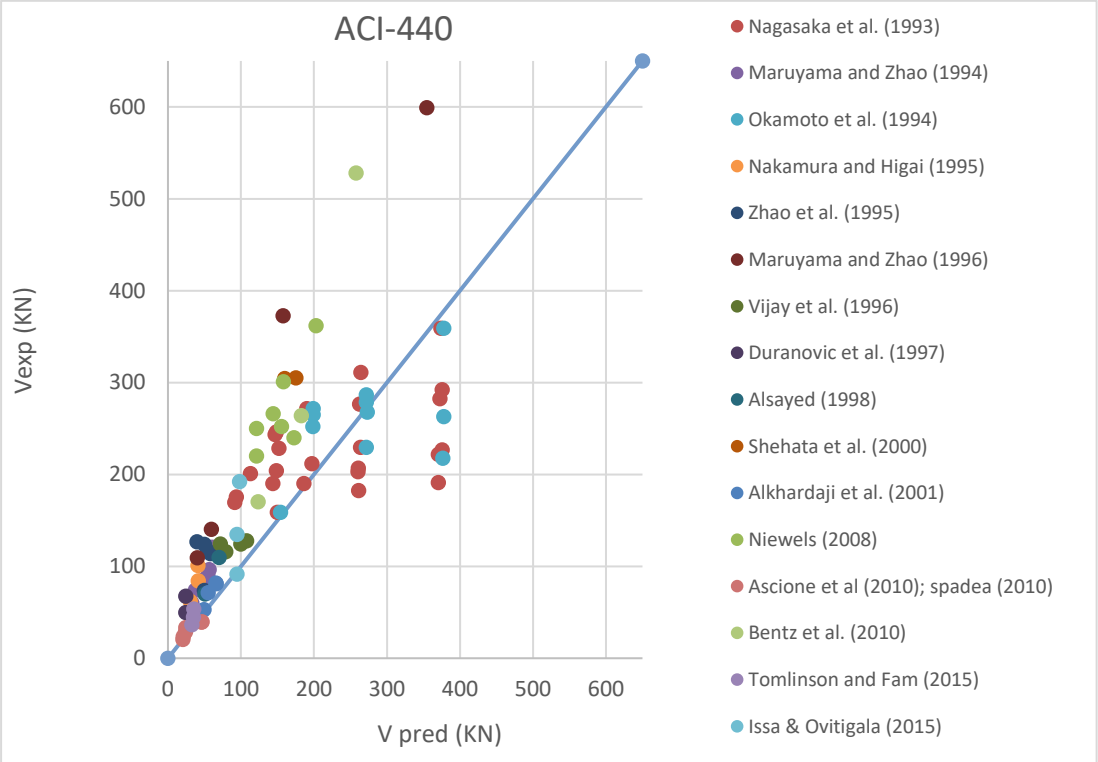

(a)

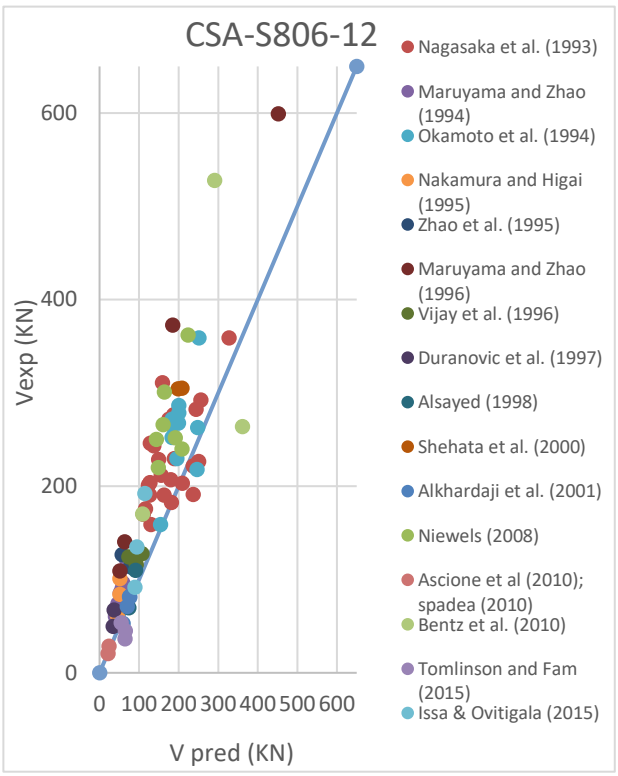

(b)

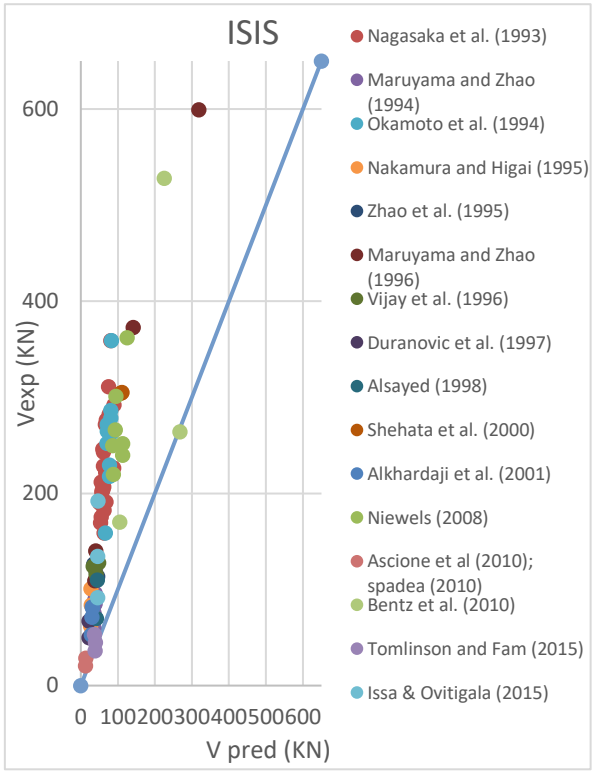

(c)

Figure 68. Comparison of experimental and predicted shear strength for beams reinforced with longitudinal FRP bars and stirrups Comparison made with following codes (a) ACI-440; (b) CSA-S806-12; (c) ISIS.

Table 8 Summary for the experimental shear capacity of beams reinforced FRP bars and stirrups compared to the predicted ones

	V_{exp}/V_{pre}		
	ACI 440-15	CSA-S806-12	ISIS
Mean	1.47	1.38	2.84
St. Dev.	0.54	0.35	0.78
Coeff. Of. Var. (%)	36.5	25.2	27.6

5.4.Comparison made for this study.

Based in this comparison between the experimental work and codes equations, it has been noticed that the predicted shear is close to the experimented result specifically the CSA S806-12 with a ratio of Vexp/Vpredict of 1.18 code and that is because the code has been taken in consideration many factors like span to depth ratio, compressive strength of the concrete, stirrups spacing and reinforcement ratio. However, the ACI 440.1R-15 considers same factors except the span to depth ratio, so it was observable that the predicted shear was conservative and far from the experimented shear as can be noticed from the Table 9. that the ratio was 1.38.

Table 9 Results for evaluating the shear behavior of beams

Beam NO.	ACI	CSA	EXP	Vexp/ Vpredict (ACI)	Vexp/ Vpredict (CSA)
B-1	78	89.15	119.71	1.54	1.34
B-2	64.4	74.4	70.76	1.10	0.95
B-3	64.4	70.14	57.66	0.90	0.82
B-4	78	85	89.85	1.15	1.06
B-5	70.6	76.3	92.65	1.31	1.21
B-6	70.6	81.2	123.79	1.75	1.52
B-7	60	69	87.5	1.46	1.27
B-8	60	64	65.75	1.10	1.03
B-9	76	109.15	142.2	1.87	1.30
B-10	67	90	90.3	1.35	1.00
B-11	83	115.5	142.2	1.71	1.23
B-12	53	55.3	54.68	1.03	0.99
B-13	53	55.3	88.39	1.67	1.60
B-14	45.4	51.4	61	1.34	1.19
		Mean		1.38	1.18

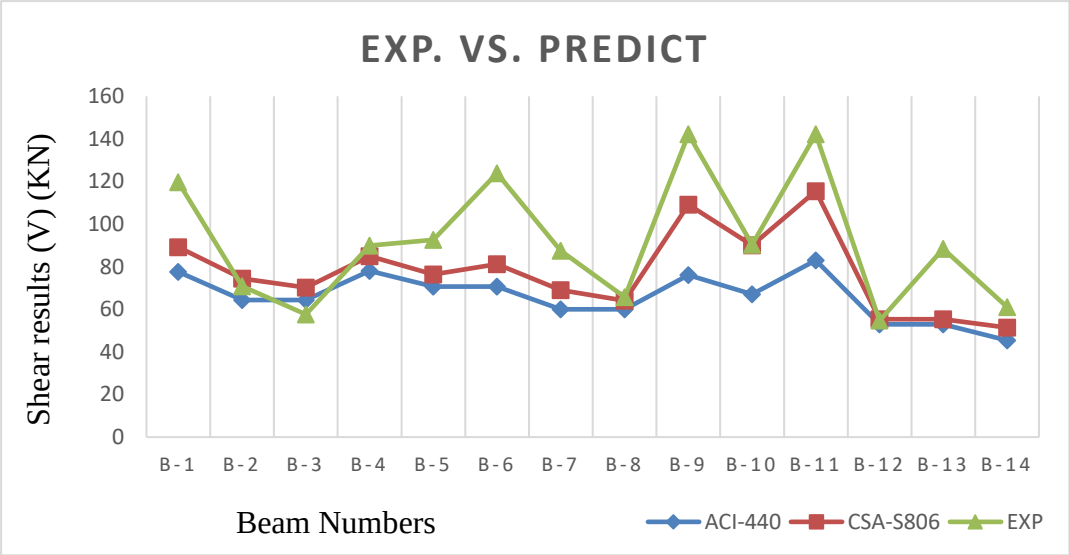

Figure 69. Comparison between the experimental work and predicted results.

CHAPTER SIX: SUMMARY, CONCLUSIONS, AND RECOMMENDATIONS

6.1.Summary

This paper presents the results of an experimental investigation on shear behavior of green concrete beams reinforced with BFRP bars and stirrups. A total of fourteen (14) full-scale beam specimens were tested in the laboratory in order to evaluate its four different variables, which are spacing of the stirrups, type of the stirrups, span to depth ratio and reinforcement ratio. Beams have experienced four modes of failures, which are shear compression failure, diagonal tension failure, shear tension failure and flexural compression failure. A comparative study of the experimental results with distributed analytical models including equations provided by ACI-440.15 and CSA-S806-12 guidelines in order to validate the experimental work and identify the influencing factors on the shear behavior of BFRP reinforced green concrete beams. Different tests were made to in order to check the mechanical properties of the green concrete, slump test for the consistency of the casted concrete, Flexural tests to check flexural capacity of the concrete and finally the compressive strength test to ensure the casted concrete is matching with the required compressive strength.

6.2.Conclusions

Based on the study, findings can be drawn as follows:

1- Green concrete can provide high compressive strength but low flexural strength as increasing the fly ash affecting the flexural strength negatively. However, it increases the workability of the concrete.

2- Using smaller stirrups spacing provides confinement to the concrete, which will help in preventing the beam from the longitudinal reinforcement splitting.

3- It was noticed that beams with a span to depth ratio of 2.5 has experienced a shear diagonal tension failure and beams with span to depth ratio of 3.5 exhibited shear tension failure. Whilst causing loss of the bond between the reinforcement and concrete and contributed the main reinforcement to slip that resulted to anchorage failure.

4- Using BFRP stirrups instead of steel resulted in a difference about 20% reduction in the stiffness.

5- It was observed that a wider crack was experienced by BFRP reinforced beams stirrups compared with steel reinforced stirrups and that is due to the low elastic modulus of the BFRP stirrups compared with the steel stirrups.

6- Beams with no stirrups have very low deflection capacity compared with BFRP stirrups by approximately 70% variance.

7- Results revealed that when minimizing stirrups spacing, the shear force capacity of the beam is increasing. Using more number of stirrups will counterattack the widen of diagonal shear crack width and that can be explained due to the distribution of the shear force amongst a high number of stirrups that acts as a dowel. Generally, minimizing spacing of the stirrups is not preventing the occurrence of the crack. However, using minimum spacing helps in decreasing the crack width. Also, it helps in improving the aggregate interlock.

8- Beams with high reinforcement ratio found to be having high load and deflection capacity compared to beam reinforced with low reinforcement ratio with almost 30%. This enhancement was due to the increased depth of the uncracked section, also improvements of the dowel action capacity

of beam.

9- From the comparison made between the experimental work and codes equations, it has been noticed that the predicted shear is close to the experimented results specifically the CSA S806-12 with a ratio of Vexp/Vpredict of 1.18 code. Consequently, the code has been taken in consideration many factors like span to depth ratio, compressive strength of the concrete, stirrups spacing and reinforcement ratio. However, the ACI 440.1R-15 considers same factors except the span to depth ratio. Hence, it was apparent that the predicted shear was conservative and far from the experimented shear with a ratio of Vexp/Vpredict 1.38.

10- The steel stirrups when reached the yield stress, the shear cracks start to widen which resulted in breakage in the aggregate interlock. As a result, the beam will experience a shear failure due to the crushing of the concrete at the compression zone over the neutral axis.

11- The experimental study shows that the BFRP stirrups was not deformed at failure stage. However, it ruptured directly due to the non-yielding properties of the FRP bars and stirrups. It was noticed that most of the rupture in the BFRP stirrups were located at the bent portion.

12- Results revealed that prediction of the shear strength using BFRP bars as a longitudinal reinforcement and also as shear reinforcement were in good harmony with the shear characteristics of the reinforced concrete beams using the other FRP bars like (GFRP, CFRP and AFRP).

6.3.Recommendations

Further work required studying the behavior of the geo-polymer concrete beams reinforced with BFRB stirrups, which means full replacement of cement in the concrete mix. As mentioned earlier that all the ruptured stirrups were located at the bend portion, so it would be better to increase the $\frac{r_b}{d_b}$ more than 3 as in the same ratio used in this study according to the ACI-440 code. It is also recommended to use different BFRP stirrups diameter in order to study the effect of the shear behavior. Further work should be done in a study of green concrete by adding some chopped fiber to examine the shear behavior of the beams by applying the same variables. In addition, examining the durability of the green concrete with regards to flexural, compressive and shear strength by exposing the specimens to harsh environment like saline and acidic environment.

REFERENCES

[1]. The international Handbook of FRP COMPOSITES IN CIVIL ENGINEERING. Edited by *Manoochehr Zoghi.*

[2]. AYUB T., SHAFIQ N., NURUDDIN M.F. 2014. Mechanical Properties of High-Performance Concrete Reinforced with Basalt Fibers. Fourth International Symposium on Infrastructure Engineering in Developing Countries, IEDC 2013. Procedia Engineering, 77: 131–139.

[3]. Issa, M.A., Ovitigala, T., Ibrahim, M. Shear Behavior of Basalt Fiber Reinforced Concrete Beams with and without Basalt FRP Stirrups (2016) Journal of Composites for Construction, 20 (4), art. no. 4015083

[4]. Reinforced Concrete mechanics and design book By James K. Wight & James G. MacGregor.

[5]. G. Shehdeh. Beam Shear Analysis of Concrete with Fiber-Reinforcement Plastic (2015) International Journal of Research in Civil Engineering, Architecture & Design, Volume 3, pp. 07-20

[6]. Steel Fiber Reinforced Concrete Behavior, Modelling, and Design By *Harvinder Singh*

[7]. A. Altalmas, A. El Refai, F. Abed, Constr. Build. Mater. 81, 162 (2015)

[8]. CSA, S806-12: Design and Construction of Building Components with Fiber-Reinforced Polymers, Canadian Standards Association, Canada, 2012.

[9]. Razaqpur, A. G., Isgor, B. O., Greenaway, S., and Selley, A. (2004). "Concrete contribution to the shear resistance of fiber reinforced polymer reinforced concrete members." J. Compos. Constr., Vol. 8:5, 452–460.

[10]. Bentz, E. C., Vecchio, F. J., and Collins, M. P. (2006). “Simplified modified compression field theory for calculating the shear strength of reinforced 15 concrete elements.” ACI Struct. J., 103(4), 614–624

[11]. Alam, M. S., and Hussein, A. (2013). “Size effect on shear strength of FRP reinforced concrete beams without stirrup.” J. Compos. Constr., 10.1061/(ASCE)CC.1943-5614.0000248, 119–126.

[12]. Santos, P. M., & Júlio, E. N. (2012). A state-of-the-art review on shear friction. Engineering Structures, 45, 435-448.

[13]. Remigijus S, Gediminas M: The influence of shear span ratio on load capacity of fiber reinforced concrete elements with various steel fiber volumes. *Civil Engg and Manag XIII* 2007, (3):209–215.

[14]. Zhao, J.K., Xu, X.S. Study on shear behavior of FRP strengthened concrete beams (2017) IOP Conference Series: Earth and Environmental Science, 61 (1), art. no. 012062

[15]. Kobraei, Mohsen & Jumaat, Zamin. (2009). Using FRP-bars in Concrete Beams: A General Review.

[16]. Hoult, N.A., Sherwood, E.G., Bentz, E.C., Collins, M.P.Does the use of FRP reinforcement change the one-way shear behavior of reinforced concrete slabs? (2008) *Journal of Composites for Construction*, 12 (2), pp. 125-133.

[17]. Yost, J.R., Gross, S.P., Dinehart, D.W. Shear strength of normal strength concrete beams reinforced with deformed GFRP bars (2001) Journal of Composites for Construction, 5 (4), pp. 268-275.

[18]. Adhikari, S. (2009) *Mechanical Properties and Flexural Applications of Basalt Fiber Reinforced Polymer (BFRP) Bars*.

[19]. Abbas, U. (2013) ‘Materials Development of Steel-and Basalt Fiber-Reinforced Concretes’, (November).

[20]. K. Pilakoutas, K. Neocleous, M. GuadagniniDesign philosophy issues of fiber reinforced polymer reinforced concrete structures. J Compos Constr, 6 (3) (2002), pp. 154-161

[21]. CEB. CEB-FIP Model Code 1990. Comite Euro-International du Beton, Thomas Telford Ltd, 1993.

[22]. fib Bulletin No. 40. FRP reinforcement in RC structures. International federation for structural concrete. Lausanne: Switzerland; 2007.

[23]. B. Benmokrane, O. Chaallal, R. MasmoudiFlexural response of concrete beams reinforced with FRP reinforcing bars.ACI Struct J, 93 (1) (1996), pp. 46-55

[24]. P. Visintin , M.S. Mohamed Ali, M. Albitar, W. Lucas(2017). “Shear Behaviour of Geopolymer Concrete Beams without Stirrups”. Construction and Building Materials 148:10-21.

[25]. Sunna R, Pilakoutas K, Waldron P, Al-Hadeed T. Deflection of FRP reinforced concrete beams. In: 4th middle east symp on struct compos inf appl (MESC-4). Alexandria, Egypt; 2005.

[26]. ACI (American Concrete Institute). (2015). “Guide for the design and construction of structural concrete reinforced with FRP bars.” ACI 440.1R-15, Farmington Hills, MI.

[27]. Design of reinforced concrete (9th edition) By JACK C. McCROMAC & RUSSELL H. BROWN.

[28]. ISIS Canada, Reinforcing Concrete Structures with Fiber Reinforced Polymers. Design Manual N8 3 Version 2, Canada ISIS Canada Corporation, Manitoba, 2007.

[29]. C. E. Bakis, A. Ganjehlou, D. I. Kachlakev, M. Schupack, P. N. Balaguru, D. J. Gee, V. M. Karbhari, D. W. Scott, C. A. Ballinger, T. R. Gentry, and others, “Guide for the Design and Construction of Externally Bonded FRP Systems for Strengthening Concrete Structures,” 2002.

[30]. Santos, P. M., & Júlio, E. N. (2012). A state-of-the-art review on shear friction. Engineering Structures, 45, 435-448.

[31]. P.S. Ambily, C.K. Madsherwaran, N. Lakhsmanan, J.K. Dattatreya, S.A. Jaffer Sathik. Experimental studies on shear behavior of reinforced geopolymer concrete thin webbed T-beams with and without fibres, 2012, 3(1):128-140.

[32]. A.K. El-Sayed, K. Soudki. Evaluation of shear design equations of concrete beams with FRP reinforcement, Journal of Composites for Construction (ASCE), 2011, 15(1):04014025-1-15.

[33]. T. Zhang, P. Visintin, D. Oehlers, M. Griffith, Presliding shear failure in prestressed RC beams. II: behavior, ASCE J. Struct. Eng. 140 (10) (2014)

[34]. P. Visintin, D.J. Oehlers, C. Wu, M. Haskett, A mechanics solution for hinges in RC beams with multiple cracks, Eng. Struct. 36 (2012) 61–69.

[35].] M. Haskett, D.J. Oehlers, M.M. Ali, Local and global bond characteristics of steel reinforcing bars, Eng. Struct. 30 (2) (2008) 376–383.

R. Muhamad, M.S.M. Ali, D.J. Oehlers, M. Griffith, The tension stiffening mechanism in reinforced concrete prisms, Adv. Struct. Eng. 15 (12) (2012) 2053–2070

[36]. D. Knight, P. Visintin, D. Oehlers, M. Jumaat, Incorporating residual strains in the flexural rigidity of RC members with varying degrees of prestress and cracking, Adv. Struct. Eng. 16 (1) (2013) 1701–1718. Zararis, P.D. Shear compression failure in reinforced concrete deep beams (2003) Journal of Structural Engineering, 129 (4), pp. 544-553.

[37]. Martin, E. (2015). Global Sustainability and Concrete. Green Building with Concrete, 311-336. doi:10.1201/b18613-12

[38]. Doye (2017).Green Concrete. Efficient & Eco-Friendly Construction Materials, IOSR Journal of Mechanical and Civil Engineering (IOSR-JMCE) e-ISSN: 2278-1684, p-ISSN: 2320-334X, Volume 14, Issue 3 Ver. II (May. - June. 2017), PP 33-35

[39]. Parbat, Dhale, V. (2015).Fly Ash as Sustainable Material for Green Concrete- A state of Art

[40]. Meyer, C. (2005). Concrete as a green Building Material. Columbia University, New York, NY 10027, USA

[41]. Alkhrdaji, T., Wideman, M., Belarbi, A., and Nanni, A. (2001). “Shear strength of RC beams and slabs.” Composites in construction, J. Figueiras, L. Juvandes, and R. Faria, eds., A. A. Balkema, Lisse, The Netherlands, 409–414

[42]. Khuntia, M., and Stojadinovic, B. (2001). “Shear strength of reinforced concrete beams without transverse reinforcement.” ACI Struct. J., 98(5), 648–656.

[43]. Shioya, T. (1989). “Shear properties of large reinforced concrete members.” Special Rep. of Institute of Technology, Shimizu Corporation, No. 25.

[44]. Tureyen, A., and Frosch, R. J. (2002). “Shear tests of FRP-reinforced beams without stirrups.” ACI Struct. J., 99(4), 427–434

[45]. Bentz, E. C., and Collins, M. P. (2006). “Development of the 2004 Canadian Standards Association (CSA) A23.3 shear provisions for reinforced concrete.” Can. J. Civ. Eng., 33(5), 521–534.

[46]. Bentz, E. C., Massam, L., and Collins, M. P. (2010). “Shear strength of large concrete members with FRP reinforcement.” J. Comp. Constr., 14(6), 637–646.

[47]. Bentz, E. C., Vecchio, F. J., and Collins, M. P. (2006). “Simplified modified compression field theory for calculating the shear strength of reinforced concrete elements,” ACI Struct. J., 103(4), 614–624

[48]. *Rizzo A and De Lorenzis L. 2009 Behavior and capacity of RC beams strengthened in shear with NSM FRP reinforcement Construction and Building Materials 23 1555-67* Crossref

[49]. *Bo C, Qunhui Z and Linjie Z 2012 Experimental study on a new method to improve the shear capacity of concrete beams Building Structure 42 144-47*

[50]. *Teng J G, Lam L and Chen J F 2004 Shear strengthening of RC beams with FRP composites Progress in Structural Engineering and Materials 6 173-84*

[51]. Knaack, A. M., & Kurama, Y. C. (2014). Behavior of reinforced concrete beams with recycled concrete coarse aggregates. *Journal of Structural Engineering*, *141*(3), B4014009.

[52]. Etxeberria, M., Mari, A. R., & Vázquez, E. (2007). Recycled aggregate concrete as structural material. *Materials and structures*, *40*(5), 529-541.

[53]. Sato, R., Maruyama, I., Sogabe, T., & Sogo, M. (2007). Flexural behavior of reinforced recycled concrete beams. *Journal of Advanced Concrete Technology*, *5*(1), 43-61.

[54]. Zaki, S. I., Metwally, I. M., & El-Betar, S. A. (2011). Flexural Behavior of Reinforced High-Performance Concrete Beams Made with Steel Slag Coarse Aggregate. *ISRN Civil Engineering*, *2011*.

[55]. Faleschini, F., & Pellegrino, C. (2013). Experimental behavior of reinforced concrete beams with electric arc furnace slag as recycled aggregate. *ACI Mater. J*, *110*, 197-206.

[56]. Awoyera, P. O., Olofinnade, O. M., Busari, A. A., Akinwumi, I. I., Oyefesobi, M., & Ikemefuna, M. (2016). Performance of steel slag aggregate concrete with varied water-cement ratio. Jurnal Teknologi, 78(10), 125-131.

[57]. E. Oller, A. Mari, J.M. Bairan, A. Cladera. Shear design of reinforced concrete beams with FRP

longitudinal and transverse reinforcement, Composites Part B: Engineering (Science Direct),2015, 15:104-122.

[58]. Design of reinforced concrete (9^{th} edition) By *JACK C. McCROMAC & RUSSELL H.*

BROWN

[59]. ACI committee 318: *Building code requirements for structural concrete and commentary*. American Concrete Institute, Detroit, USA; 2002.

[60]. ACI Committee 222, " Protection of Metals in Concrete Against Corrosion (ACI 222R-01)," *ACI Manual of Concrete Practice,* American Concrete Institute, Farmington Hills, MI.

[61]. EI Refai, F. Abed. Concrete contribution to shear strength of beams

reinforced with basalt fiber-reinforced bars. J Compos Constr 10.1061/(ASCE)CC.1943-5614.0000648, 04015082

[62]. Kocaoz, S., Samaranayake, V.A., Nanni, A. Tensile characterization of glass FRP bars (2005) Composites Part B: Engineering, 36 (2), pp. 127-134.

[63]. (2002) *Recommended Test Methods for FRP Rods and Sheets* ACI Committee 440. In: Unpublished draft specifications. Farmington Hills, MI: American Concrete Institute

[64]. Tomlinson, D., and Fam, A. (2014). "Performance of concrete beams reinforced with basalt FRP for flexure and shear." J. Compos. Constr., 10.1061/(ASCE)CC.1943-5614.0000491, 04014036.

[65]. Upadhyay, R., & Srivastava,V. (2014). Effects of fly ash on Flexural Strength of Portland Pozzolana Cement Concrete. f Academia and Industrial Research, ISSN: 2278-5213, Volume 3, Issue 5 (October 2014).

[66]. Agrawal, S.K. and Sharma, P. 2009. Role of additives in optimization of fly ash in cement. NBM CW. 14(9): 134-136.

[67]. Sidheshwar Murkute, Madan S. H, and Dr. V. A. Patil, "Comparative study of green concrete and conventional concrete on strength and durability properties," International Research Journal of Advanced Engineering and Science, Volume 3, Issue 4, pp. 229-232, 2018

[68]. Harison, A., Srivastava, V. and Herbert, A. 2014. Effect of fly ash on compressive strength of Portland Pozzolona Cement Concrete. J. Acad. Indus. Res. 2(8): 476-479. 3. IS: 10262-1982.

[69]. Rajdev, R., Yadav, S. and Sakale, R. 2013. Comparison between Portland Pozzolana Cement and processed fly ash blended Ordinary Portland Cement. Int. Conf. on Recent Trends in Appl. Sci. with Engg. Appl. 3(6): 24-29.

[70]. Siddique, R. 2002. Effect of fine aggregate replacement with Class F fly ash on the mechanical properties of concrete. Cement Concre. Res. 33(2003): 539-547.

[71]. Venkatakrishanaiah, R. and Mohankumar, G. 2013. Experimental study on strength of high-volume high calcium fly ash concrete. IOSR J. Mech. Civil Engg. 5(4): 48-54.

[72]. . A. El Refai, F. Abed, A. Altalmas, J. Compos. Const.-ASCE 19, 04014078 (2014)

[73]. A. El Refai, F. Abed, J. Compos. Const.-ASCE, 20, 040150824 (2015)

[74]. A. El Refai, F. Abed, A Al-Rahmani, Constr. Build. Mater. 96, 518 (2015)